Electronic Engineering

VOL. 39. No. 476.

Explosion, or muffled report?

ALL the experts tell us, and the growing amount of written material seems to indicate, that there is an information 'explosion'. On our part, we do not admit that the explosion is all information.

It has always been the practice for technologists, engineers and scientists to publish papers in periodicals so that the world at large is informed and some measure of credit attached to the author and to his colleagues; both of these are laudable and necessary objectives in themselves. As a secondary role, the publication of papers provides a *raison d'etre* for periodicals and books. Indeed, were it not for commercial and national security, much more publishable material would be available.

These are the facts of the situation, but there is one facet that needs to be examined more closely concerning the rush for publication. It is our editorial task, and sometimes pleasure, to peruse many publications in our field of electronics and its related disciplines. During this perusal, we have noticed that not only considerable redundancy is incorporated within a single article but a good deal of overlap occurs between quite separate material. A case can be made out for both of these phenomena: an author often creates redundancy to clarify his presentation and two authors often go through similar processes of thought to reach somewhat different conclusions. This is all very right and proper and one cannot be critical of redundancy of this kind; after all, one employs redundancy in data transmission to reduce the possibility of errors in reception.

There is, however, another kind of writing which is really the theme of this editorial. This kind of writing is overwriting—the filling out with Latin- and Greek-based polysyllables where simpler Anglo-Saxon is superior, the unnecessary historical prologue, oversubtle descriptions where diagrams are obviously better, and so on and on. Much overwriting is born of inexperience; on the other hand, much of it stems from a belief that portentous construction adds weight and authority to something which may have neither.

We are sure that some of the daunting problems of the so-called information explosion could be mitigated by succinct writing, by not putting pen to paper unless one really has something to add to the corpus of knowledge, and (dare we say it) by stricter editorial control. These are the ways to help those who have to handle and disseminate the vast written outpourings of scientists and engineers throughout the world.

It has been suggested to us that what we have said above is the worst possible example of our own criticism—it is overwritten and full of prolixity and redundancy. So, in brief: if you really must write, write with economy and to the point. Rodomontade is for the grammarians, not the authors.

Time-amplitude and amplitude-time converters using linear ramps

by **C. Riddle,** B.Sc., M.I.E.E., *Royal Armament Research and Development Establishment.*

A linear ramp is generated when a capacitor is charged from a constant-current device such as a transistor. A complementary transistor can be used to discharge the capacitor linearity. With the aid of such ramps, a variety of linear generators can be designed; these include pulse generators and frequency generators in which the repetition rate or frequency is proportional to the input voltage, pulse generators in which the time interval between pulses is proportional to the input voltage, voltage generators in which the voltage generated is proportional to the time intervals or frequency of the input pulses, linear monostable delay units in which the delay is proportional to the input voltage etc. A linear sawtooth generator is described which has some advantages over the standard Miller integrator normally used for this purpose, because there is no initial step and and the ramp starts from the rail potential. A practical circuit is given for each of the various generators, with some indication of limits. In most cases these limits are fairly wide; for instance, the delay unit operates by decade switching from 1μs to a minute or more.

(Voir page 664 pour le résumé en français: Zusammenfassung in deutscher Sprache auf Seite 665)

THE basic circuit is shown in Fig. 1, and consists simply of a transistor with its collector connected to the positive rail *via* a capacitor. If the current into the base is

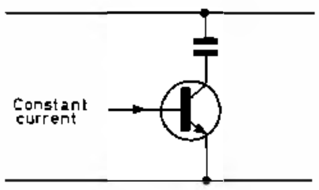

Fig. 1 Basic circuit

constant, linear charging of the capacitor will occur until the transistor saturates. The capacitor can be discharged in a similar way by connecting a second transistor across the capacitor (Fig. 2). Linear charging will now occur when the input is at $+V_B$ potential, and linear discharge will follow when the input is switched to zero potential.

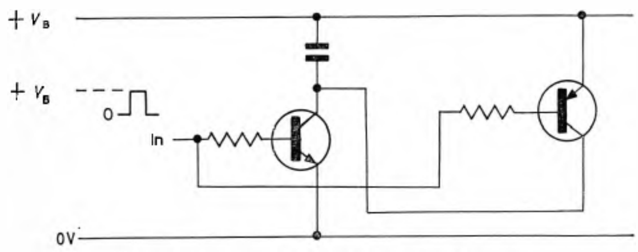

Fig. 2 Linear charge and discharge circuits

The charge voltage V acquired in time t is equal to it/c, where i is the charge current and c the capacity. Nonlinearity will occur if there is any shunt resistance across the capacitor. With modern low-leakage transistors, the nonlinearity due to leakage into the transistors is very small over quite a wide range of charging currents. Also high-low impedance converters can easily be built to monitor the waveform. A circuit of this sort can be used as a linear sawtooth generator. The pulse generator necessary to provide the drive can be free-running or triggered. This generator has two advantages over the standard Miller integrator: there is no step, and the charge starts from the bottomed collector voltage of the second transistor, i.e. very nearly V_B.

Linear pulse generators

A standard squarewave generator such as that shown in Fig. 3 is of limited use. The switching time is determined by the time constants of the capacitors and the base resistors; if the two combinations are different, the mark/space ratio will not be equal. The period can be altered to a limited extent by varying the base resistors. If the resistances are too low, oscillations may cease when the transistors saturate; if the resistances are too high, oscillations cease when the transistors are almost cut off.

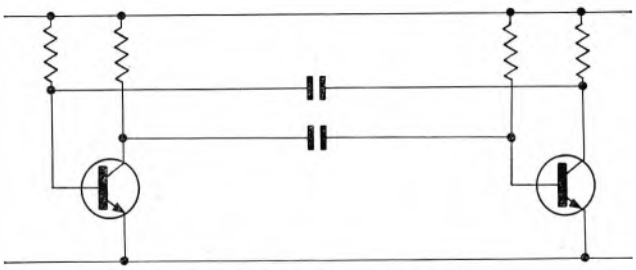

Fig. 3 Squarewave generator

The output waveshape is not very good, because the positive-going portion rises exponentially with a time constant proportional to the product of the collector resistance and the coupling capacitance.

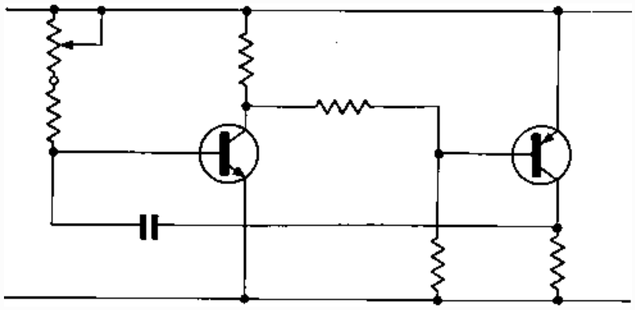

Fig. 4 Pulse generator

A more versatile generator can be derived from the circuit shown in Fig. 4. This constitutes a pulse generator with a short ON period and an OFF period determined by the discharge of the capacitor into the first transistor base resistance. The period can be adjusted over a fairly wide range by altering the first transistor base resistance, because the gain of the second stage remains high at all times. The scale is nonlinear, because the period depends on the discharge of the capacitor into a resistor, which is an exponential function. It can be made linear by replacing the resistor by a transistor, as shown in Fig. 5.

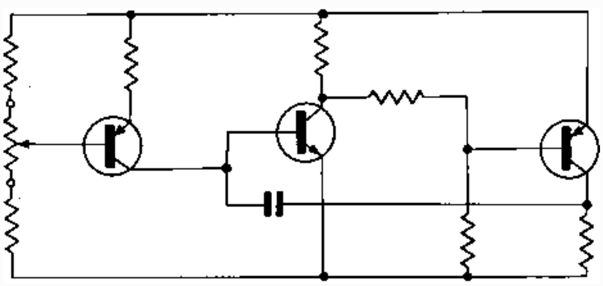

Fig. 5 Linear pulse generator

For any given setting of the potentiometer, the first transistor is now a constant-current device, its current being independent of the voltage on its collector. The discharge of the capacitor is now linear, and the period depends directly on the current in the first transistor. By a suitable zeroing arrangement, the current in the transistor can be made proportional to the voltage applied to the transistor base. The system is now a linear pulse generator in which the period is directly proportional to an input voltage applied to the base of the first transistor. A linear squarewave generator can be derived from this by feeding the output pulses into a standard binary divider. The resultant squarewave has sharp leading and trailing edges, and unity mark/space ratio.

Pulse generator with repetition frequency proportional to input voltage

Fig. 6 gives the circuit details of a linear pulse generator derived from the circuit of Fig. 5. The output frequency is proportional to the voltage V across the 500Ω potentiometer. To ensure that there is always a reasonable voltage between the collector and base of the constant-current BCY31 transistor, the voltage across the 500Ω potentiometer is halved by the 4·7kΩ voltage divider. The zeroing device comprises a 100Ω potentiometer which can be preset so that the voltage between the l.h. terminal and the centre point is equal to the base-emitter voltage of the BCY31. When this is done, the voltage across the 4·7kΩ emitter resistance is equal to $V/2$. The emitter current is then equal to $V/(2 \times 4700)$ amperes, and this is also nearly equal to the capacitor charging current; the period is thus directly proportional to V. Because the base-emitter voltage is, to some extent, temperature dependent, a silicon diode is shunted across the 100Ω resistor to compensate for variations in this voltage due to ambient-temperature fluctuations.

In Fig. 6, coupling between the P346A and HT101 is by a capacitor rather than the resistor in Fig. 5, to avoid the loss associated with resistive coupling. However, it is essential for correct operation that the repetition frequency is determined solely by the discharging time for capacitor C_1. To ensure this the discharging time for C_2 should be less than that of C_1. If C_2 is made smaller than C_1, the drive to the second stage might be too small to saturate the HT101. The excursion of C_1 would then be reduced, and the repetition frequency increased proportionally. A better way to reduce the discharge time of C_2 is to connect a diode across the base-emitter of the HT101. This restricts the positive excursion of the HT101 to a fraction of a volt. The value of C_2 can now be fixed at half that of C_1, and under these conditions the discharging of C_2 is completed before that of C_1, even for the highest values of V. To ensure self-starting under all conditions, the gain of the second stage should be as high as possible. On the other hand, the first-stage (P346A) base is d.c.-coupled to a varying current source,

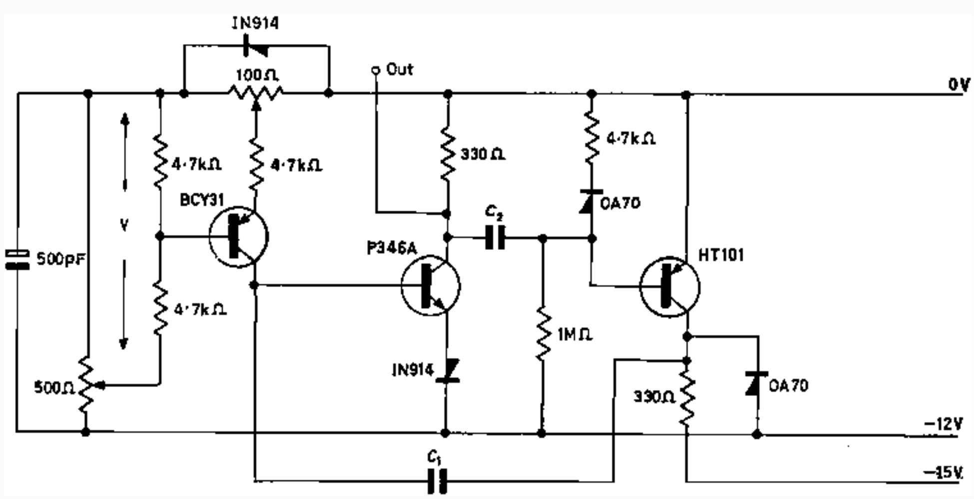

Fig. 6 Linear-pulse-generator detailed circuit

and, to avoid saturation troubles, a low-gain transistor with a low-value collector resistor is preferred for this position.

The P346A has a reverse base-emitter voltage limit of 4V, and so a diode is inserted in the emitter so that the excursion is limited only by the 12V rail voltage. This diode is a fast-switching type, with low reverse current, so that it does not form a significant discharge path for the capacitor. The discharge period of the capacitor is proportional to the negative-going voltage swing. This must not be allowed to vary, and to ensure this a limiter is incorporated. The HT101 collector resistor is connected to a −15V rail, but the maximum excursion is limited by the OA70 diode to −12V. It should be noted that the peak voltage across the BCY31 is nearly twice the rail voltage, and a 24V transistor is therefore required in this position. The time interval between pulses is equal to the time taken to discharge C_1 fully from its maximum negative excursion. Since the charge current is constant, time interval t is equal to the voltage excursion multiplied by C_1 divided by the charging current. In the circuit shown, the voltage excursion is nearly 12V and the charging current is approximately $V/(2 \times 4700)$ amperes; therefore the pulse-repetition frequency is $V/(12C_1 \times 2 \times 4700)$.

There are various factors which affect the range and accuracy of the system: the system will cease to oscillate if the discharge current is too high or too low. When the current is low, the accuracy may be impaired by leakage currents; when it is high, the accuracy will be impaired unless the time interval between pulses is long compared with the pulse duration. If C_1 is too small, there will be a loss of charge during the switching period, resulting in a reduced excursion, which shortens the discharge period. However, within these limitations, the circuit works well. With the circuit values given, and with $C_1 \geqslant$ 1000pF, the system is self-starting and linear over much more than a decade.

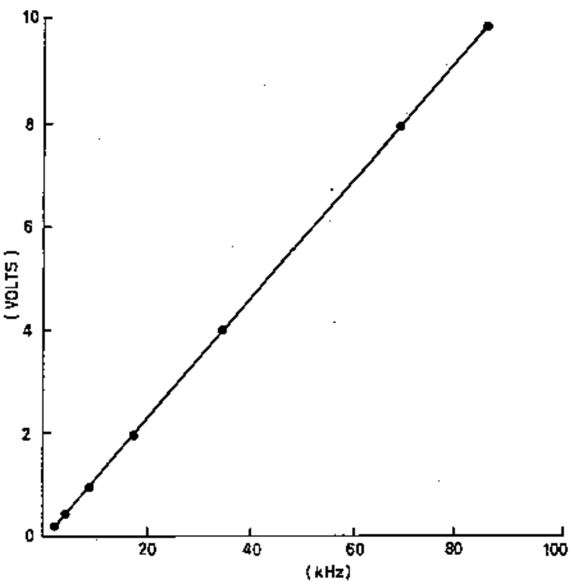

Fig. 7 Pulse generator with repetition frequency proportional to input voltage (C_1 = 0·001μF)

The graph in Fig. 7 shows the linearity when C_1 = 1000pF. Every point measured between 0·5 and 10V lies on the straight line, within the limits of test measurement (Avometer for voltage measurements, oscilloscope for time measurements). The pulse length is 0·3μs, and the frequency range 4·3 to 86kHz. With C_1 = 1μF, the pulse length is 150μs, and the frequency range 1000 times lower.

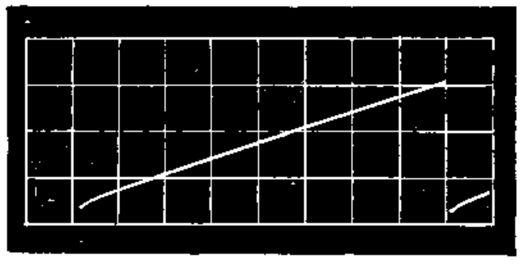

Fig. 8 Linear discharge of C_1 (C_1 = 100pF; scale 1μs/square)

Fig. 8 shows that the discharge is reasonably linear, even when the capacitance is reduced to 100pF. However, when capacitances below 1000pF are used, an appreciable loss of charge occurs during the switching-off process, so that the peak negative excursion on the P346A base does not reach −12V.

Linear sawtooth generators

The circuit shown in Fig. 9 is similar to that shown in Fig. 2 with a high/low-impedance converter added. It can be driven from the output of the circuit shown in Fig. 6.

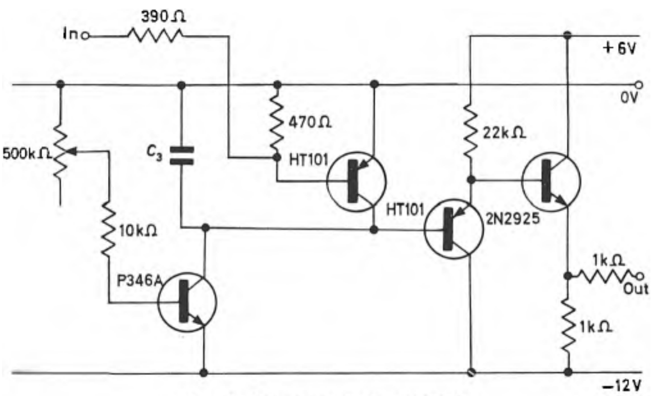

Fig. 9 Linear sawtooth generator

Fig. 10 shows a typical output waveform; C_1 = 1000pF, C_3 = 3300pF. This is a double exposure, showing the zero rail voltage at the top, and the ramp going negative from the rail voltage until it saturates, followed shortly afterwards by a very rapid reset to zero. A 3300pF capacitor charged to 12V is discharged completely by a 200mA current in about 0·20μs. The 0·3μs pulse generated in the circuit of Fig. 6, with C_1 = 1000pF, is thus sufficient to discharge the 3300pF capacitor. By switching C_1, C_2

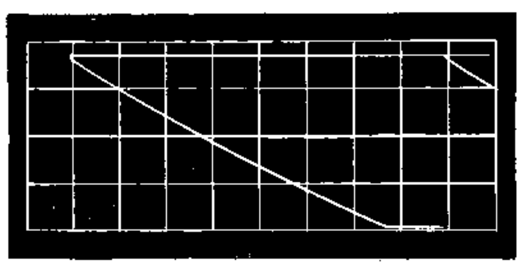

Fig. 10 Linear ramp (C_1 = 1000pF, C_3 = 3300pF; scale 20μs/square)

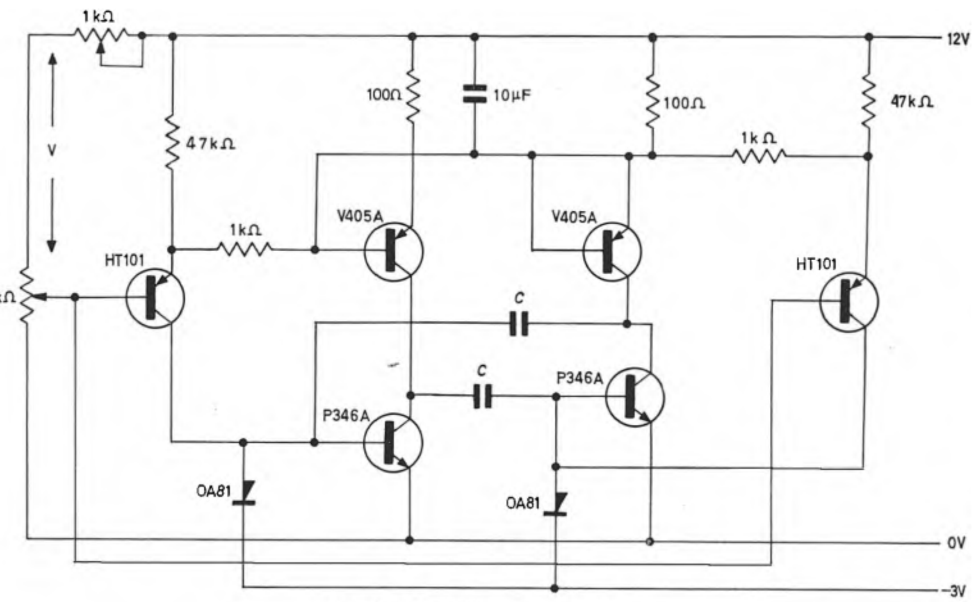

Fig. 11 Linear frequency generator

and C_3 in proportion, charging periods may be varied over a range of at least 100 000 : 1, from 4µs upwards, and probably much more if necessary. The charging current can be adjusted over a 50 : 1 range by the 500kΩ potentiometer, or the current can be stabilized using an emitter resistor.

The main advantage of a 2-stage complementary impedance converter of the type shown is that the base-emitter voltage drops of the two complementary transistors are equal in value but opposite in sign, and so tend to cancel out. The output therefore follows the input without change in d.c. level. It will be noted from Fig. 9 that the ramp starts quite accurately from zero voltage, with no step. There is thus no need to provide a separate zero-bias adjustment.

Linear frequency generator with frequency proportional to input voltage

It has already been mentioned that a squarewave generator of the type shown in Fig. 3 is not easily controllable by potentiometer to cover a wide frequency range. This situation can be remedied by replacing the collector resistors by transistors, which act as variable resistors whose values are controlled by a potentiometer. An example of this method is shown in Fig. 11. An HT101 transistor acting as a constant-current device feeds both the first P346A flip-flop, and the series V405A, which acts as the P346A collector load. A portion of the first V405A emitter current is drained off so that the P346A base current is greater than that of its series V405A transistor. Under static conditions, the P346A would therefore be nearly bottomed. Under oscillatory conditions, the potentiometer controls the frequency in a linear manner over a range much greater than 10, and, by decade switching of C, a frequency range of at least 10Hz to 1MHz is obtained.

In the circuit shown, the excursion of the capacitor C is limited by the diode to an invariable −3V. In the absence of this diode, the excursion would be limited by the reverse base-emitter maximum excursion, which is somewhat variable. The waveshape at the collector junction has a sharp negative-going trailing edge, but the positive-going front is a linear ramp, generated by the

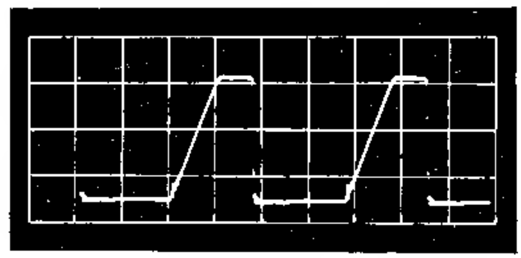

Fig. 12 Linear-frequency-generator waveshape at collector junction (C = 1000pF; scale 0·5µs/square)

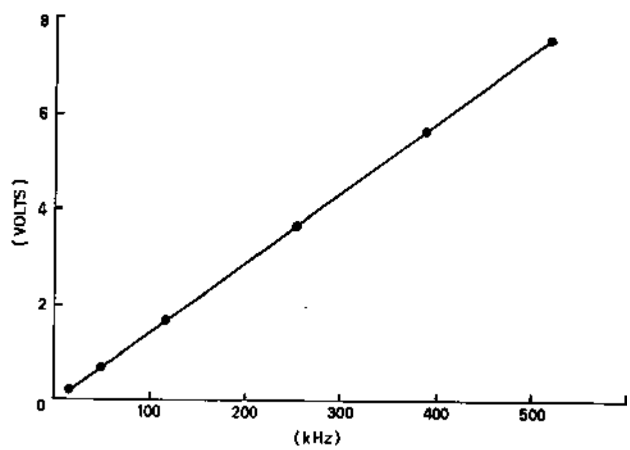

Fig. 13 Frequency generator with frequency proportional to input voltage (C = 1000pF)

charging of C through the constant-current V405A (Fig. 12). Also the mark/space ratio depends on the balance of two similar circuits, and is likely to vary over the range of potentiometer control. This circuit is rather more complicated than the pulse generator of Fig. 5 and seems to have few advantages over the latter. A squarewave, with uniform mark/space ratio can, however, be generated by operating a binary flip-flop from the negative-going trailing edge, and the repetition frequency is proportional to the control voltage V (Fig. 13).

(To be continued)

Solid-state h.l.t.t.l. 16-bit memory element

by **Anh Nguyen-huu,** Dipl.-Ing., and **R. H. Murphy,** B.Sc.(Eng.), *Transitron Electronic Ltd.*

The article describes a large-scale-integration (l.s.i.) circuit—the high-level transistor/transistor logic (h.l.t.t.l.) 16bit memory element—and its function, together with typical applications for which it has been designed.

(Voir page 664 pour le résumé en français: Zusammenfassung in deutscher Sprache auf Seite 665)

DURING the past two years, high-level transistor/transistor logic (h.l.t.t.l.) integrated circuits have come to be regarded by most users as among the better devices of the various types of integrated circuits brought on to the market. This is due to the fact that these circuits have high fan-out, high noise immunity, high-capacitance driving capability and high-speed performance, and are consequently reliable in many applications. In order to make these circuits more useful, further developments, including the recently introduced large-scale-integration (l.s.i.) circuits have been undertaken; in fact, the h.l.t.t.l. family now comprises more than 40 types. Among many large-scale-integration circuits developed to date, the h.l.t.t.l. 16bit memory element is perhaps the most successful.

Development

During the early days of its development, a goal was set for this solid-state memory element: the circuit involved had to be flexible and cheap enough to be used instead of ferrite-core memories in some applications. For scratch-pad ferrite-core memories of less than 10000 bits, the cost per bit was relatively high, because of the inefficient utilization of the necessarily complex WRITE and SENSE circuitry. It became feasible to complete such systems with monolithic flip-flop arrays incorporating their own SENSE and WRITE amplifiers and at the same time gain advantage from their inherent high operating speeds from random-access applications. Further, the solid-state memory circuit had to be compatible with existing h.l.t.t.l. circuits and could not be composed of too many components, because it had to be diffused on a relatively small silicon chip and capable of being supplied in the 14-lead flat package. This development results in the present 16-bit memory element, which consists of 16 single set/reset flip-flops, two SENSE and two WRITE amplifiers, consisting altogether of 46 transistors, 87 resistors (including underpaths) and 12 diodes. The 16 set/reset flip-flops form a 4×4 matrix which provides the storage of information. Each flip-flop comprises two 3-emitter transistors and two collector resistors of 4·5kΩ each. Two emitters of these two transistors are tied together and connected logically to the X_i or Y_i address lines. The third emitter is internally connected between all the 16 flip-flops and the input of one of the two SENSE amplifiers as well as the output of one of the two WRITE amplifiers (Fig. 1).

The output stage of the SENSE amplifier is a single transistor with no pull-up network. This permits the ORing of many SENSE-amplifier outputs when an expansion, of the bit number is required, for example, to build a 64bit memory using four 16bit memory elements. An external resistor is needed to pull up the ORed collectors of such an expansion and connected to the voltage supply.

Circuit function

To analyse the operation of the 16bit memory element, let us first study the WRITE and the SENSE amplifiers. If the input of a WRITE amplifier does not have a potential higher than 0·75V, the WRITE amplifier output is off, and the SENSE line, which is also the SENSE amplifier input, is kept at a potential of 1·5V, which represents two V_{be} voltage drops. If the input of a WRITE amplifier has a potential higher than 2·1V, its output transistor will be on, and the potential of the SENSE line is pulled down to 0·75V, approximately one V_{be} voltage drop (Fig. 2).

Sensing a selected bit

Assuming that the bit location (X_1, Y_1) has been selected with transistor Q_1 on and Q_2 off, if both selected inputs are low, say near ground, all the collector current of the transistor Q_1 will flow through the two emitters e_1 and e_2, while the emitter e_3, and thus the SENSE line, is disconnected from the cell. If one of the selected ADDRESS inputs, for example X_1, is brought to a high potential, it will be considered as disconnected from the cell. If the remaining selected ADDRESS input is also brought to a high potential, this will also be disconnected from the cell, and the whole collecter current of the transistor Q_1 is forced to flow into the SENSE line. This current will be detected and the SENSE-amplifier output S_1 will be low; the current forced to flow into the SENSE-amplifier input will open the input transistor VT_1 harder, and thus cause VT_2 to be on. The collector of VT_2 will then have a potential of approximately 0·8V (which is about one V_{be} voltage drop), which will turn VT_3 off, and cause the output transistor VT_5 to be on. The output S_1 will thus have a low potential.

Since Q_2 is off, only a small leakage current flows in the equivalent SENSE line. This current, therefore, does not cause a change of state of the input transistor VT_1 of the second SENSE amplifier. The collector of VT_2 has a potential of 2·3V, which represents approximately three V_{be} voltage drops. This is high enough to turn VT_3 on. With the difference between the collector voltage of VT_3 and the voltage drop on MR_3, the base potential of VT_5 is kept at about 0·1V, which guarantees completely a turn-off of this transistor, and thus causes the output S_0 to be high.

As we have seen, both data and complement data of one selected bit are provided at the two SENSE-amplifier outputs. Furthermore, the information stored in this bit location will not be destroyed by sensing, since the two inputs of the SENSE amplifiers are kept at the same potential, and these amplifiers work only as current detectors. All these characteristics help to make the 16bit memory element more flexible and very useful for such applications as scratch-pad memories.

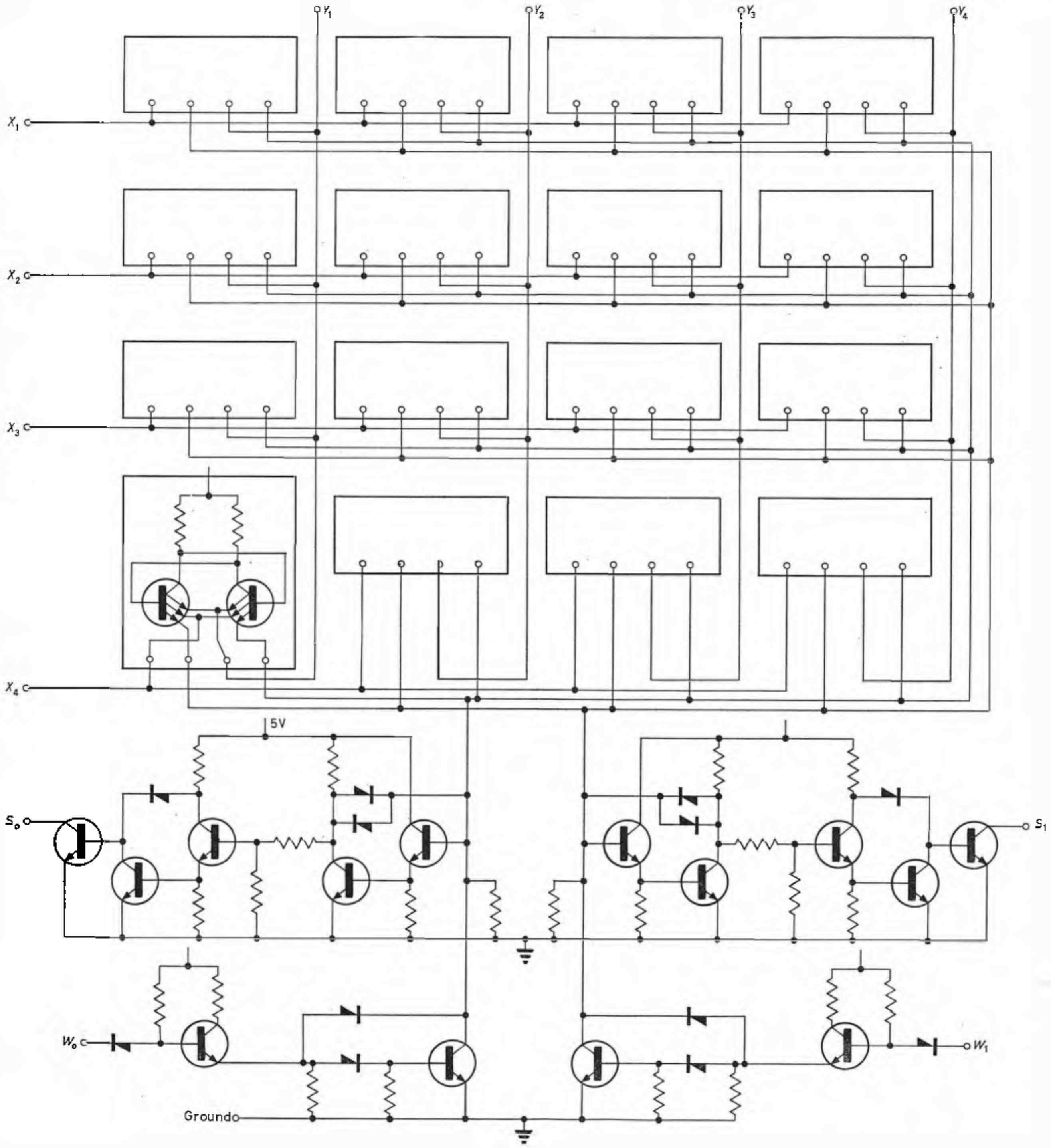

Fig. 1 16-bit memory element

Input characteristics

The input characteristics of a 16bit memory element at 25°C and three different values of voltage supply V_{cc} are shown in Fig. 3. The selected inputs (one X and one Y input) are tied together, while others are grounded. If the selected inputs are also at ground level, a relatively large current will flow to ground. This is the sum of the base and collector currents of the ON transistor, which is carried to ground through the two ADDRESS-line emitters. Since the third emitter is kept at 1·5V, it is back-biased, and no current flows to the sense input. As the input voltage increases, between 0V and the point A, the input current decreases, rapidly. This is due to the fact that the current from the half-selected bit is shared by selected inputs and grounded inputs. At an input voltage between the points A and B, the input current decreases only slightly; there is still no current flowing to the SENSE line. Between the points B and C, the input current again decreases rapidly. This is caused by the fact that the collector current of the ON-transistor is being transferred from the selected inputs to the SENSE line. The input voltage at the point A is defined as $V_{37}\overline{(S)}$, the threshold voltage on X and Y address lines to prevent the SENSE amplifier from sensing. This is one of the values given in the data sheet. An input voltage

Fig. 2 H.L.T.T.L. 16-bit memory element

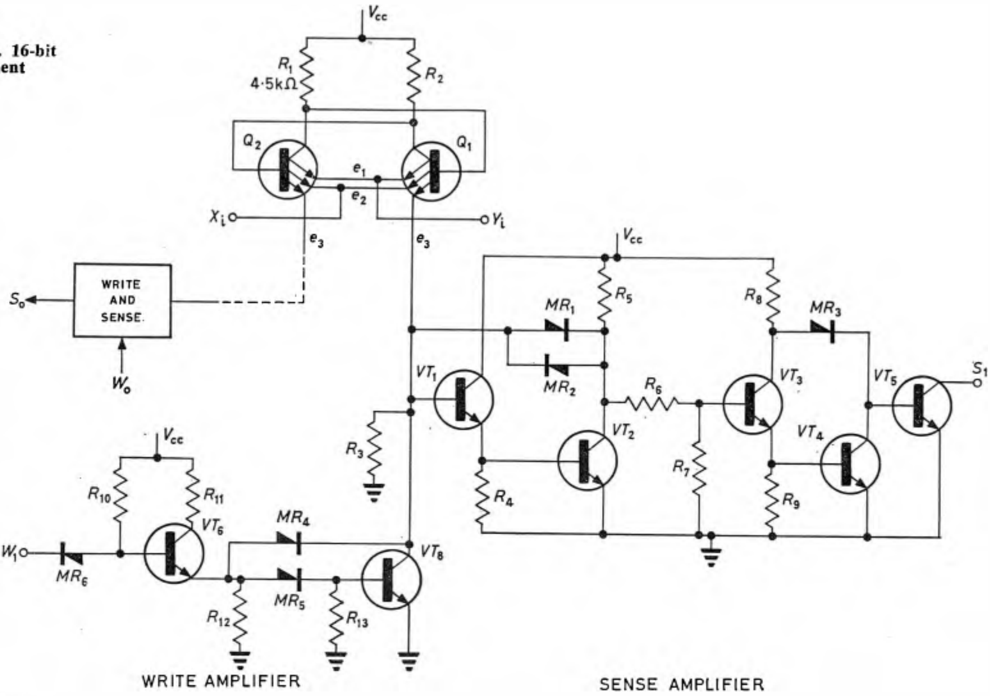

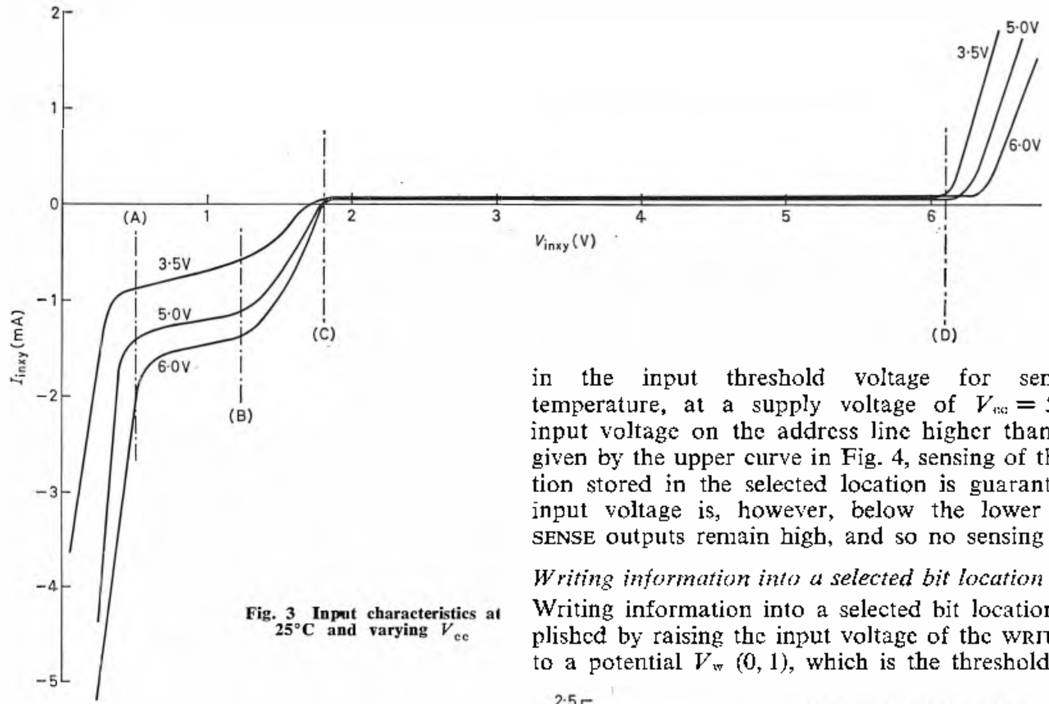

Fig. 3 Input characteristics at 25°C and varying V_{cc}

higher than this applied to the selected inputs can activate the SENSE amplifier and the equivalent output will change its state to indicate the information stored in the selected bit.

At the point C, specified as V_{xy} (S), the threshold voltage on X and Y ADDRESS lines to ensure sensing, and thereafter the input voltage, is high enough to disconnect these inputs from the cell. All the flip-flop current is forced to flow to the SENSE line; this will be detected by the SENSE amplifier. The input current changes its direction and is reduced to a leakage current. If the input voltage continues to rise (at a potential slightly higher than that of the point D), the input breakdown voltage will be exceeded, and a large current is forced to flow into the selected inputs. Fig. 4 shows the variations in the input threshold voltage for sensing with temperature, at a supply voltage of $V_{cc} = 5$V. At an input voltage on the address line higher than the limits given by the upper curve in Fig. 4, sensing of the information stored in the selected location is guaranteed. If the input voltage is, however, below the lower curve, the SENSE outputs remain high, and so no sensing is possible.

Writing information into a selected bit location

Writing information into a selected bit location is accomplished by raising the input voltage of the WRITE amplifier to a potential V_w (0, 1), which is the threshold voltage of

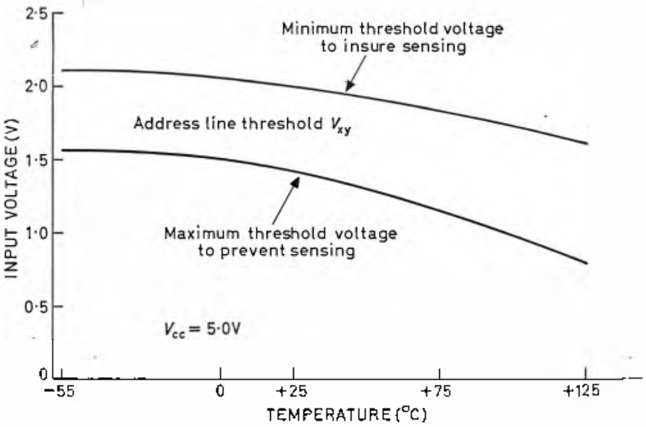

Fig. 4 Sensing threshold *versus* temperature

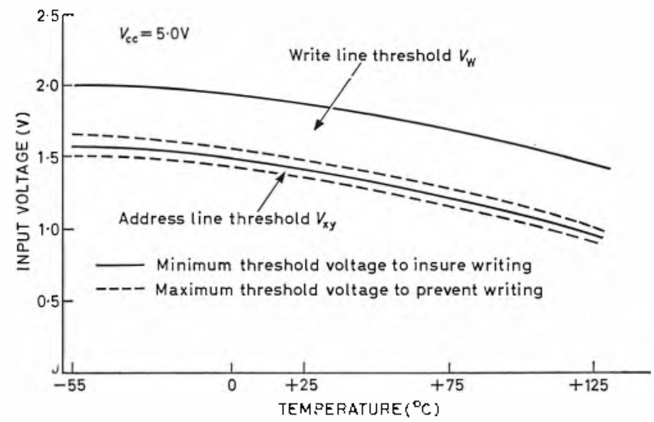

Fig. 5 Writing threshold *versus* temperature

the WRITE line in logic 0 or 1 condition. Since the selected inputs are at high potentials to ensure writing, they can be considered as disconnected from the cell. Assume that Q_1 is on while Q_2 is off, as in the case discussed above; if the WRITE-amplifier input W_0 is at a potential higher than 2·1V, the WRITE-amplifier output transistor is on, and the SENSE-line potential appearing at the third emittter of Q_2 is dropped to 1 V_{be} (about 0·75V). Since Q_1 is on, its collector potential is $1{\cdot}5V + V_{ce}(sat)$. This is also the base potential of Q_2. With its third emitter pulled down to 1 V_{be}, Q_2 will be on and cause Q_1 to turn off.

Writing is accomplished and guaranteed if the input voltage of the selected bit is higher than the minimum threshold voltage on the ADDRESS line to ensure writing, and the input voltage of the WRITE amplifier is higher than the minimum threshold voltage on the WRITE line to ensure writing, as shown in Fig. 5. No writing is possible if the ADDRESS-line input voltage is below the maximum threshold voltage on the ADDRESS line to prevent writing, or if the input voltage of the WRITE line is below the maximum threshold voltage on the WRITE line to prevent writing.

Switching and loading characteristics

Owing to the circuit arrangement using the clamp-diode network, the 16bit memory element can operate satisfactorily at high speed. Delay time between addressing and sensing or writing is less than 20ns, which allows the device to be used in memory systems with a cycle time of less than 120ns. Each ADDRESS-line input represents a fan-in of eight equivalent h.l.t.t.l. input loads, and each WRITE line a fan-in of 1. The output-loading characteristic (output voltage/output current) at 25°C is shown in Fig. 6. At an output current of 40mA, for the device TMC 3162, the output voltage in logic 0 condition is still under 0·45V.

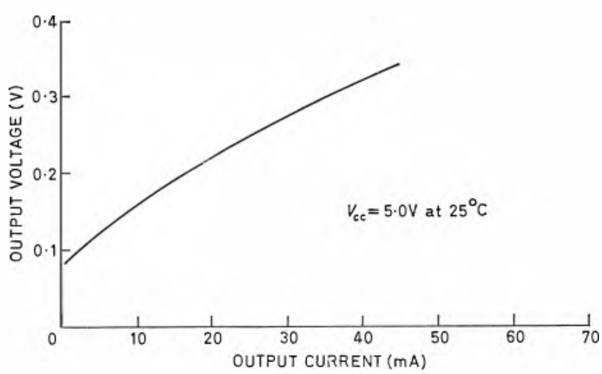

Fig. 6 Output loading characteristics for logic 0 condition

This means that the SENSE-amplifier output of this 16bit memory element (TMC 3162) can drive as many as 30 equivalent h.l.t.t.l. input loads.

Applications

64bit memory

A 64bit memory can be made out of four 16bit memory elements, as indicated in Fig. 7. As discussed above, the SENSE outputs S_1 or S_0 can be paralleled and all WRITE inputs W_0 and W_1 tied together, as shown. Each ADDRESS-line input represents now a fan-in of 16 h.l.t.t.l. input loads.

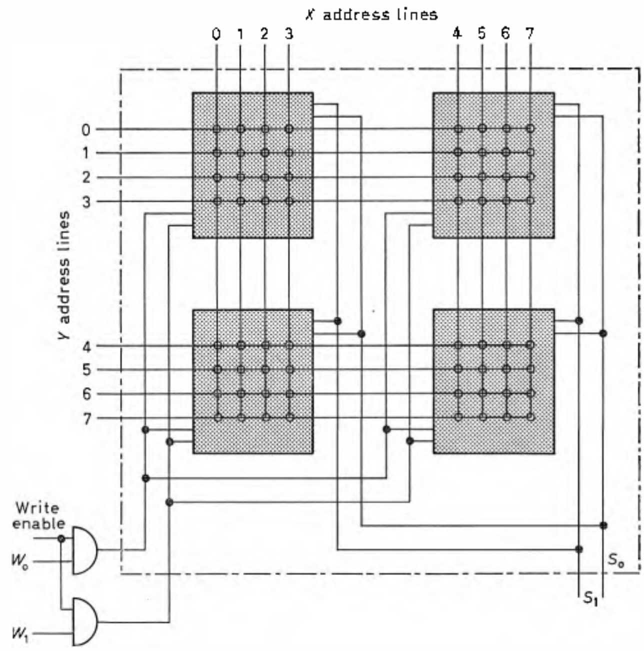

Fig. 7 64-bit memory element using four 16-bit h.l.t.t.l. memory elements

64-word-of-n-bit memory

A 64-word memory n bits/word can be realized from $4n$ 16bit memory elements. Fig. 8 shows such an arrangement, using the TMC 3164. The address will be decoded by an x- and a y-decode network which can be realized using the h.l.t.t.l. noninverting gates. Since the fan-in of an address line increases with every additional bit (16 input loads per bit), a driver network is necessary, and can be economically built with quad 2-input line-driver type TNG 5511. Data and complement data of each bit will appear at the outputs $S_{01}, S_{11}, \ldots S_{0n}, S_{1n}$. When information is to be written into the memory system, the selected x- and y-address lines are set at a high potential (in the WRITE condition with WRITE inputs $W_{01}, W_{11} \ldots W_{0n}, W_{1n}$); the equivalent gate output will then be high and energize the selected locations. This information will also appear at the sense outputs, thus enabling the written information to be checked again.

16bit memory element as storage device in computer

Another application is shown in Fig. 9. The information stored in the selected bit can be read and then supplied to the flip-flop. With a certain clock pulse, this information will be added to 1 and then written back to the same location as soon as the WRITE condition is satisfied. This application is often met in the computer logic, where subtraction or selection of a new bit is required. Because of the short delay time between addressing and sensing or writing, the 16bit memory element is very useful for this application, especially in high-speed systems.

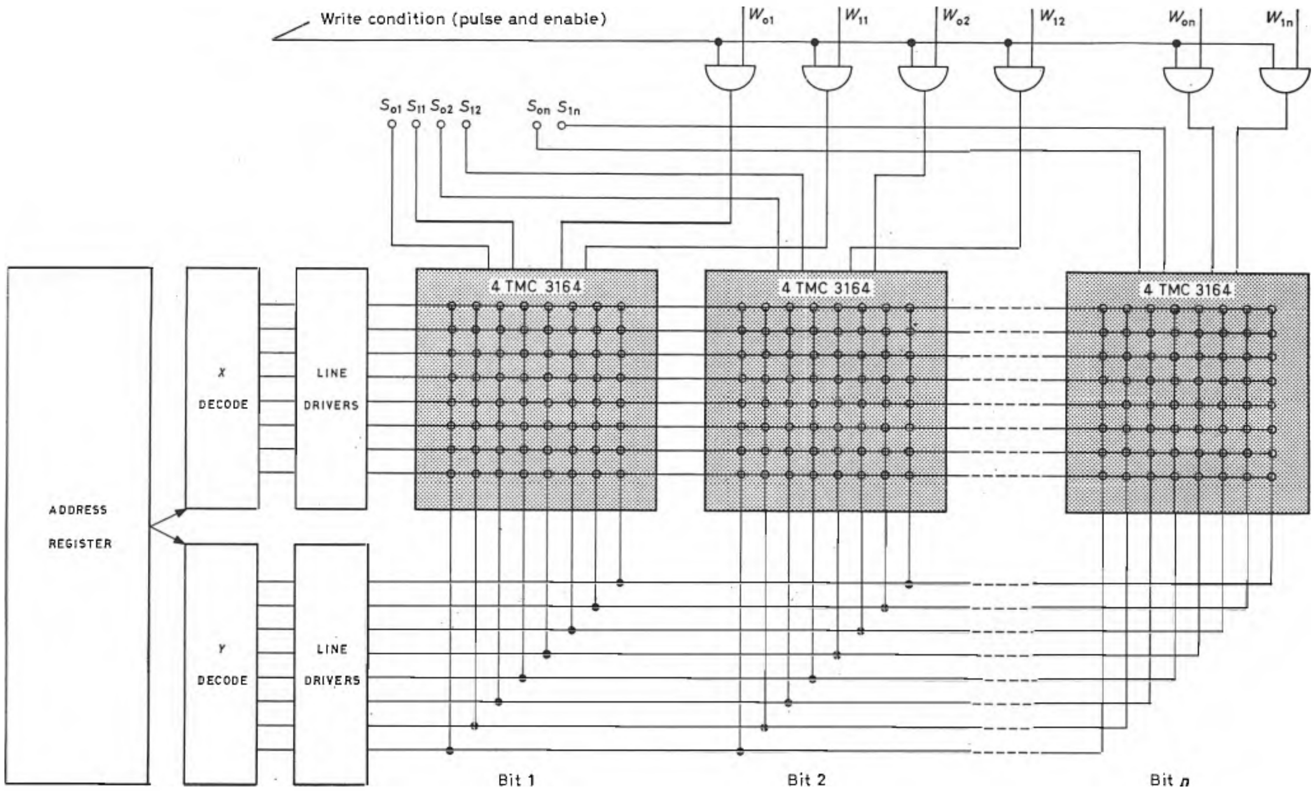

Fig. 8 Logic diagram of a 64-word memory with *n* bits (quad 2-input line driver TNG 5511, can be used for driver network and h.l.t.t.l. noninverting gate TNG 6252 for decode network)

Summary

The main characteristics of the 16bit memory element are:

(a) Both data and data complement are provided.

(b) The stored informataion is not destroyed while sensing.

(c) It is compatible with other h.l.t.t.l. circuits, both in logic levels and noise immunity.

(d) High-speed operation is possible with delay times between addressing and sensing or writing of less than 20ns.

(e) Sensing is performed by addressing a bit location and bringing the selected inputs to a high potential (typically 3·5V) while other inputs are held at near ground level.

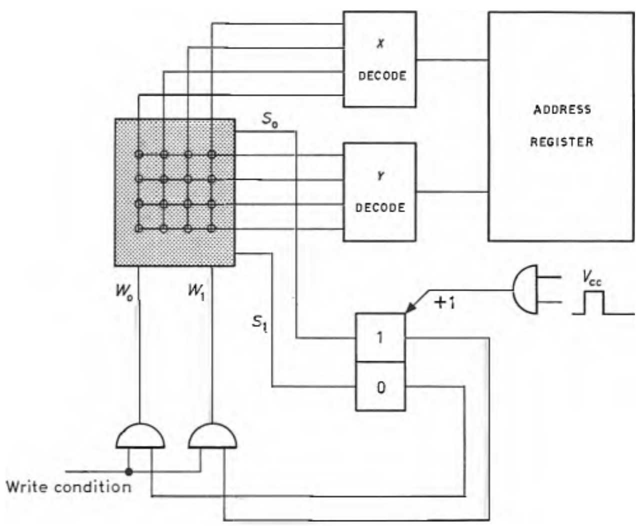

Fig. 9 Element as storage device in a computer (information stored in the selected bit can be read, plus 1 and written back in the same location)

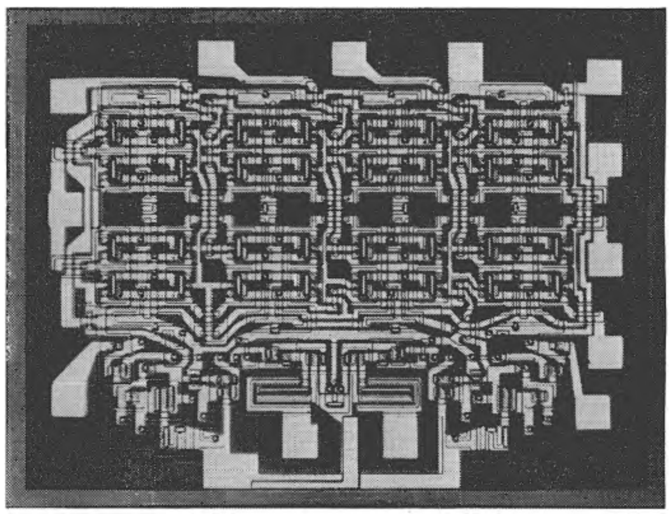

Fig. 10 Photograph of the element

(f) Writing is accomplished by raising the input potential of one of the WRITE amplifiers.

Acknowledgments

This article has been based partly on information supplied by the Digital Integrated Circuits Division of Transitron Electronic Corporation, Wakefield. Acknowledgment is due to the Directors of Transitron Electronic Ltd for permission to publish this material.

REFERENCES

1 MURPHY, R. H.: H.L.T.T.L., *Electronic Equipment News* (Aug. 1965).
2 RUTHAZER, L. B.: High-speed integrated-circuit memories, *Nerem Record* (1965).
3 HART, T. W.: Integrated-circuit memory system, *Nerem Record* (1966).

Stabilized power supply for 3kV, 60mA

by **G. Klein** and **C. W. Bodenhausen**, *Philips Research Laboratories, Eindhoven, Netherlands*

This article describes a well stabilized high-voltage power supply in which use is made of a series element consisting of a transmitting valve and a transistor. In this way, it is possible to obtain excellent stabilization and instantaneous regulation without a large loop gain.

(Voir page 664 pour le résumé en français: Zusammenfassung in deutscher Sprache auf Seite 665)

In an earlier article[1], a method was indicated which made it possible to design a stabilized power supply for 2kV, 10mA, without a large loop gain and, accordingly, without having to use large output capacitances.

The principle of this method follows from a consideration of Fig. 1, in which the basic circuit of a stabilized

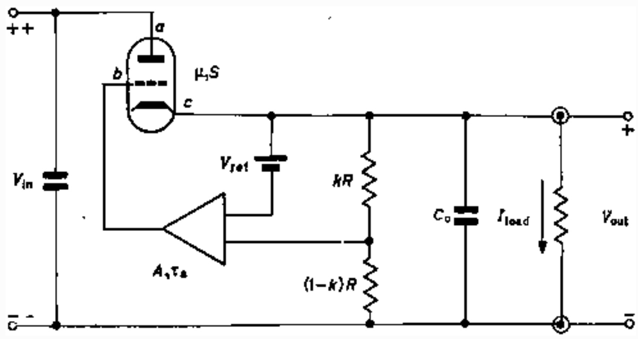

Fig. 1 Principle of stabilized power supply

power supply is shown. On the assumption that the control amplifier and the reference element are ideal, changes in the output voltage V_{out} can occur only as a result of changes in the unstabilized voltage V_{in} and in I_{load}:

$$\Delta V_{out} = \frac{\Delta V_{in}}{Ak\mu} + \frac{\Delta I_{load}}{AkS}$$

where k = fraction of the output voltage which is compared with the reference voltage V_{ref}

A = amplification of the control amplifier; so that Ak is the loop gain from the output to the grid of the series element

μ = amplification factor of the series element

S = mutual conductance of the series element.

To keep the changes in V_{out} below a certain level for given variations ΔV_{in} and ΔI_{load}, the products $Ak\mu$ and AkS must have certain minimum values. The ratio of these products, known, respectively, as the stabilization factor and the regulation factor, is μ/S, i.e. the internal resistance of the series element. Therefore, whether the required value of Ak is determined by the changes in V_{in} or by those in I_{load} will depend on this parameter. In low-voltage supplies, it is generally the latter which determine the loop gain, but the more V_{out} increases and thus, for the same delivered power, $(I_{load})_{max}$ decreases, the more important the effect of changes in V_{in} becomes. With high-voltage apparatus, such as that described here, which can deliver 200W, a power valve with a relatively low internal resistance has to be used as the series element, and this implies that the loop gain will be determined by changes in V_{in}, and therefore should be very large. This is illustrated by the following numerical example.

If it is required that a change of 10% in V_{in} should have the same effect on V_{out} as a change in the load current of 0·1 $(I_{load})_{max}$, this would, with $V_{in} \simeq 2V_{out}$, lead to the same value of Ak if

$$\frac{0{\cdot}2V_{out}}{Ak\mu} = \frac{0{\cdot}1(I_{load})_{max}}{AkS}$$

or

$$\mu/S = \frac{2V_{out}}{(I_{load})_{max}}$$

With V_{out} = 3kV and $(I_{load})_{max}$ = 60mA, an internal resistance of the series element of 100kΩ would result. However, in a power valve, the anode resistance rarely exceeds 10kΩ, so that the required loop gain would then be determined by the stabilization factor. There would be little objection to this alone, if it were not for the fact that an upper limit is also imposed on the admissible loop gain. The reason for this is that, in feedback systems, the ratio of the two largest time constants determines the admissible loop gain. If this value is exceeded in systems with more than two time constants, oscillations will in general occur, while, in systems with just two time constants, although oscillations cannot occur, free resonances of large amplitude are possible. A regulated power supply can generally be included in the latter category, and here the conditions for proper operation[1,2] is that the loop gain Ak should preferably remain smaller by a factor of 4 than the ratio of the two determining time constants, namely the time constant τ_a, corresponding to the decay of the frequency characteristic of the control amplifier A, and the time constant C_0/S of the output circuit. As far as the stability of the system is concerned, it is optional which of those two time constants is made the greater; with regard to the effect of sudden changes in I_{load}, however, this does make a great difference. If C_0 is small, a change ΔI_{load} will cause a relatively large change ΔV_{out}, which, because of the large value of τ_a, will only slowly be brought under control. If, on the other hand, C_0 is large the change ΔV_{out} will be much smaller and also can be controlled quickly, owing to the fast response of A.

Frequently, the former solution is chosen, since there is no need for a large output capacitance. For general purposes, such a supply with a 'recovery time' should, however, be avoided. The condition for the ratio of the time constants then requires that

$$Ak < C_0/4S\tau_a \quad \text{or} \quad C_0 > 4AkS\tau_a$$

For a given value of τ_a, it is thus necessary to make C_0 vary in accordance with the regulation factor AkS. For this reason, it is preferable to make Ak no greater than is necessary for the regulation factor, and so this factor and not the stabilization factor should determine Ak. This can be achieved if a series element with large internal resistance is chosen. If this element has in addition a high mutual conductance, the loop gain can be kept very

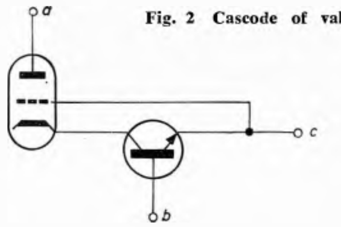

Fig. 2 Cascode of valve and transistor

small indeed, so that r_a, and thus also C_0, can remain as small as possible. With a load current of 60mA and a conventional rectifier unit, there is little sense in making C_0 extremely small; in order to limit the ripple voltage in V_{in} to a few hundred volts, the capacitor in the rectifier unit must already be several microfarads, and there is no point in making C_0 much smaller than this.

In the previous article[1] it was suggested that the series element used should be a cascode consisting of a transistor and a valve, as shown in Fig. 2. Because of the high power and high voltages involved in the apparatus described here, the valve used was the small transmitting type QB3/300, while, as the transistor must be able to cope with a power of several hundred milliwatts, a type AC127 was used. This combination gave an amplification factor of no less than 10^6; the mutual conductance was 40mA/V at a current of 1mA, and about 1A/V at a current of 60mA. It is clear that with a series element like this the loop gain need hardly be greater than unity.

Fig. 3 shows the principle of the control circuit. To make the mutual conductance of the series element less dependent on I_{load}, a resistor of 10Ω is placed in series with the emitter of the transistor. Although in principle the valve E80CC could be replaced by a transistor pair it is simpler to use valves in the comparator stage because of the occurrence of heavy voltage pulses during the switching from one voltage range to another. The output resistance of the amplifier stage is too large for driving the series element, and thus an emitter follower is used for matching. A reference voltage of approximately 83V is supplied by the neon valve 83A1.

The principle of the current limitation and overload protection is shown in Fig. 4. The load current I_{load} flows through the resistor R_1 in series with the cascode valve and cascode transistor. As the cathode of the

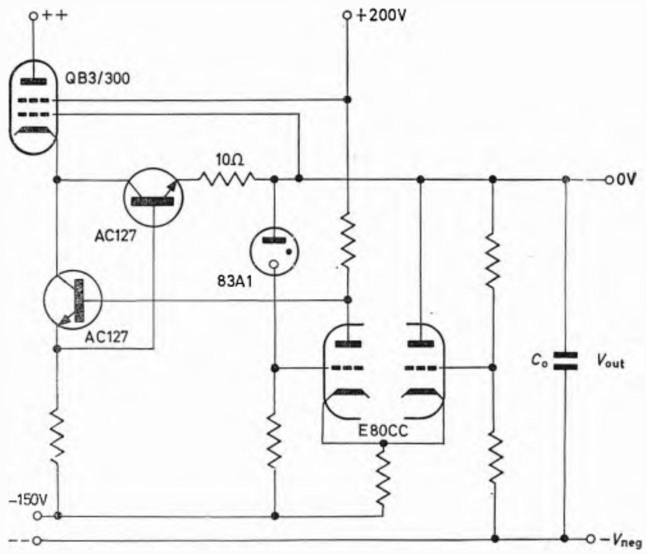

Fig. 3 Basic circuit of h.t. supply

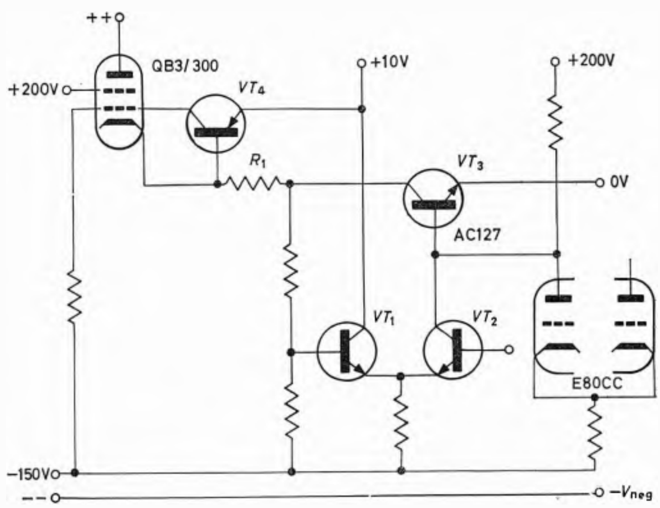

Fig. 4 Principle of current stabilization and limitation

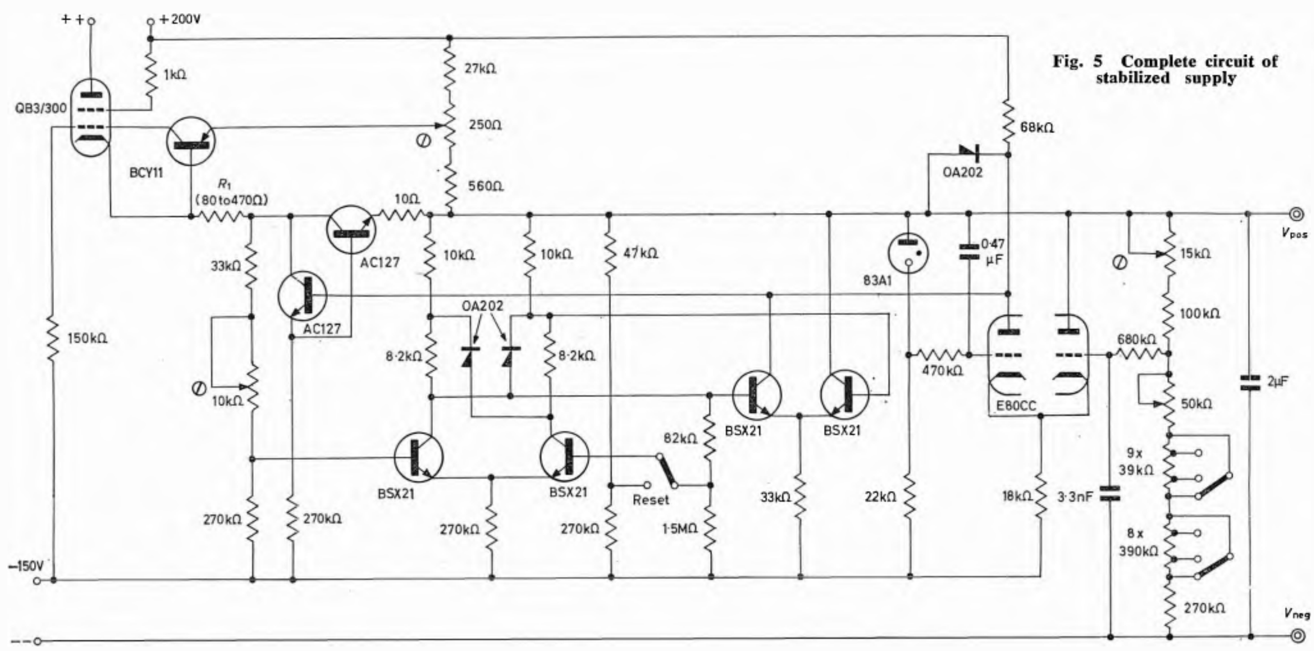

Fig. 5 Complete circuit of stabilized supply

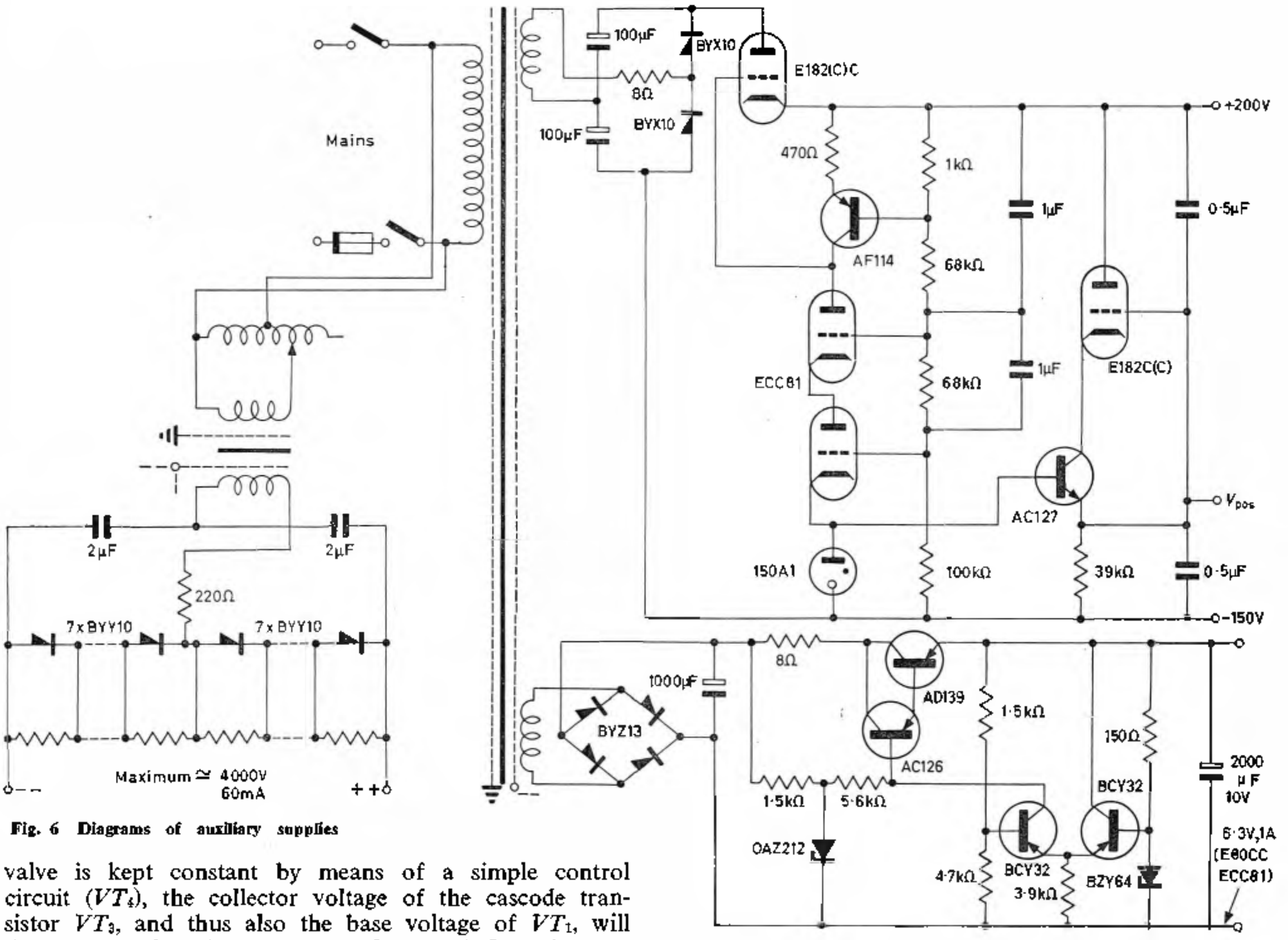

Fig. 6 Diagrams of auxiliary supplies

valve is kept constant by means of a simple control circuit (VT_4), the collector voltage of the cascode transistor VT_3, and thus also the base voltage of VT_1, will decrease as I_{load} increases. As VT_1 and VT_2 form a differential stage, VT_2 will become conductive at a certain I_{load}. With sufficient amplification, this control circuit will then determine the adjustment of the series element. If the base voltage of VT_2 is kept constant, I_{load} will be stabilized at a certain value. If, however, this base voltage is made a small fraction of the output voltage, it will diminish when the maximum load is exceeded, and this ensures that the load current is completely cut off.

The complete diagram of the control circuit, omitting only nonessential details, is shown in Fig. 5. The circuit used for the current limitation consists of two stages and corresponds to the second of the two methods just mentioned. Fig. 6 shows the diagram for the more important auxiliary voltages. The slider of the variable transformer is coupled mechanically to the switch for the 300V steps in the output voltage.

Results

V_{out}: Adjustable from 300 to 3000V in steps of 300 and 30V; continuous adjustment over a range of 50V.

I_{load}: 0-60mA.

Stabilization: A change of 10% in the mains voltage gives a relative change in V_{out} of less than 3×10^{-6}.

Regulation: The internal resistance for direct current is less than 1Ω per 100V, so that a change of $0{\cdot}1\,(I_{load})_{max}$ produces a relative change in V_{out} of less than 6×10^{-5}. For alternating current the modulus of the internal impedance is less than 2·5Ω for all frequencies and for all output voltages. At 300V this means that an alternating current of 6mA peak-to-peak produces a relative change in the output voltage of 5×10^{-5}. At 3000V this is smaller by a factor of 10. With discontinuous loads, the circuit has no recovery time: the output voltage always remains within the above specification.

Hum and ripple: Depending on the position of the range selector, the load current and the mains voltage, the sum of hum and ripple varies from 0·6 to 1·5mV peak-to-peak.

Long-term stability: Measured with a time constant of 10s, the relative changes in V_{out} were found to be less than 10^{-5} for all voltage ranges. The variations over periods of hours, after a warming-up time of 10min, remained smaller than 10^{-4} at a constant ambient temperature. The effect of temperature changes is determined by the temperature coefficient of the reference valve and the resistors in the voltage divider (3×10^{-6} and 2×10^{-5} per degC, respectively).

Overload protection: The apparatus is protected against short-circuiting. If the maximum current to be drawn is set to a certain value, the voltage stabilization continues to work perfectly up to this value. There is thus no premature influence of the current-limiter circuit on the output voltage. If the maximum current is exceeded, V_{out} becomes practically zero, and remains at this value until the overload is removed and the reset button is pushed in. The current-limiter delay depends on the magnitude of the excess current, and varies between 1 and 6μs.

REFERENCES

1. Klein, G., Zaalberg van Zelst, J. J. Combinations of valves and transistors in a stabilized 2000V power supply. *Philips Tech. Rev. 25*, 181 (1963/4).
2. Klein, G., Zaalberg van Zelst, J. J. *Instrumental Electronics*. Philips Technical Library, Eindhoven, Netherlands (1967).

Noise analysis of feedback amplifiers

by **P. J. Finnegan**, B.E., M.I.E.E.E., *Woolwich Polytechnic, London*

The noise within any linear time-invariant 2-port may be expressed as two noise sources outside a noiseless, but otherwise equivalent, 2-port. Using this concept, approximate but generally accurate expressions are derived for the overall noise generators, noise factor and optimum source resistance of certain classes of feedback amplifier. A study is made of the manner in which the introduction of feedback degrades noise factor and alters optimum source resistance, and of the design of amplifiers with negligible noise-factor degradation due to feedback. Finally, a simple method is proposed for the approximate analysis of a wider range of feedback amplifiers.

(Voir page 664 pour le résumé en français: Zusammenfassung in deutscher Sprache auf Seite 665)

It has been established[1,2] that the noise produced within any linear time-invariant 2-port may be represented by two noise generators with a complex correlation coefficient, connected externally to the 2-port itself, which is then considered noiseless but otherwise equivalent. The two external noise generators can be connected in any of six ways, corresponding to the six matrix combinations, and will be constant-current or constant-voltage sources, depending on the chosen configuration. Bogner[3] and Feifel[4] have shown that this approach has useful application in the noise analysis of feedback amplifiers. It will be used in this article to derive simple approximate expressions for the overall noise generators, noise factor and optimum source resistance of certain classes of feedback amplifiers.

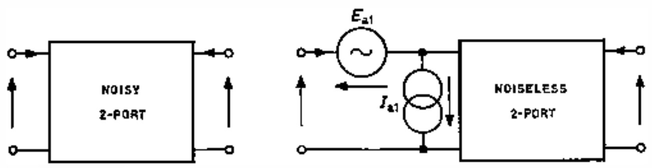

Fig. 1 2-port noise expressed as equivalent noise generators at the 2-port input

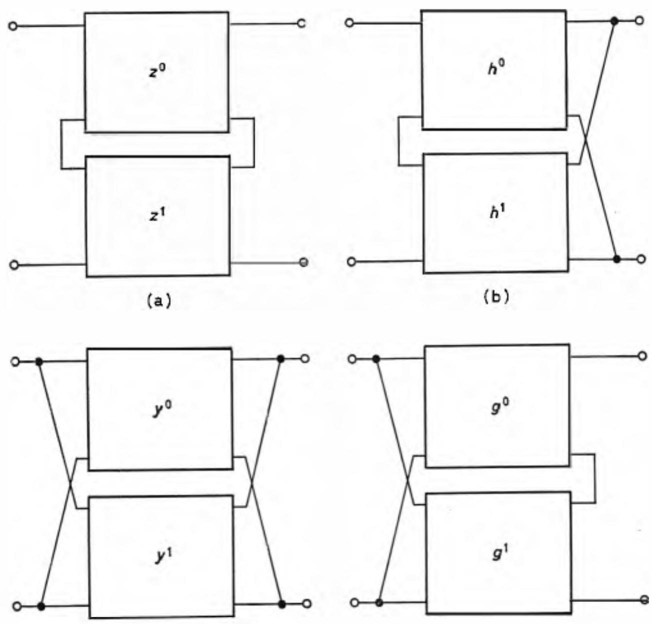

Fig. 2 Four basic feedback combinations

Noisy 2-ports

Fig. 1(a) shows a noisy 2-port which is separated in Fig. 1(b) into a noiseless 2-port and two noise generators: a constant-voltage generator E_{a1} in series with the input and a constant-current generator I_{a1} in shunt with the input. In general, the correlation between them is complex, but in this article it will be considered real and denoted by γ. The value of this representation lies in the simplicity of the expressions for noise factor, E_{a1}, I_{a1}, γ and the source impedance, using no other parameters of the network. As noise is a fluctuating quantity whose average value is zero, one should strictly speak in terms of mean squares, and write $\sqrt{(\overline{E_{a1}^2})}$ and $\sqrt{(\overline{I_{a1}^2})}$, the equivalent root-mean-square quantities. However, for simplicity and where no ambiguity is likely to arise E_{a1} and I_{a1} will be written.

The mathematical expression for Fig. 1(b) in matrix form is

$$\begin{bmatrix} V_1 \\ I_1 \end{bmatrix} = \begin{bmatrix} a_{11} & a_{12} \\ a_{21} & a_{22} \end{bmatrix} \begin{bmatrix} V_2 \\ -I_2 \end{bmatrix} + \begin{bmatrix} E_{a1} \\ I_{a1} \end{bmatrix} \quad \ldots\ldots\ldots\ldots (1)$$

Corresponding expressions apply for the remaining five combinations.

Feedback

The simplest forms of feedback are those which can be separated into the four combinations shown in Fig. 2, where superscripts 0 and 1 denote the amplifier and feedback networks, respectively. The first designation describes the connection of the two input ports, the second that of the output ports. Both the amplifier and the feedback 2-port are treated as noisy 2-ports. The location of the noise generators and the matrix notation chosen in a particular case are such that the resultant noise and matrix parameters for the overall network are obtained by simple addition.

Series-series feedback

Fig. 3 shows the series-series combination to be examined in detail; the amplifier noise generators are readily transformed from the usual a-notation of Fig. 1(b) to the z-notation of Fig. 3 by means of the transformation[5]

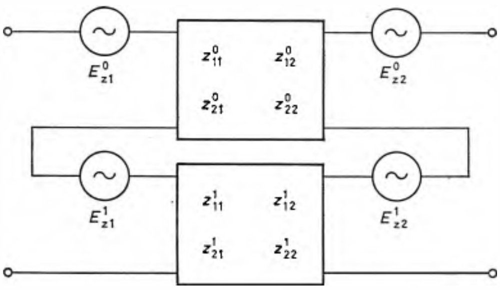

Fig. 3 Series-series combination of two noisy 2-ports

$$\begin{bmatrix} E_{z1}^0 \\ E_{z2}^0 \end{bmatrix} = \begin{bmatrix} 1 & -z_{11}^0 \\ 0 & -z_{21}^0 \end{bmatrix} \begin{bmatrix} E_{a1}^0 \\ I_{a1}^0 \end{bmatrix} \quad \ldots\ldots\ldots\ldots (2)$$

Summing gives

$$\left.\begin{aligned} E_{z1} &= E_{z1}^0 + E_{z1}^1 \\ E_{z2} &= E_{z2}^0 + E_{z2}^1 \\ Z &= Z^0 + Z^1 \end{aligned}\right\} \quad \ldots\ldots\ldots\ldots (3)$$

This final z-form is now converted back to the a-form:

$$\begin{bmatrix} E_{a1} \\ I_{a1} \end{bmatrix} = \begin{bmatrix} 1 & -(z_{11}/z_{21}) \\ 0 & -(1/z_{21}) \end{bmatrix} \begin{bmatrix} E_{z1} \\ E_{z2} \end{bmatrix} \quad \ldots\ldots\ldots\ldots (4)$$

Inserting equation (2) into equation (3), and the result into equation (4), and multiplying out,

$$\left.\begin{aligned} E_{a1} &= E_{a1}^0 + I_{a1}^0\,[z_{11}(z_{21}^0/z_{21}) - z_{11}^0] \\ &\quad + E_{z1}^1 - E_{z2}^1\,(z_{11}/z_{21}) \\ I_{a1} &= I_{a1}^0 - E_{z2}^1\,(1/z_{21}) \end{aligned}\right\} \quad \ldots\ldots\ldots (5)$$

Equation (5) gives the resultant input noise generators E_{a1} and I_{a1} for the feedback amplifier as a single 2-port, in terms of the original noise generators of the amplifier, the noise generators of the feedback 2-port and the impedance parameters.

At this stage, it is convenient to simplify equation (5). Examining the coefficient of I_{a1}^0 in the first equation,

$$\begin{aligned} z_{11}(z_{21}^0/z_{21}) - z_{11}^0 &= (z_{11}^0 + z_{11}^1)\frac{z_{21}^0}{z_{21}^0 + z_{21}^1} - z_{11}^0 \\ &= z_{11}^1\frac{z_{21}^0}{z_{21}^0 + z_{21}^1} + z_{11}^0\left(\frac{z_{21}^0}{z_{21}^0 + z_{21}^1} - 1\right) \\ &= z_{11}^1\frac{z_{21}^0}{z_{21}^0 + z_{21}^1} + z_{11}^0\frac{-z_{21}^1}{z_{21}^0 + z_{21}^1} \end{aligned}$$

In most practical amplifiers,

$$z_{21}^0 \gg z_{21}^1$$

and the expression then reduces to

$$z_{11}^1 - \frac{z_{11}^0 z_{21}^1}{z_{21}^0} = z_{11}^1\,[1 - (z_{11}^0/z_{21}^0)\,(z_{21}^1/z_{11}^1)]$$

But $z_{21}^0/z_{11}^0 = A_{vo}^0$ is the open-circuit voltage gain of the amplifier 2-port; similarly $z_{21}^1/z_{11}^1 = A_{vo}^1$ is the open-circuit voltage gain of the feedback 2-port. This gives

$$z_{11}^1\,[1 - (A_{vo}^1/A_{vo}^0)] \simeq z_{11}^1$$

as $A_{vo}^0 \gg A_{vo}^1$, the forward open circuit voltage gain of the amplifier 2-port is much greater than that of the feedback 2-port.

In terms of power, the joint significance of these two assumptions is that the feedforward through the feedback 2-port is negligible in comparison with that through the amplifier 2-port.

Furthermore, as $z_{21}/z_{11} = A_{vo}$, the overall amplifier voltage gain, it is seen that

$$E_{z1}^1 \gg E_{z2}^1\,(z_{11}/z_{21})$$

Similarly $\qquad I_{a1}^0 z_{21} \gg E_{z2}^1$

or $\qquad I_{a1}^0 \gg E_{z2}^1\,(1/z_{21})$

To illustrate the magnitudes in question, an example is given of a typical low-noise low-level bipolar transistor whose rounded-off noise sources at the chosen operating point are

$$E_{a1}^0 = 0{\cdot}01\mu\text{V}/\sqrt{\text{Hz}}$$
$$I_{a1}^0 = 1{\cdot}0\text{pA}/\sqrt{\text{Hz}}$$

Typical z-parameters are

$$\begin{bmatrix} 5\text{k}\Omega & 200\Omega \\ 1\text{M}\Omega & 100\text{k}\Omega \end{bmatrix}$$

Assuming the feedback network is a simple emitter resistor R_E of value 100Ω, as shown in Fig. 4(c), the z-parameters of the feedback network are

$$\begin{bmatrix} 100\Omega & 100\Omega \\ 100\Omega & 100\Omega \end{bmatrix}$$

It is obvious that $z_{21}^0 \gg z_{21}^1$, i.e. $1\text{M}\Omega \gg 100\Omega$,

$$A_{vo}^1 = z_{21}^1/z_{11}^1 = 1 \text{ and } A_{vo}^0 = z_{21}^0/z_{11}^0 = \frac{10^6}{5 \times 10^3} = 2 \times 10^2.$$

Hence $A_{vo}^0 \gg A_{vo}^1$, which justifies the second assumption. As will be shown later, for this case,

$$E_{z1}^1 = E_{z2}^1 = \sqrt{(4KTR_E)}/\sqrt{\text{Hz}}$$

$\sqrt{(4KT)} = 1{\cdot}3 \times 10^{-10}$ and $R_E = 10^2$, giving

$$E_{z1}^1 = E_{z2}^1 = 1{\cdot}3 \times 10^{-9}$$

which justifies $\qquad E_{z1}^1 \gg E_{z2}^1\,(z_{11}/z_{21})$

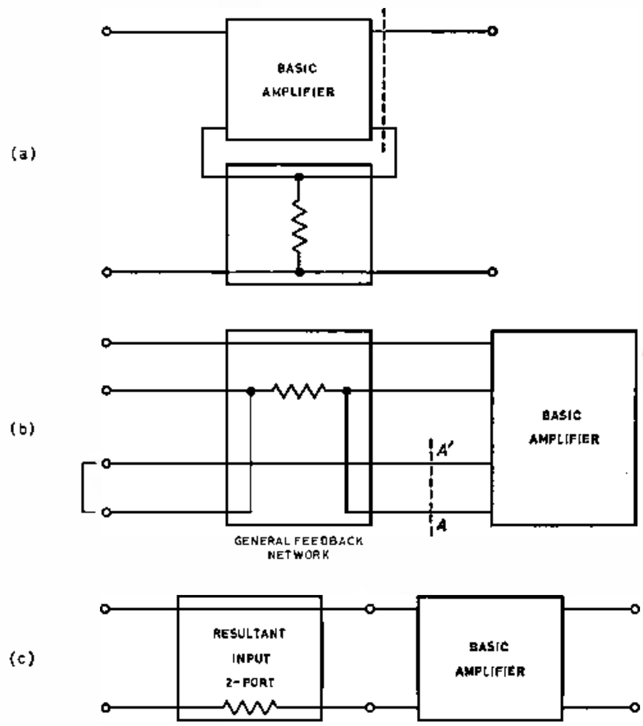

Fig. 4 Reduction of series-series feedback

Finally, $I_{a1}{}^0 z_{21} = 10^{-12} \times 10^6 = 10^{-6}$ which is much greater than $1{\cdot}3 \times 10^{-9}$, the value of $E_{z1}{}^1$.

Applying the above assumptions to equation (5) gives

$$\left.\begin{aligned} E_{a1} &= E_{a1}{}^0 + I_{a1}{}^0 z_{11}{}^1 + E_{z1}{}^1 \\ I_{a1} &= I_{a1}{}^0 \end{aligned}\right\} \quad \cdots\cdots\cdots\cdots (6)$$

The term $I_{a1}{}^0 z_{11}{}^1$ is a 'circuit effect', while $E_{z1}{}^1$ is a 'thermal effect' representing the additional noise introduced by the feedback components. In other words, even if noiseless feedback components could be used, the noise properties would still be effected.

If the feedback network is passive (usually), as in the example, then $E_{z1}{}^1$ is due to the thermal noise of its input impedance: i.e.

$$E_{z1}{}^1 = \sqrt{[4KT\,\mathrm{Re}\,(z_{11}{}^1)]} \text{ per unit bandwidth}$$

where Re = real part
K = Boltzmann's constant
T = absolute temperature

Writing $4KT = \Delta$, equation (6) is then

$$\left.\begin{aligned} E_{a1} &= E_{a1}{}^0 + I_{a1}{}^0 z_{11}{}^1 + \sqrt{[\Delta \mathrm{Re}\,(z_{11}{}^1)]} \\ I_{a1} &= I_{a1}{}^0 \end{aligned}\right\} \quad \cdots\cdots (7)$$

This result is identical to that of placing an impedance of value $z_{11}{}^1$ in series with the original amplifier.

Similarly, the series-shunt combination gives

$$\left.\begin{aligned} E_{a1} &= E_{a1}{}^0 + I_{a1}{}^0 h_{11}{}^1 + \sqrt{[\Delta \mathrm{Re}\,(h_{11}{}^1)]} \\ I_{a1} &= I_{a1}{}^0 \end{aligned}\right\} \quad \cdots\cdots (8)$$

which is equivalent to inserting a series impedance $h_{11}{}^1$. In other words, for noise analysis, any series-series or series-shunt combination which has a passive feedback 2-port reduces approximately to placing a noisy impedance equal to $z_{11}{}^1$ or $h_{11}{}^1$, respectively, in series with the original amplifier.

Call this series impedance Z_s and let its real part be R_s; then equations (7) and (8) may be combined to give

$$\left.\begin{aligned} E_{a1} &= E_{a1}{}^0 + I_{a1}{}^0 Z_s + \sqrt{(\Delta R_s)} \\ I_{a1} &= I_{a1}{}^0 \end{aligned}\right\} \quad \cdots\cdots\cdots\cdots (9)$$

A similar analysis for the shunt-shunt combination gives

$$\begin{aligned} E_{a1} &= E_{a1}{}^0 \\ I_{a1} &= I_{a1}{}^0 + E_{a1}{}^0 y_{11}{}^1 + \sqrt{[\Delta \mathrm{Re}\,(y_{11}{}^1)]} \end{aligned}$$

which is the effect of adding a shunt admitance $y_{11}{}^1$. The shunt-series combination likewise reduces to a shunt admittance $g_{11}{}^1$.

These two sets may be combined into one set of expressions corresponding to equations (8):

$$\left.\begin{aligned} E_{a1} &= E_{a1}{}^0 \\ I_{a1} &= I_{a1}{}^0 + E_{a1}{}^0 Y_p + \sqrt{(\Delta G_p)} \end{aligned}\right\} \quad \cdots\cdots\cdots\cdots (10)$$

where Y_p is the effective shunt conductance: this is $y_{11}{}^1$ in the case of shunt-shunt feedback and $g_{11}{}^1$ in the case of shunt-series feedback.

In many practical circuits, additional components such as biasing resistors need be taken into account, and thus Z_s and Y_p will be resultant values.

To show how to obtain approximately the resultant noise network, without any computation, by applying the assumptions initially, the simple example of series-series feedback used earlier is chosen. This is the emitter resistor shown in Fig. 4(a) redrawn in the form of a general feedback network, as in Fig. 4(b). This can now be reduced to the approximate noise circuit of Fig. 4(c) by

(a) short-circuiting the load

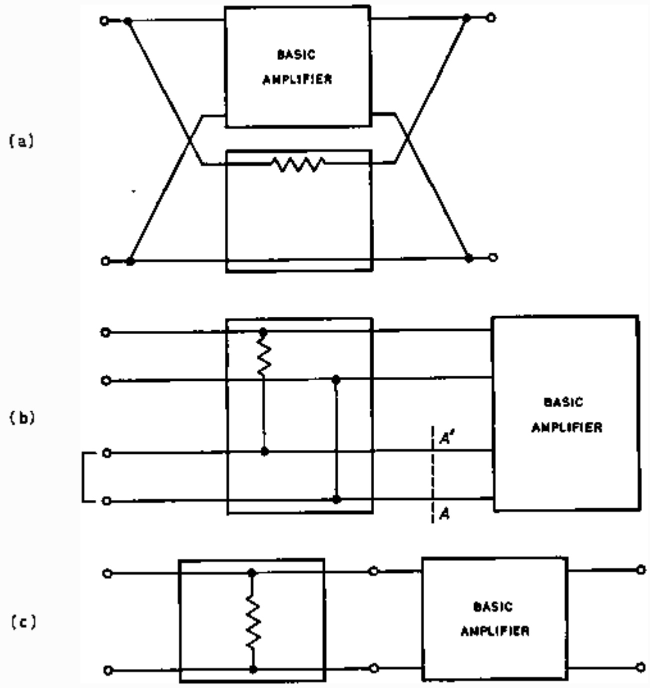

Fig. 5 Reduction of shunt-shunt feedback

(b) open-circuiting the output of the basic amplifier, as shown at AA'.

At first sight, the rearrangement of Fig. 4(b) appears unnecessary, as the same result is obtained by the single operation of open-circuiting at the amplifier output independent of the load termination. Fig. 2(a), being series output feedback, may be similarly reduced.

However, if the shunt-shunt case of Fig. 5 (e.g. a collector-base feedback resistor) is now considered, it is clear that short-circuiting the load is necessary to arrive at the resultant noise 2-port of Fig. 5(c). The reason for this operation should now be clear; namely, to cover a general feedback combination. Short-circuiting the load is always permissible, since noise factor is independent of the load when the noise in the load is neglected. Open-circuiting at AA' is the physical interpretation of the assumptions. This is a simple technique for obtaining the resultant noise network which holds for combinations of Fig. 2. It also holds for combinations of these and it appears that it might be true in general.

The suggestion, then, is that the equivalent noise circuit of a single-loop feedback amplifier is obtained by short-circuiting the load and open-circuiting the basic amplifier output. In general, this results in a noisy 2-port at the amplifier input and its noise properties may be expressed by $E_{a1}{}^1$ and $I_{a1}{}^1$ as shown in Fig. 6.

The basic amplifier noise generators $E_{a1}{}^0$ and $I_{a1}{}^0$ may be transferred to the input by means of the conversion

$$\begin{bmatrix} E_{a1}{}^+ \\ I_{a1}{}^+ \end{bmatrix} = \begin{bmatrix} a_{11} & a_{12} \\ a_{21} & a_{22} \end{bmatrix} \begin{bmatrix} E_{a1}{}^0 \\ I_{a1}{}^0 \end{bmatrix}$$

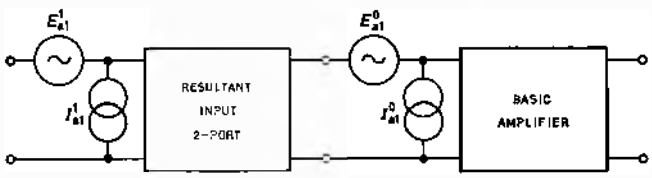

Fig. 6 General reduced-feedback amplifier

Then the resultant E_{a1} is

$$\begin{aligned} E_{a1} &= E_{a1}{}^{+} + E_{a1}{}^{1} \\ &= a_{11}E_{a1}{}^{0} + a_{12}I_{a1}{}^{0} + E_{a1}{}^{1} \\ &= a_{11}E_{a1}{}^{0} + a_{12}I_{a1}{}^{0} + a_{11}E_{g2} \\ &= a_{11}\,[E_{a1}{}^{0} + I_{a1}{}^{0}g_{22} + E_{g2}] \quad \ldots\ldots\ldots\ldots\ (11a) \end{aligned}$$

Similarly $\quad I_{a1} = a_{22}\,[I_{a1}{}^{0} + E_{a1}{}^{0}h_{22} + I_{h2}]$ .... (11b)

where, with reference to the resultant noise 2-port,

$g_{22} = 1/y_{22}$ = output impedance with short-circuit input

$h_{22} = 1/z_{22}$ = output admittance with open-circuit input

$E_{g2} = \surd[\Delta \mathrm{Re}\,(g_{22})]$

$I_{h2} = \surd[\Delta \mathrm{Re}\,(h_{22})]$

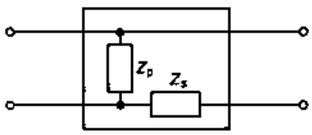

Fig. 7 Usual resultant noise 2-port

Noise factor

The noise factor of any network is the degradation in signal/noise ratio in passing through the device. It can also be regarded as the total mean-square noise voltage at the output to that portion of it due to the thermal noise in the source alone. For a resistive source R_g and using the input noise generators E_{a1} and I_{a1},

$$F = 1 + \frac{\overline{E_{a1}{}^{2}} + \overline{I_{a1}{}^{2}}R_g{}^{2} + 2\gamma\, \overline{E_{a1}I_{a1}}R_g}{\Delta R_g} \quad \ldots\ldots\ (12)$$

where γ is the real part of the correlation coefficient and $\Delta = 4KT$. The optimum source resistance R_{go} is obtained by differentiating F with respect to R_g and setting to zero, giving

$$R_{go}{}^{2} = \overline{E_{a1}{}^{2}}/\overline{I_{a1}{}^{2}} \quad \ldots\ldots\ldots\ldots\ldots\ldots\ (13)$$

Thus optimum source resistance is independent of correlation when using a resistive source. Substituting for R_g in equation (12) gives the expression for the optimum noise factor F_o as

$$F_o = 1 + \frac{2E_{a1}I_{a1}\,(1+\gamma)}{\Delta}$$

Noise factor of feedback amplifier

To find the noise factor of a feedback amplifier $\overline{E_{a1}{}^{2}}$, $\overline{I_{a1}{}^{2}}$ and γ are replaced by their appropriate gross values. For instance, in the series examples, squaring equation (9) gives

$$\left.\begin{aligned} \overline{E_{a1}{}^{2}} &= \overline{(E_{a1}{}^{0})^{2}} + \overline{(I_{a1}{}^{0})^{2}}\,Z_s{}^{2} + 2\gamma^{0}E_{a1}{}^{0}I_{1a}{}^{0}Z_s + \Delta R_s \\ \overline{I_{a1}{}^{2}} &= \overline{(I_{a1}{}^{0})^{2}} \end{aligned}\right\} \ldots\ldots\ (14)$$

For two correlated sources, such as E_{a1} and I_{a1}, the normalized correlation coefficient is[6]

$$\gamma = \frac{\overline{E_{a1}I_{a1}{}^{*}}}{\surd(\overline{E_{a1}{}^{2}}\,\overline{I_{a1}{}^{2}})} \quad \ldots\ldots\ldots\ldots\ldots\ (15)$$

where the asterisk denotes a conjugate.

Inserting the values of E_{a1} and I_{a1} from equation (9) gives

$$\begin{aligned} \gamma &= \frac{\overline{[E_{a1}{}^{0} + I_{a1}{}^{0}Z_s + \surd(\Delta R_s)]\,(I_{a1}{}^{0})^{*}}}{\surd(\overline{E_{a1}{}^{2}}\,\overline{I_{a1}{}^{2}})} \\ &= \frac{\overline{E_{a1}{}^{0}I_{a1}{}^{0*}} + \overline{(I_{a1}{}^{0})^{2}}\,Z_s}{\surd(\overline{E_{a1}{}^{2}}\,\overline{I_{a1}{}^{2}})} \\ &= \frac{\gamma^{0}\,\surd[\overline{(E_{a1}{}^{0})^{2}}\,\overline{(I_{a1}{}^{0})^{2}}] + \overline{(I_{a1}{}^{0})^{2}}Z_s}{\surd(\overline{E_{a1}{}^{2}}\,\overline{I_{a1}{}^{2}})} \end{aligned}$$

Then the last term in equation (12) is

$$2\gamma\, \overline{E_{a1}I_{a1}}R_g = 2\gamma^{0}E_{a1}{}^{0}I_{a1}{}^{0}R_g + 2\overline{(I_{a1}{}^{0})^{2}}\,Z_sR_g \quad \ldots\ (16)$$

Inserting equations (16) and (14) into equation (12) and rearranging gives

$$F_s{}^{1} = 1 + R_s/R_g + \frac{\overline{(E_{a1}{}^{0})^{2}} + \overline{(I_{a1}{}^{0})^{2}}\,R_g{}^{2}\,(1+Z_s/R_g)^{2} + 2\gamma^{0}E_{a1}{}^{0}I_{a1}{}^{0}R_g\,[1+Z_s/R_g]}{\Delta R_g} \quad \ldots\ldots\ldots\ (17)$$

Equation (17) is thus the noise-factor expression for any simple series-series or series-shunt feedback network, where Z_s is the resultant series impedance and R_s is its real part. This is, for example, the expression for an amplifier with a simple emitter resistor R_s, as in Fig. 4(a).

It is apparent that the ratio Z_s/R_g is critical. If only low-noise amplifiers are considered, specifying that the degradation due to feedback is small, then it is necessary to keep $Z_s/R_g \ll 1$; i.e. the series impedance must be much less than the source resistance. For the shunt feedback combinations reducing to a shunt admittance Y_p, the expression for noise factor is

$$F_p{}^{1} = 1 + R_g/R_p + \frac{\overline{(E_{a1}{}^{0})^{2}}\,(1+R_g/Z_p)^{2} + \overline{(I_{a1}{}^{0})^{2}}\,R_g{}^{2} + 2\gamma^{0}E_{a1}{}^{0}I_{a1}{}^{0}\,[1+R_g/Z_p]}{\Delta R_g} \quad \ldots\ldots\ldots\ (18)$$

where the critical condition is now that R_g/Z_p be $\ll 1$; i.e. the shunt impedance must be much greater than the source resistance. Equation (17) is the expression for a single-stage transistor amplifier with a collector-base feedback impedance Z_p.

The overall conclusion from equation (17) and (18) is that the effective series impedance or the effective shunt admittance is much less than the source impedance or admittance, respectively.

Combined feedback

The case of combined feedback is now considered: Fig. 6 is the combination of simple series-series and shunt-shunt. However, an examination of other combinations reveals that many circuits reduce to an approximate effective series and shunt impedance, as in Fig. 7. Thus Fig. 7 represents a frequently encountered equivalent noise circuit:

$$\begin{aligned} a_{11} &= 1 & a_{22} &= 1 + Z_s/Z_p \\ g_{12} &= Z_s & E_{g2} &= \surd(\Delta R_s) \\ h_{22} &= 1/(Z_s + Z_p) & I_{h2} &= \surd[\Delta\ 1/(Z_s + Z_p)] \\ &= \frac{1/Z_p}{1 + Z_s/Z_p} & &= \sqrt{\left(\Delta\,\frac{1/Z_s}{1 + Z_s/Z_p}\right)} \end{aligned}$$

But, from the previous conclusions that $Z_s \ll R_g \ll Z_p$, it follows that $Z_s/Z_p \ll 1$.

Then $h_{22} = 1/Z_p$ and $I_{h2} = \surd(\Delta G_p)$

giving

$$\left.\begin{aligned} E_{a1} &= E_{a1}{}^{0} + I_{a1}{}^{0}Z_s + \surd(\Delta R_s) \\ I_{a1} &= I_{a1}{}^{0} + E_{a1}{}^{0}Y_p + \surd(\Delta G_p) \end{aligned}\right\} \ldots\ldots\ldots\ (19)$$

By inserting equations (19) into equation (15), γ can now be calculated. Inserting the results of this together with equations (19), into equation (12) gives, after some rearranging,

$$\begin{aligned} F^{1} = 1 + R_s/R_g + R_g/R_t &+ \frac{\overline{(E_{a1}{}^{0})^{2}}\,(1 + R_g/Z_p)^{2} + \overline{(I_{a1}{}^{0})^{2}}\,R_g{}^{2}\,(1 + Z_s/R_g)^{2}}{\Delta R_g} \\ &+ \frac{2\gamma^{0}\,E_{a1}{}^{0}I_{a1}{}^{0}\,[1 + R_g/Z_p]\,[1 + Z_s/R_g]}{\Delta R_g} \quad \ldots\ldots\ (20) \end{aligned}$$

This is a superposition of equations (17) and (18). As stated earlier, many systems reduce to an approximate effective series and shunt impedance, and equation (20) is widely applicable.

Equations (17), (18) and (20) may also be obtained by regarding the network as a cascade, in the manner of Fig. 5, and using the expression for cascaded noise factors[7]

$$F = F_1 + \frac{F_2 - 1}{G_1} + \frac{F_3 - 1}{G_1 G_2} + \ldots \quad (21)$$

Optimum source

Expressions (17), (18) and (20) have corresponding values for optimum source resistance. Taking the series combination of equation (17) and differentiating in the usual manner yields an optimum $R_{go}{}^1$ given by

$$(R_{go}{}^1)^2 = R_{go}{}^2 [1 + R_s\Delta/(E_{a1}{}^0)^2 + 2\gamma^0 Z_s/R_{go} + (Z_s/R_{go})^2]$$

$(Z_s/R_{go})^2 \ll 1$ and if $2\gamma^0 Z_s/R_{go} \ll 1$ then, letting $(E_{a1}{}^0)^2/\Delta = R_N{}^0$, this reduces to

$$R_{go}{}^1 = R_{go} \sqrt{(1 + R_s/R_N{}^0)} \quad (22)$$

Similarly, the shunt combination is

$$R_{go}{}^1 = R_{go}/\sqrt{(1 + G_p/G_N{}^0)} \quad (23)$$

where $G_N{}^0 = (I_{a1}{}^0)^2/\Delta$

Thus feedback which is in series at the input increases the optimum source resistance while that in shunt decreases it.

For the combination in Fig. 6, the optimum source resistance is given by

$$R_{go}{}^1 = R_{go} \sqrt{\frac{1 + R_s/R_N{}^0}{1 + G_p/G_N{}^0}} \quad (24)$$

Degradation of noise factor

For the series example equation (17) gives the expression for F^1 for any R_g. The corresponding expression without feedback is

$$F = 1 + \frac{\overline{(E_{a1}{}^0)^2} + \overline{(I_{a1}{}^0)^2} R_g{}^2 + 2\gamma^0 E_{a1}{}^0 I_{a1}{}^0 R_g}{\Delta R_g} \quad (25)$$

It would be instructive to have an expression relating F^1 and F. This is a convenient way to assess the degradation due to feedback for any fixed value of R_g, and furthermore the expression can be modified to special conditions, e.g. the old optimum in terms of the new.

For simplicity it will be assumed that the noise 2-port is purely resistive. Then subtracting equations (25) from (17) gives

$$F^1 - F = R_s/R_g [1 + 2\sqrt{(R_N{}^0/G_N{}^0)} \{R_g/R_{go} + \gamma^0\}] \quad (26)$$

This is the actual degradation due to feedback for any fixed R_g.

If $R_g = R_{go}$ then it is easily seen that equation (26) simplifies to

$$F^1 = F_o (1 + R_s/R_{go}) \quad (27)$$

Let $R_g = R_{go}{}^1 = R_{go} \sqrt{(1 + R_s/R_N{}^0)}$;

If $R_s/R_N{}^0 \ll 1$

then $\sqrt{(1 + R_s/R_N{}^0)} \simeq 1 + 1/2\,(R_s/R_N{}^0)$

Inserting this into equation (26) and neglecting R_s/R_{go} relative to F_o gives new optimum noise factor in terms of the old:

$$F_o{}^1 = F_o [1 + R_s/R_{go} (1 - 1/2\ R_s/R_N{}^0)] \quad (28)$$

As $R_s/R_N{}^0$ is much less than unity for low-noise systems, it may be said that, to a first approximation,

$$R_{go}{}^1 = R_{go}$$

This means that equations (27) and (28) now reduce to

$$F_o{}^1 = F_o (1 + R_s/R_{go}) \quad (29)$$

So the minimum degradation due to a feedback resistor R_s is

$$\Delta F = F_o\, R_s/R_{go} \quad (30)$$

Similarly, for the shunt combination,

$$\Delta F = F_o\, R_{go}/R_p \quad (31)$$

and for the combination

$$\Delta F = F_o (R_s/R_{go} + R_{go}/R_p) \quad (32)$$

For feedback combinations which do not simplify to that of Fig. 6, and when a_{11} and a_{22} are not equal to unity, the expressions for $R_{go}{}^1$ and ΔF are more complex:

$$R_{go}{}^1 = R_{go} \sqrt{\frac{1 + g_{22}/R_N{}^0}{1 + h_{22}/G_N{}^0}} \quad (a_{11}/a_{22}) \quad (33)$$

$$\Delta F = F_o (g_{22}/R_{go} + R_{go}/h_{22}) (a_{11}a_{22}) + (F_o - 1) \{(a_{11}a_{22}) - 1\} \quad (34)$$

Conclusion

The results derived here are based on one main assumption,namely that the feedforward through the feedback network may be neglected in comparison with that through the amplifier. This assumption is usually justified in practise. From the expressions, it is obvious that feedback *per se* does not alter the noise figure. However, the magnitudes of the feedback components will alter noise performance because of their circuit effect at the amplifier input; an example of this is the term $I_{a1}{}^0 z_{11}{}^1$ in the expression for E_{a1} in equation (6). In addition, resistive elements introduce further corresponding noise sources, expressed by $E_{z1}{}^1$ in equation (6). Both these effects will degrade the amplifier noise performance.

For the approximate analysis of this noise performance the feedback amplifier reduces to the basic amplifier preceded by an equivalent noise 2-port, as in Fig. 7. It has been shown how this network is obtained. For the four simple combinations in Fig. 2, which were described in detail, the noise 2-port is a simple series or shunt impedance. For more complex feedback combinations, an approach is suggested whereby single-loop feedback combinations may be quickly and easily reduced to their equivalent noise 2-ports. Having obtained the equivalent noise 2-port, the noise factor expression is then obtained. Further expressions show the degradation due to feedback and the alteration in optimum source resistance. Amplifiers may be designed with negligible noise-factor degradation due to feedback if the effective series impedance is much less than the optimum source resistance and the effective shunt impedance is much longer than the optimum source resistance. This requirement is not usually incompatible with other design demands. If the amplifier is multistage, then the cascade formula due to Friis may be used. If it is multiloop, then it may be analysed in stages by starting at the innermost loop and working outwards.

Acknowledgements

The author thanks the Principle and governing body of Woolwich Polytechnic for permission to publish, and K. B. Reed for his assistance and encouragement during its preparation.

REFERENCES

1 Becking, A. G. T., *et al.*: The noise factor of four-terminal networks, *Philips Res. Rep. 10 (Oct. 1955).*
2 Rothe, H., and Dahlke, W.: Theory of noisy fourpoles, *Proc. Inst. Radio Engrs. 44 (June 1956).*
3 Bogner, R. E: *Electronic Engng. 37,* 115 (Feb. 1965).
4 Feifel, B.: *A.E.U. 20,* 12 (1966).
5 Vasseur, J. P.: *Properties and applications of transistors.* (Pergamon, 1964).
6 Van der Ziel, A.: *Noise* (Prentice-Hall, 1954).
7 Friis, H. T.: Noise figure of radio receivers, *Proc. Inst. Radio Engrs. 42,* (July 1944).

X-band omnidirectional double-slot array antenna

by **T. Takeshima**, Ph.D.(Eng.), *Kobe Industries Corporation, Akashi, Japan*

The article describes an omnidirectional slotted array composed of a relatively thin X-band rectangular waveguide with pairs of longitudinal shunt slots placed opposite each other on the broad faces of the waveguide (this is simply referred to as a double-slot antenna). Measurements show that, for a slotted waveguide 1 × 0·126in outside dimensions, the azimuth radiation pattern is circular within 1dB (measured frequency: 9375MHz). Furthermore, comparisons with circular waveguide or coaxial-type slot antennas, practical design methods for slot conductance and the power-handling capacity of the double-slot antenna are discussed.

(Voir page 664 pour le résumé en français: Zusammenfassung in deutscher Sprache auf Seite 665)

In general, horizontally polarized antennas with an omni-directional azimuth pattern in the microwave region, such as circular-waveguide- or coaxial-type slotted-array antennas, are studied in u.h.f. television relaying or as radar-beacon antennas. But normal circular slotted-array antennas give rise to practical design difficulties as follows.

Circular waveguide

The most important factor is that the line must carry a radially symmetrical mode, so that the slots are excited equally. This condition is fulfilled by a circular waveguide propagating the TM_{01} mode. However, for this case, a slot cut parallel to the guide axis does not radiate. It is therefore necessary to excite the slots by means of probes; and, to ensure symmetrical excitation, the probe depth must be uniform. The theoretical design of the distance between the slots, the diameter and the depth of the probes is very difficult. Furthermore, the adjustment of matching screws between each bay of slots for increasing bandwidth is more complex.

A second factor is that the minimum number of slots required to produce a pattern having a satisfactory azimuth circularity is found to depend on the size of the line: the larger the guide diameter, the greater the number of elements. For a 1¼in circular waveguide operating in the X-band, the minimum is seven[1].

A third factor is that, in the construction of this antenna, it is necessary to construct a TE_{10}-to-TM_{01}-mode converter, a mode filter for TE_{11} mode, absorber, and so on. Accordingly, the structure is very complex.

Coaxial line

In this type, it is necessary to excite the slots by means of probes, as with the circular-waveguide type; but, in this case, there are branching feeder systems to excite the slots[2]. However, the theoretical designs for both methods are complex and difficult.

Instead of the usual cylindrical-slot antenna, it is necessary to produce a small lightweight simple-structure low-cost omnidirectional slot array for simple radar-beacon antennas. In this article, circularity-forming processes in a double-slot array antenna (experimental findings), a comparison between a double-slot antenna and a cylindrical-slot antenna, and some problems in practical design of rectangular-waveguide double-slot-array antennas are discussed. This double-slot antenna is an omnidirectional slotted array composed of longitudinal shunt slots placed opposite each other on the broad faces of the waveguide. In conclusion, the experimental results show excellent radiation patterns (circularity within 1dB) and complete practicability for this antenna.

Circularity-forming process (experimental findings)

Consider three slots *A*, *B* and *C* on the broad faces of a rectangular waveguide, as shown in Fig. 1. In this case, the pair of slots *A* and *B* are in phase, and the pair of slots *B* and *C* are out of phase. The radiation pattern of the *B* and *C* slot pair is therefore not omnidirectional. Accordingly, the *A* and *B* slot pair is prepared in order to obtain an omnidirectional radiation pattern. There are two methods of obtaining circularity by means of a rectangular-waveguide double-slot antenna. The first method is by means of a large groundplane, as shown in Fig. 2(a). This method is based on the concept that the ideal radiation pattern of the slot on an infinite metallic plane is semicircular. Actually, circularity within about 6dB has been obtained by applying a groundplane of three wavelengths[3]. The second method is by means of relatively thin rectangular waveguide, as shown in Fig. 2(b). This depends on the concept that the ideal radiation pattern of the slot on an infinitely thin metallic plane is circular.

Both of the above methods are confirmed experimentally. Radiation patterns were measured for double-slot antennas having various combinations of narrow-

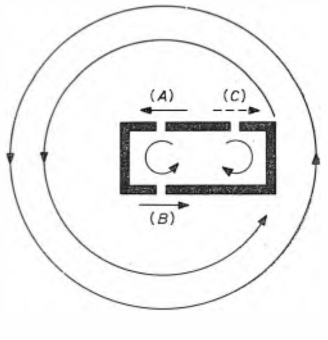

Fig. 1 Radiation mechanism of double-slot antenna

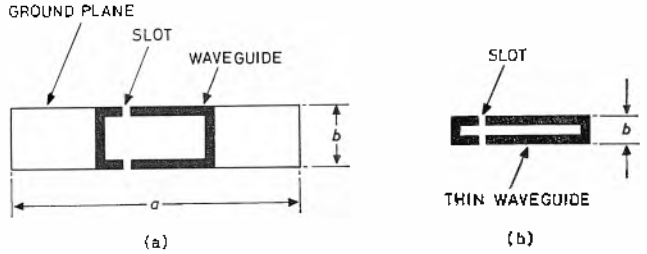

Fig. 2 Construction of slot

wall widths of rectangular waveguide and lengths of ground-plane, as shown in Fig. 3 and Table 1, and experimental results were obtained for circularity-forming processes, as shown in Fig. 4 and Table 2. From these experimental results, it is found that the double-slot antenna with a narrow-wall width of 0·1 wavelength has an excellent circularity without a groundplane, as shown in Fig. 4(j).

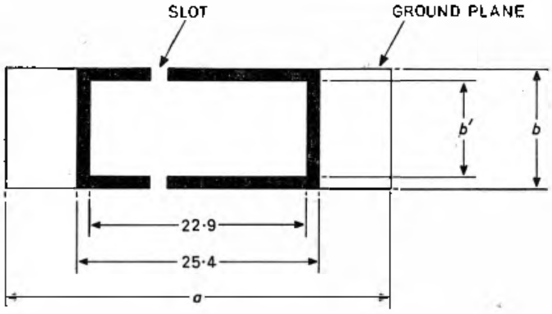

Fig. 3 Dimensions of samples

TABLE 1
Classification of samples

SAMPLES	b', mm	b, mm	b/λ
A	10·2	12·7	0·3969
B	3·8	6·35	0·1988
C	2·2	3·2	0·1

TABLE 2
Circularity of double-slot antennas

SAMPLES	a/λ	b/λ	CIRCULARITY, dB	ILLUSTRATION
A	0·794	0·3969	8·2	Fig. 4(a)
A	1·5	0·3969	7·0	Fig. 4(b)
A	2·0	0·3969	6·0	Fig. 4(c)
A	3·0	0·3969	5·7	Fig. 4(d)
B	0·794	0·1988	3·8	Fig. 4(e)
B	1·5	0·1988	3·6	Fig. 4(f)
B	2·0	0·1988	3·4	Fig. 4(g)
B	3·0	0·1988	3·4	Fig. 4(h)
C	0·794	0·1	1·0	Fig. 4(i)
C	3·0	0·1	1·0	Fig. 4(j)

Comparison between double-slot and cylindrical-slot antennas

A slot-feeding structure for cylindrical-slot antennas is complex, as indicated above; but it has been shown by Sinclair[4] that the radiation pattern of a cylindrical-slot antenna can be obtained theoretically and experimentally. Consider the situation where two slots are used, with slot 1 located at $\phi = 0°$, and slot 2 at $\phi = \phi_2$, as shown in Fig. 5. The field radiated by slot 1 is given by

$$E_{\phi 1} = A/j\pi\,(a_0 + \sum_{n=1}^{\infty} a_n \cos n\phi) \quad \ldots\ldots\ldots\ldots (1)$$

Assume that slot 2 is fed in such a way that the field it produces is given by

$$E_{\phi 2} = MA/j\pi\,[a_0 + \sum_{n=1}^{\infty} a_n \cos n\,(\phi_2 - \phi]\,e^{j\psi} \quad \ldots\ldots (2)$$

Fig. 4 Horizontal pattern of a double-slot antenna

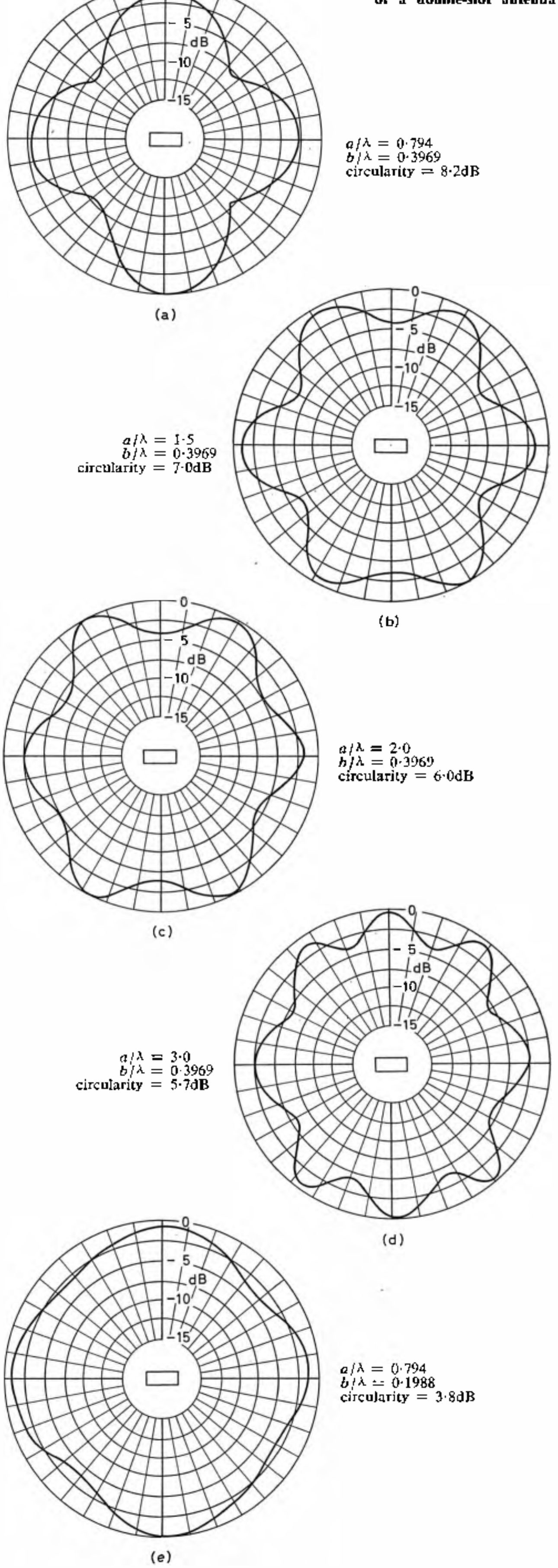

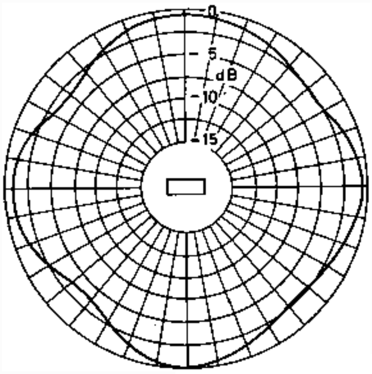

$a/\lambda = 1{\cdot}5$
$b/\lambda = 0{\cdot}1988$
circularity = 3·6dB

(f)

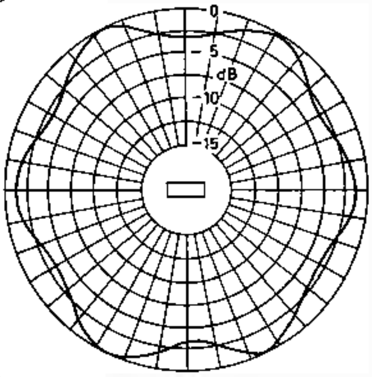

$a/\lambda = 2{\cdot}0$
$b/\lambda = 0{\cdot}1988$
circularity = 3·4dB

(g)

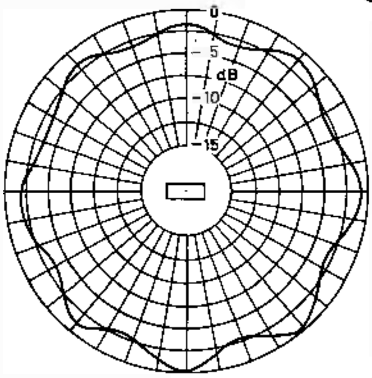

$a/\lambda = 3{\cdot}0$
$b/\lambda = 0{\cdot}1988$
circularity = 3·4dB

(h)

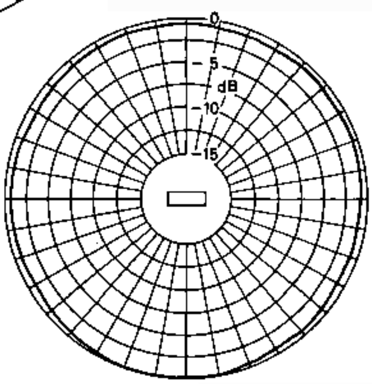

$a/\lambda = 0{\cdot}794$
$b/\lambda = 0{\cdot}1$
circularity = 1·0dB

(i)

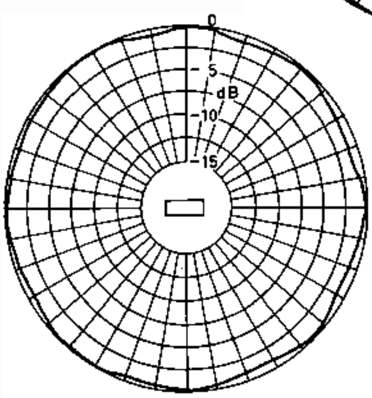

$a/\lambda = 3{\cdot}0$
$b/\lambda = 0{\cdot}1$
circularity = 1·0dB

(j)

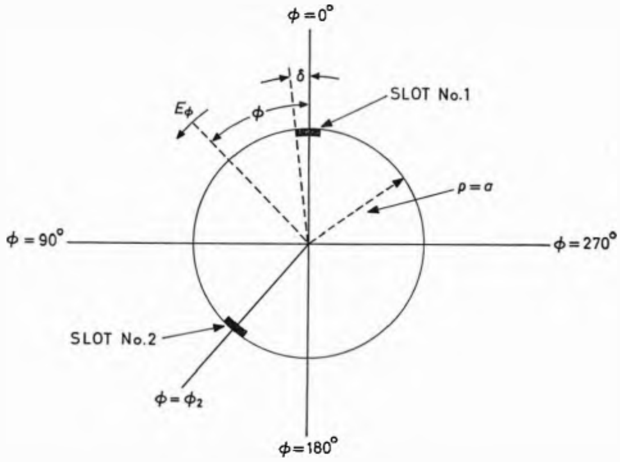

Fig. 5 Diagram showing the co-ordinate system

where
$$a_0 = \frac{1}{2H_0^{(2)\prime}(ka)}$$
$$a_n = \frac{j^n}{H_0^{(2)\prime}(ka)}$$
$$ka = \frac{2\pi a}{\lambda}$$

A is the relative exciting amplitude, M is the ratio of the amplitude of the field radiated in a given direction by slot 2 to the amplitude radiated by slot 1 in a similar direction, and Ψ is the time phase difference between these fields. The field produced by the array of the two slots is the sum of the fields in equations (1) and (2).

In Fig. 6, the circularity of the cylindrical double-slot-array antenna, assuming $M = 1$, $\Psi = 0$ and $\phi_2 = 180°$, has been calculated from equations (1) and (2) as a function of cylinder diameter D, for comparison with the corresponding measured circularity for a rectangular-waveguide double-slot antenna without a groundplane. It appears that the measured circularity of the double-slot antenna coincides with the calculated circularity of the cylindrical 2-slot-array antenna when the cylinder diameter D and the narrow-wall width b are normalized

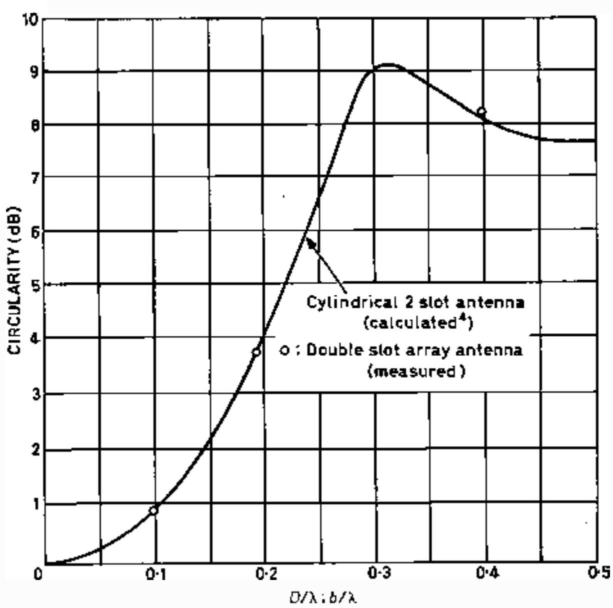

Fig. 6 Comparison of circularity

to wavelength λ, in order to make a comparison between each circularity.

But, in X-band, it is impossible to make the cylindrical antenna with a diameter less than 0·1 wavelength, because of a design problem in transmission lines. However, it is very easy to obtain the condition $b/\lambda = 0{\cdot}1$ in rectangular waveguide. From this point of view, the double-slot antenna is therefore superior.

Problems in practical design

Vertical patterns

It is very easy to design a slot-conductance distribution in order to obtain a specified vertical pattern by means of simple linear-array theory. In this article, the measurements are carried out by a uniform and resonant array for the sake of simplification, and experimental results for the vertical pattern are shown in Fig. 7.

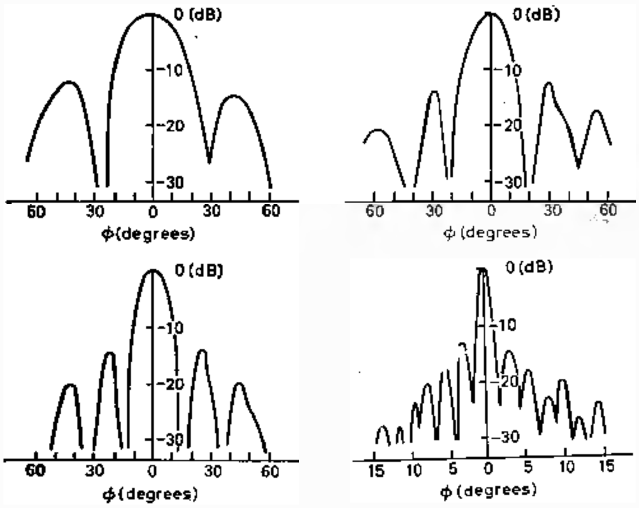

Fig. 7 Vertical pattern of double-slot-array antennas
top left: 3 stack, beamwidth = 24·3°
top right: 4 stack, beamwidth = 18·6°
bottom left: 5 stack, beamwidth = 14·3°
bottom right: 37 stack, beamwidth = 2·1°

Slot conductance and input impedance

A calculation equation of the slot conductance for the longitudinal shunt slot is given as follows:

$$g = g_1 \sin^2(\pi x/a) \quad \ldots\ldots\ldots\ldots\ldots\ldots \quad (3)$$
$$g_1 = 2{\cdot}09\ \lambda_g/\lambda\,(a/b)\cos^2 \pi\lambda/\lambda_g$$

where g = slot conductance

x = slot displacement from the centre line of the rectangular waveguide

λ_g = guide wavelength

a = broad-face width of waveguide

b = narrow-face width of waveguide

Accordingly, the slot conductance of the thin rectangular waveguide increases with a decrease in the narrow-wall width b. Furthermore, the experimental results confirm that the internal mutual coupling between the slots of the two sides is negligible. For instance, the input impedance of a 4-stack double-slot-array antenna is shown in Fig. 8. The bandwidth of this array is relatively narrow because of the resonant design, but it can be broadened by using a nonresonant array.

Power-handling capacity

In general, the fundamental equation of the power-handling capacity for rectangular waveguide is given as follows[5]:

$$P = E_{max}^2\, 6{\cdot}63 \times 10^{-4}\, ab\ \lambda/\lambda_g$$

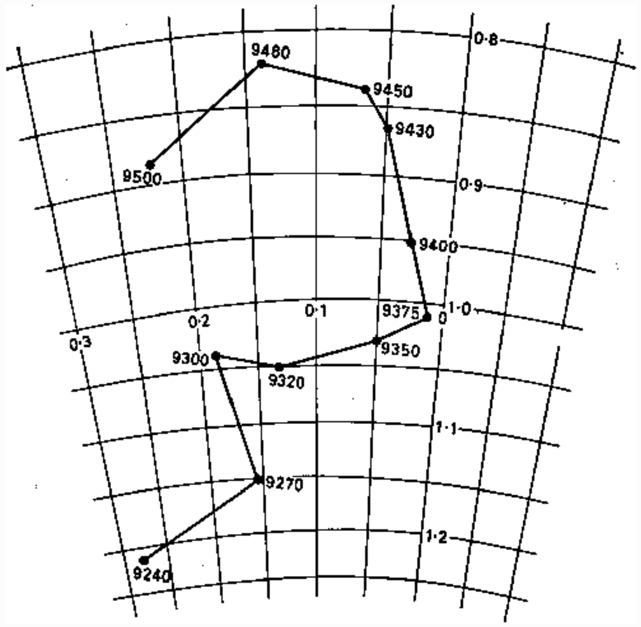

Fig. 8 Input impedance of 4-stack double-slot-array antennas

where P is in watts, E_{max} is in volts/centimetre, a and b are in centimetres. Assuming that $E_{max} = 15\,000V$/cm, $\lambda = 3{\cdot}2$, $\lambda_g = 4{\cdot}47$, $a = 2{\cdot}29$cm, $b = 0{\cdot}22$cm, then P is calculated as approximately 53kW. Also, with a reduction factor[5] of 0·2, power-handling capacity is estimated as $P \simeq 10$kW. Accordingly, the above conclusions confirm that the double-slot-array antenna may be used not only as a receiver antenna but also as a small power-transmitting antenna.

Beam tilt in the vertical plane

In circular-waveguide slot-array antennas, the beam tilt from the array normal is obtained by a groundplane. But, in this double-slot array antenna, it is very easy to obtain the required beam tilt by means of the nonresonant method or Rutz's method[6], in which the length of the slot is variable.

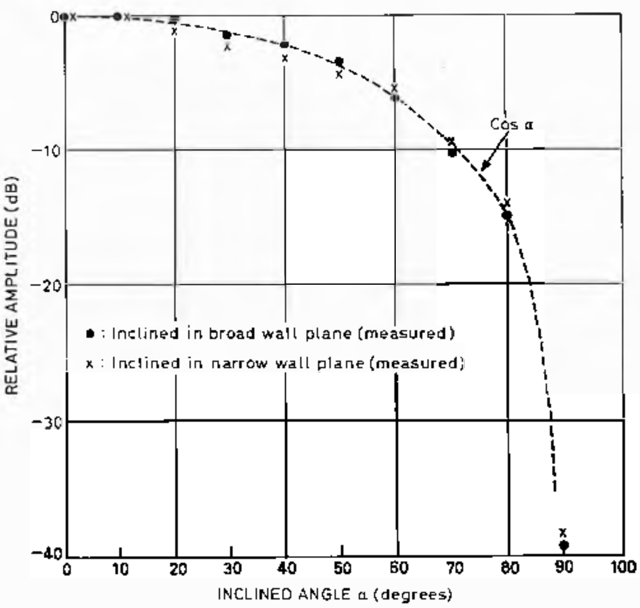

Fig. 9 Polarization character of double-slot-array antennas

POLARIZATION CHARACTER

The horizontal and vertical patterns have been discussed previously. When the antenna is used as a transponder antenna in a secondary radar system, the polarization character is very important. The experimental polarization character as a function of the angle of inclination of the array axis from perpendicular are shown in Fig. 9.

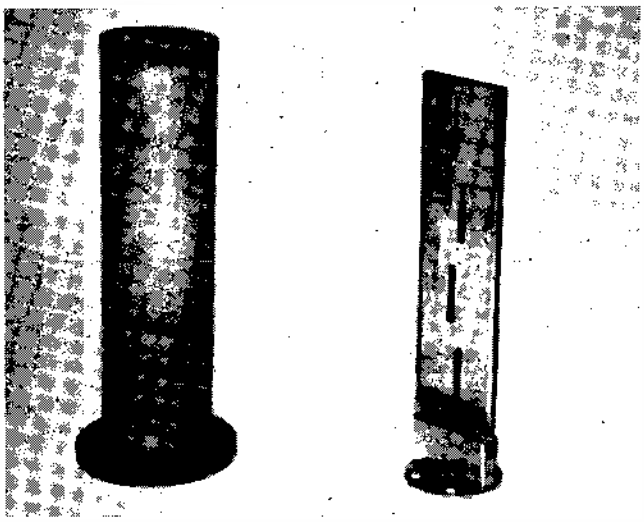

Fig. 10 Outline of double-slot-array antennas

OUTLINE

As an example, an outline of a 4-stack double-slot-array antenna is shown in Fig. 10; this is a cylindrical glass-base-polyester radome, highly resistant to erosion from rain, and which has virtually no effect on the antenna pattern.

Conclusion

Horizontally polarized antennas with an omnidirectional azimuth pattern in *X*-band can be obtained by using the double-slot array; and this double-slot array has many superior characteristics:

(i) It is small and lightweight in comparison with conventional cylindrical-slot antennas.
(ii) Only two slots per bay are required.
(iii) Only an impedance transformer is needed to convert to feed line, and no filter absorber etc. are required.
(iv) Exciting probes are not necessary.
(v) It has a flexibility in design of the vertical pattern.
(vi) It is possible to use as a small-power beacon-transmitter antenna.

Further investigation of the double slot array antenna is therefore worthwhile.

Acknowledgment

The author wishes to thank Prof. T. Makimoto of Osaka University, as well as S. Nishitake and S. Matsuda, for their guidance and encouragement during the course of this work, and Y. Isogai for his assistance with the measurements.

REFERENCES

1 SILVER, S.: *Microwave antenna theory and design*. McGraw-Hill (1949)
2 EPSTEIN, J., *et al.*: Some types of omnidirectional high-gain antenna for use at ultra-high frequencies, *RCA Rev.*, *13*, 137-162 (June 1952)
3 STEGEN, R. J.: UHF TV radiators using slot arrays, *Electronics*, 152-155 (July 1953)
4 SINCLAIR, G.: The patterns of slotted-cylinder antennas, *Proc. Inst. Radio Engrs*, *36*, 1487-1492 (Dec. 1948)
5 RIDENOUR, L. N.: *Microwave transmission circuits*. McGraw-Hill (1948)
6 RUTZ, E. M.: Resonant antenna array with tilted beam, *IRE Trans.*, *AP-8*, 435-436 (July 1960)

Timers using unijunction transistors

by **J. F. Young**, C.G.I.A., M.I.E.E., A.M.I.E.R.E., *The University of Aston in Birmingham*

The unijunction transistor has potential advantages for use in industrial timer circuits, but various difficulties are encountered. Two possible circuits are described: the first gives a train of pulses after an initial delay but cannot give enough output power for direct use with an electromechanical relay; the second incorporates diodes to isolate the CR timing arrangement from the relay, both being in the emitter circuit. Delay time is almost independent of both supply-voltage and ambient-temperature variations.

(Voir page 664 pour le résumé en français: Zusammenfassung in deutscher Sprache auf Seite 666)

THE construction of the unijunction transistor is basically so simple that one would expect the cost to be quite low; however, this is not the case in practice. One probable reason for this is that limited application of these devices has kept the number produced relatively low. One field of application has been as a firing arrangement for thyristors, although other devices are often used. As part of a timing circuit, the unijunction transistor has potential advantages over other devices; even here the application has been limited by difficulties.

The potential advantages of the unijunction transistor in timing circuits can be seen by reference to the relaxation oscillator in Fig. 1. Capacitor *C* charges *via* resistor *R* until the emitter diode conducts; current then flows into the emitter, introducing carriers into the lower region (E to B_1) of the unijunction transistor, and so reducing the resistivity of this region. Since the resistivity of the upper region (B_2 to E) is not changed, the voltage at the emitter tends to fall, thus increasing further the current

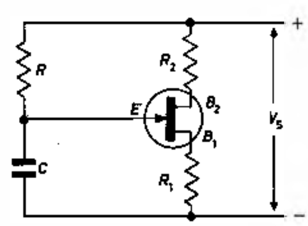

Fig. 1 Unijunction-transistor relaxation oscillator

flowing from the capacitor into the emitter. The action is cumulative, and the capacitor is discharged to a low voltage. Provided that the emitter resistor R has a high enough value, there is insufficient emitter current to maintain the conductivity of the lower section (E to B_1); so the emitter voltage rises and the emitter diode becomes reverse biased once more, while C recharges *via* R and the cycle repeats.

The cycle time depends mainly on the time taken by C to charge *via* R to a sufficiently high voltage to fire the unijunction transistor. The time depends on the supply voltage V_s, on C and R, and on the required emitter-firing voltage V_e. The latter depends on the 'stand-off ratio' k, the supply voltage V_s and the forward drop V_f of the internal emitter diode:

$$V_e = kV_s + V_f$$

The forward voltage V_f is temperature dependent; fortunately, so is the interbase resistance R_{bb} measured between the ohmic contacts B_1 and B_2. Because of this, R_2 can be selected to have such a value that the changes in the interbase resistance counteracts that due to the change in diode forward drop. A typical value for R_2 suggested by manufacturers is 400Ω although, with the lower-cost unijunction transistors, it has been found that the smallest variation of time with temperature is obtained if R_2 is zero. With any particular type of transistor, a suitable value for R_2 should preferably be chosen experimentally from tests on a large number of devices. Provided that the forward drop is temperature-compensated, the firing-point emitter voltage can be approximated as

$$V_a = kV_s$$

The voltage V_e applied to the emitter is equal to the capacitor voltage, and, since C charges *via* R towards the supply voltage V_s,

$$V_e = V_s\,[1 - \exp(-t/CR)]$$

where t is the time from the commencement of charging. Thus the unijunction transistor fires when

$$V_e = kV_s = V_s\,[1 - \exp(-t/CR)]$$

or

$$k = 1 - \exp(-t/CR)$$

The time is therefore

$$t = CR/(1-k)$$

assuming that the capacitor is initially completely discharged.

Thus it is not difficult to make the time independent of both supply voltage and temperature. This is advantageous compared with some other devices used in timers[1,2,3]. However, there are practical difficulties encountered with the unijunction transistor which will be seen best by considering a well known unijunction-transistor timer circuit. This circuit, shown in Fig. 2, is sometimes suggested by manufacturers of unijunction transistors. When the unijunction transistor fires, the discharge current from the large capacitor C flows *via* the emitter and base 1 into the 150Ω relay. This causes the relay to operate its changeover contacts, and it is then retained by the current flowing through R_1 for as long as the switch S is closed. Additional contacts on the relay are used to operate external circuits.

There are two basic difficulties with the arrangement of Fig. 2. First, a relatively large C is required, and inevitably an electrolytic unit must be used in order to obtain long times and store sufficient energy to operate the relay. This immediately rules out the circuit for many applications, since, although electrolytic capacitors are now much more reliable than previously, they deform if inactive. Consequently, in any applications where the device might remain de-energized for a considerable time, the use of electrolytic capacitors is out of the question. In addition, it is unreasonable to expect an accurately maintained delay despite temperature and ageing if electrolytic capacitors are used.

The second difficulty with this circuit is less severe but of importance. The relay, which is inductive, is operated by the discharge of a capacitor. Consequently, the relay is operated by a purely transient process in an oscillatory circuit, and great care is required to ensure long-term reliability in such a case. Having operated, the relay is dependent on its own retaining contacts, and care must be taken to keep these clean.

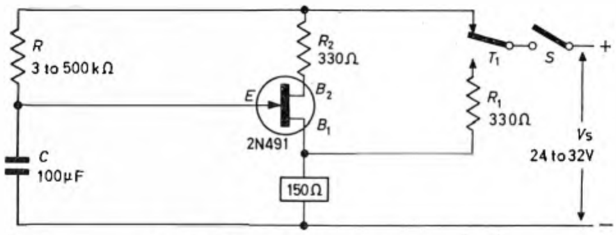

Fig. 2 Usual suggested timer circuit

Because of the difficulties encountered and anticipated with the circuit in Fig. 2, an investigation has been made into the possibilities of various other circuits, and some of these are now described. In the circuit in Fig. 3, when the switch is first closed, C (4µF) charges slowly in parallel with the 0·001µF capacitor *via* R. When the voltage across the capacitor achieves a sufficient amplitude, the emitter diode of the unijunction transistor conducts, and the device fires. The emitter voltage then falls below the voltage of C, and MR_1 cuts off. This effectively disconnects C, and a more rapid relaxation oscillation commences at a frequency depending on R and C_1. The resulting pulses of current in base 2 are used to produce a direct voltage across the output smoothing capacitor C_2. Consequently, with this circuit, a d.c. output appears, following an initial delay after the supply switch is closed. While this arrangement is satisfactory for use with a high-resistance load, it is not possible to obtain successful operation with a low-impedance-relay load unless a buffer transistor is interposed. However, if two transistors are to be used, it is probably not worth using a unijunction transistor at all.

Ideally, the load should be connected in the emitter circuit, since here it is possible to obtain a much higher value of current after the unijunction transistor has fired than before firing. The circuit finally arrived at is shown

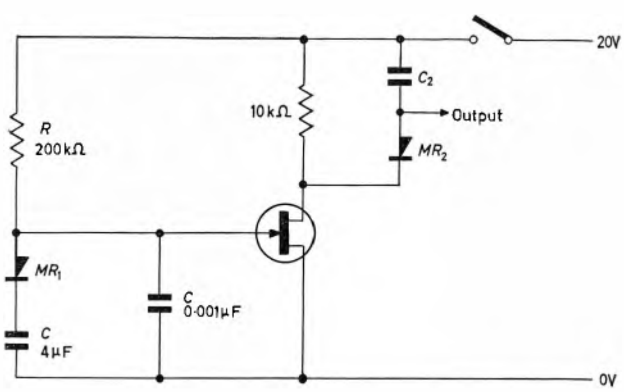

Fig. 3 Timer giving repetitive pulse output

in Fig. 4. Here, silicon diode MR_1 is used to isolate the charging circuit while C is charging *via* R. This isolating-diode arrangement has been used in earlier transistor timers[3,5]. The relay is connected to a low-resistance supply potentiometer formed by R_1 and R_2. The voltage across R_2 is arranged to be always, even under worst tolerance conditions, below the peak-voltage point on the emitter voltage current curves of the unijunction transistor. Consequently, the unijunction transistor does not fire *via* MR_2. After the switch is closed, C charges *via* R. Eventually the voltage across C exceeds the emitter voltage, and MR_1 conducts while MR_2 becomes reverse-biased and cut-off. As C continues to charge *via* R, the emitter voltage is increased until the unijunction transistor eventually fires. The emitter voltage then drops drastically

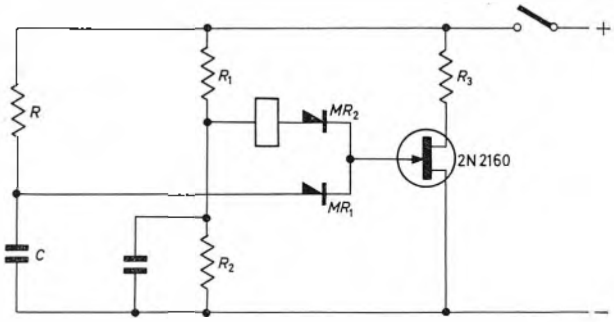

Fig. 4 Timer operating electromechanical relay

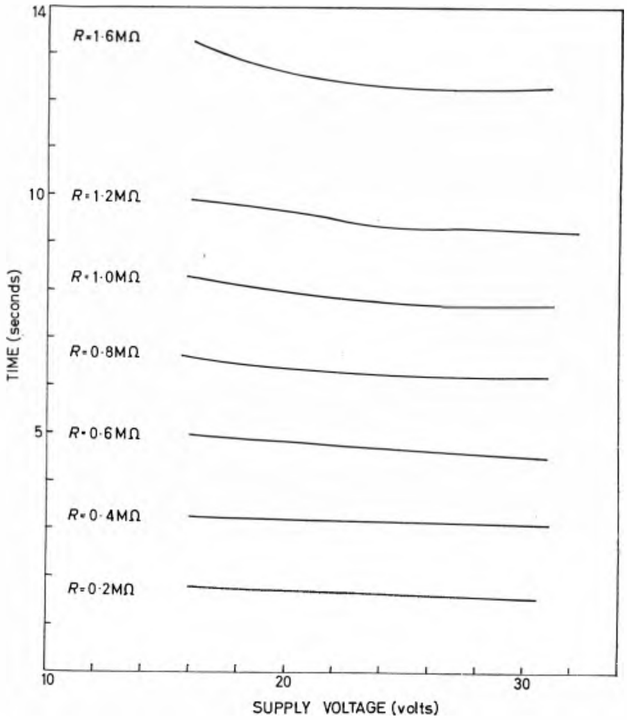

Fig. 5 Variation of delay time with supply voltage

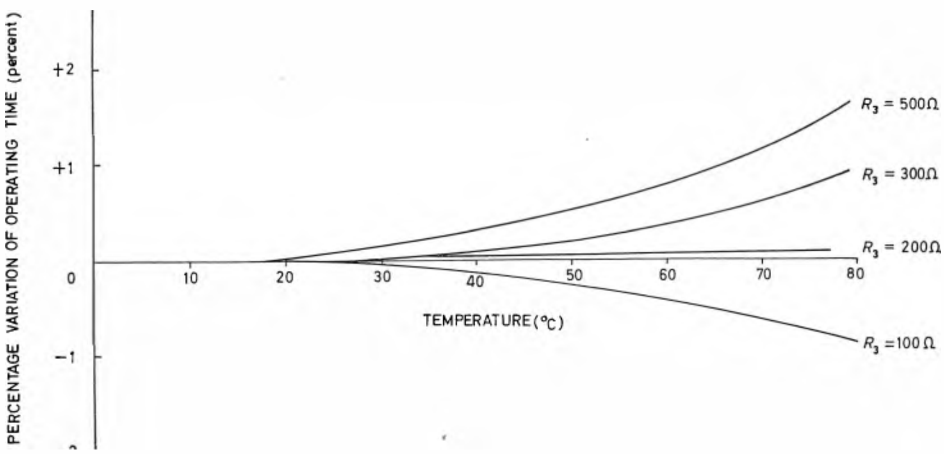

Fig. 6 Effects of ambient-temperature variation

as a heavy emitter current flows through the relay and causes it to operate. The circuit then remains in this condition until the supply switch is opened.

Results obtained with the arrangement of Fig. 4 are shown in Fig. 5, where it is seen that the delay time is reasonably independent of supply-voltage variations over a wide range. The effects of ambient-temperature variation are shown in Fig. 6 for various values of the temperature-compensating resistor R_3 in the circuit of base 2. When the optimum value of 200Ω was used for R_3, virtually no variation of operating time was observable over a wide temperature range.

It was found easy to arrange the semiconductor circuit components within an international octal plug for encapsulation, this now being a very popular method of construction for industrial semiconductor equipment. The metallized-paper capacitor C is the largest external component of the circuit. In some of the tests, a Zener diode was used to reduce the impedance of the relay supply circuit by replacing R_1. However, although it can increase the relay power, this arrangement introduces dangers of poor operation due to supply-voltage spikes. The circuit was also successfully tested as a one-shot type of photoelectric relay for use in such applications as burglar alarms. For this, a cadmium-sulphide photocell was connected instead of C, so that, if the light was interrupted, the relay operated. In this connection, it is possible to make the unijunction transistor itself photosensitive[6] and so avoid the need for the extra photocell.

Acknowledgment

The author wishes to thank R. A. Smith for the experimental results obtained in the course of undergraduate work at the University of Aston in Birmingham.

REFERENCES

1 Young, J. F.: Design factors for industrial cold-cathode timers, *Electronic Engng.*, *31*, 422 (July 1959)
2 Young, J. F.: Scale linearisation for thyratron timers, *Electronic Engng.*, *34*, 835 (Dec. 1962)
3 Young, J. F.: The use of transistors in industrial timer circuits, *Electronic Engng.*, *35*, 366 (June 1963)
4 Cleary, J. F. (Ed.): *GE Transistor manual*, 4th Edition, p. 198 (1962)
5 Young, J. F., and GEC Ltd: *Transistorised timer circuit*. British Patent 836 074
6 Granville, J. W.: A two-state light-activated circuit element using germanium, *Brit. J. Appl. Phys.*, *6*, 172 (May 1955)

Series-connected tunnel-diode-scaler design considerations

by **Z. C. Tan**, M.Sc., M.I.E.E.E., and **J. B. Earnshaw**, M.Sc., Ph.D., F.Inst.P., *University of Auckland, New Zealand*

This article discusses the results of calculations relating to the transient characteristics of a pair of similar tunnel diodes connected in series, biased by an ideal current source and triggered by pulses from an a.c.-coupled voltage source. The purpose of these calculations is to investigate quantitatively the design conditions for scalers employing chains of series-connected tunnel diodes. A qualitative explanation of these scalers is also presented and its limitations are indicated. The principal conclusion of this investigation is that, although series-connected tunnel-diode scalers can be made to operate satisfactorily with critically selected components, their design does not appear to be a feasible proposition from an engineering standpoint.

(Voir page 664 pour le résumé en français: Zusammenfassung in deutscher Sprache auf Seite 666)

A VERY interesting composite characteristic is produced when a number of similar tunnel diodes are connected in series to form a chain[1] ('similar' is used here to describe tunnel diodes fabricated from the same semiconductor material and with approximately equal peak currents). When such a chain is biased by a constant current I_b, the situation is represented by a horizontal load line drawn on the composite characteristic and passing through $I_a=I_b$.

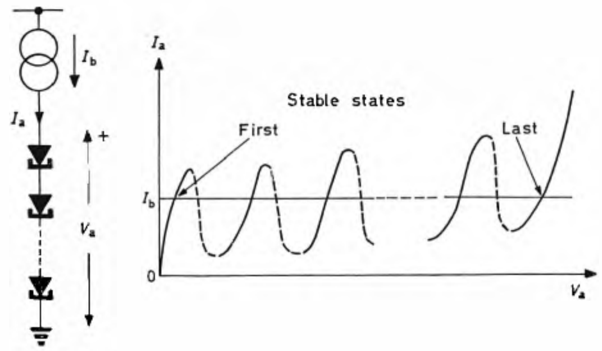

Fig. 1 Tunnel diode biased with a constant current
(a) Tunnel-diode chain
(b) Composite characteristic

As shown in Fig. 1, this load line makes a number of intersections with the composite characteristic, and each intersection with a positive-resistance region represents a stable state in which the tunnel-diode chain can exist. Owing to their multistate capabilities, tunnel-diode chains would appear to have applications in high-speed scaling, analogue-to-digital encoding, binary addition and other similar logic functions. In scaling, for example, successive input pulses may be arranged to switch the chain progressively from one state to another. When the chain switches to its final state, a reset may be initiated to return the chain to its initial state; thus a chain possessing 10 stable states may perform as a decade scaler (Fig. 2). Because of the apparent simplicity and potential speed of scalers of this type, they have aroused considerable interest and have been the subject of a number of publications[2-7]. In most of the papers, the authors have based their designs on the static composite characteristic of the chain and have described the operation of their scalers accordingly. This approach appears to be rather naïve, since many of the assumptions made regarding the static composite characteristics are invalid under transient conditions. In order that the limitations of this approach may be discussed, a qualitative description based on the static composite characteristic is first presented.

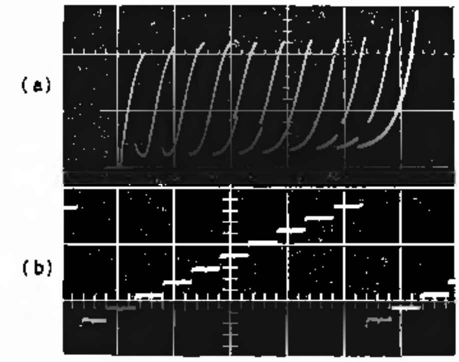

Fig. 2 Experimental decade-scaler waveforms
(a) Static composite characteristic (vertical: 2mA/division; horizontal: 1V/division)
(b) Waveform across the chain (vertical: 2V/division; horizontal: 2μs/division)

Qualitative description

Presented below is a qualitative description of the operation of a scaler employing a chain of tunnel diodes. The progressive 'stepping' of the chain from one stable state to another is explained by considering the manner in which successive input pulses shift an appropriately drawn load line across the composite characteristic. The basic circuit of the scaler is given in Fig. 3. A constant bias current I_b establishes the multistate capabilities of the chain. Input

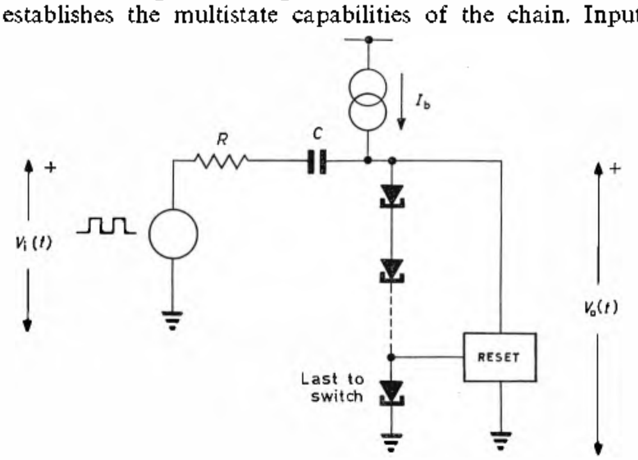

Fig. 3 Basic circuit using a tunnel-diode chain

This article was originally presented at the 1st New Zealand Electronics Conference, Auckland, August 1966, under the title 'Transient characteristics of series-connected tunnel diodes'.

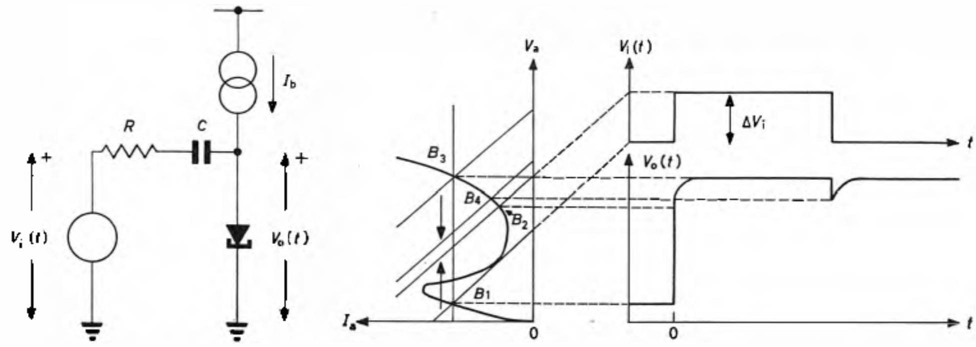

Fig. 4 Graphic illustration of the response of a single tunnel diode to a rectanglar input-voltage pulse

pulses from a voltage source are *RC*-coupled to the chain and these switch the chain from one stable state to the next. When the chain is switched to its final state, the reset temporarily removes the bias current and the chain is returned to its initial condition. This reset may be initiated by the switching of the tunnel diode which is selected to be the last in the chain to switch (a study of the composite characteristic indicates that this should be the tunnel diode with the maximum value of I_p). Figs. 4 and 5 provide graphical illustrations of the operation of this form of scaler. The basic assumptions made are that

(i) the switching time of the tunnel diodes is very much smaller than the time constant of the input coupling circuit

(ii) the static composite characteristic remains unchanged during the switching transients.

These assumptions imply that no significant charging of the input coupling capacitor takes place during the switching interval, so that the switching trajectory on the static composite characteristic follows a path determined by the input resistive load line and the amplitude of the input pulse.

In Fig. 4, only one tunnel diode is considered. Initially no current flows through the coupling capacitor *C*, so that only the bias current I_b flows through the tunnel diode and the bias point B_1 on the characteristic diagram is established by the horizontal load line through $I_a = I_b$. The application of a rectangular input-voltage pulse changes the horizontal load line into a composite one of $-1/R$ passing through B_1. This load line is then displaced instantaneously along the V_a-axis by an amount equal to the input voltage amplitude, so that it then passes through B_2. The operating point shifts from B_1 to B_2 along a trajectory determined by the composite load line, and then moves from B_2 to B_3 as the coupling capacitor *C* charges up to its final steady-state value. When *C* is fully charged, current ceases to flow through it, and the load line is again horizontal. For the trailing edge of the input pulse, the procedure is that the composite load line is again formed and shifted so that the operating point initially moves from B_3 to B_4 and then returns to B_3 as *C* charges to its equilibrium value, at which time the load line is again horizontal.

In the discussion so far, it has been tacitly assumed that the amplitude of the input pulse and the slope of the composite load line are such that the load line is shifted beyond the peak point by the leading edge of the input pulse but not returned to the original side of the valley point by the trailing edge. These assumptions ensure that, for a rectangular input pulse only forward switching takes place. Typical input and output waveforms are shown alongside the characteristic diagram in Fig. 4.

Fig. 5 illustrates the operation of a 5-tunnel-diode (quinary) scaler. The composite load line is formed and displaced as explained above; but now, because there is more than one peak, the amplitude of the input pulses must only be large enough to shift the load line beyond one peak at a time. The voltage across the chain corresponding to a train of input pulses is in the form of a series of 5-step staircases.

The assumptions made above have enabled the operation of the scaler to be described in a simple manner. Although this description predicts staircase waveforms that are typical of those sometimes observed (Fig. 6), it does not describe the operation of the scaler sufficiently well to allow circuit values to be determined accurately. This is because, in order to take advantage of the inherently high switching speeds of the tunnel diodes, the scaler is normally operated under conditions which are somewhat different from those

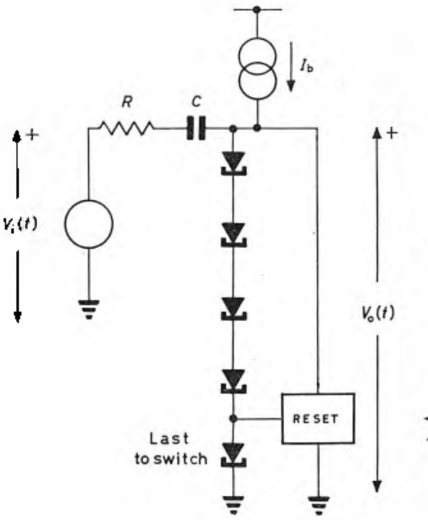

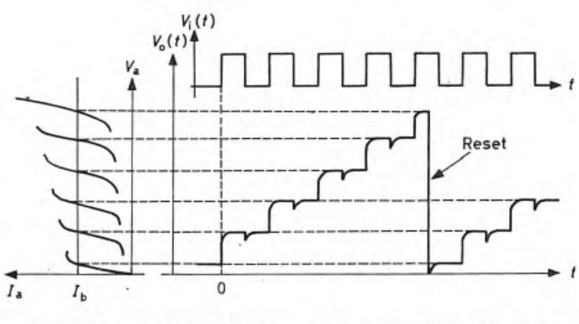

Fig. 5 Graphic illustration of the operation of a scaler employing a chain of five tunnel diodes

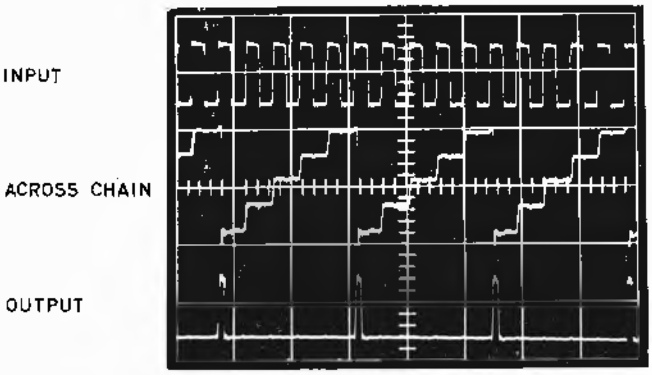

Fig. 6 Experimental quinary-scaler waveforms
Vertical: top and bottom 0·5V/division, middle 1V/division; horizontal: 0·2μs/division

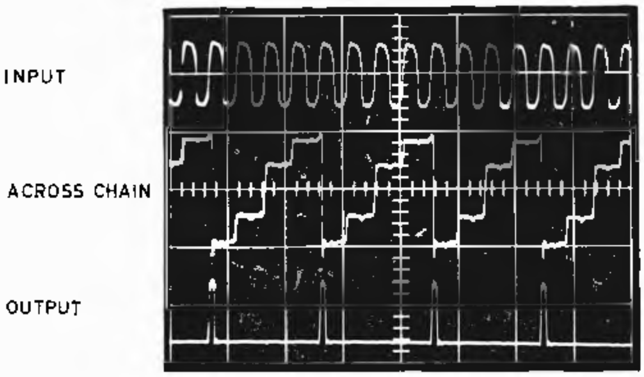

Fig. 7 Waveforms showing double switching
Vertical: top and bottom 0·5V/division, middle 1V/division; horizontal: 0·2μs/division

described, and for which the basic assumptions are invalid. Furthermore, during the switching intervals, the transient characteristics of the tunnel-diode chain may differ significantly from the static composite characteristics. For these reasons, the simple explanation cannot accurately predict the occurrence of 'double switching', nor account for the phenomenon of 'anomalous switching'. (Double switching[8,9] is illustrated in Fig. 7, and it occurs when the operating point skips a stable state. The normal order of switching of tunnel diodes in the chain is the same as that of increasing I_p values, but with anomalous switching this is not so.)

Any attempt to represent the transient characteristics of the tunnel-diode chain by a static composite curve must be discarded and replaced by a set of differential equations which accurately describes the operating conditions and, in particular, takes account of the tunnel-diode junction capacitances. Such an approach is adopted in the next section, where the simple case of a chain of two tunnel diodes is considered.

Transient analysis

Since the static composite characteristic is unsatisfactory for describing the detailed operation of the scaler, the differential equations which describe it more accurately are examined for possible solutions. An initial consideration of the problem indicates that a general solution for a chain of n tunnel diodes is not a practical proposition, owing to the large number of differential equations and variable parameters involved. As a consequence, the simpler case of a chain of two tunnel diodes is studied first. Fig. 8 sets out the problem for a scaler employing a chain of two tunnel diodes. Each of the diodes is represented by an equivalent circuit consisting of a parallel combination of a current-function generator and the tunnel-diode junction capacitance.

For the current-function generator of one of the tunnel diodes, a 60-section linear piecewise approximation to the static characteristic of a typical 5mA germanium tunnel diode with the following principal parameters is adopted: $I_p = 5\text{mA}$, $I_v = 1\text{mA}$, $V_p = 60\text{mV}$, $V_v = 340\text{mV}$, and $V_f = 500\text{mV}$. For the current-function generator of the other tunnel diode, a static characteristic of the same basic shape but with a different current scale is assumed, [Fig. 8(b)], so that

$$i_2(v) = A i_1(v)$$

where A is the ratio of the two peak currents; i.e. $A = I_{p2}/I_{p1}$.

The junction capacitances of both the tunnel diodes vary with voltage according to the relation

$$C(v) = C_v \left(\frac{V_d - V_v}{V_d - v}\right)^{1/2}$$

where V_d = diffusion voltage ($\simeq$0·7V for germanium)
V_v = valley voltage
C_v = valley capacitance, i.e. junction capacitance when $v = V_v$.

The series inductance of the individual tunnel diodes is omitted, because, being of the order of a nanohenry or so, it does not significantly affect the results, as presented below.

The equations below follow directly from an inspection

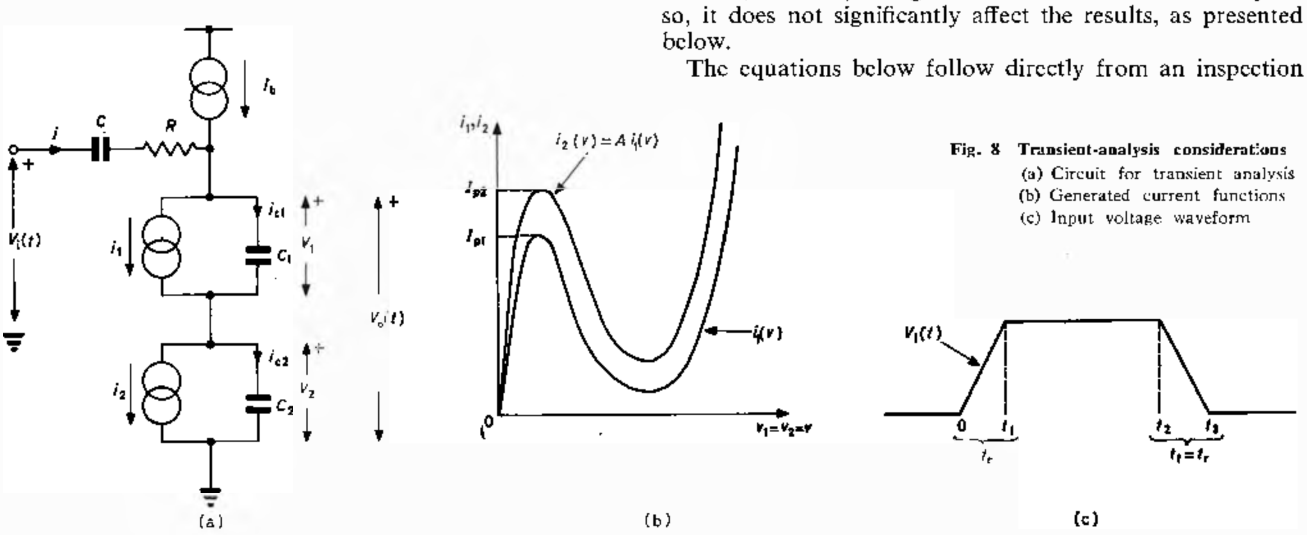

Fig. 8 Transient-analysis considerations
(a) Circuit for transient analysis
(b) Generated current functions
(c) Input voltage waveform

of the circuit of Fig. 8. At the current nodes,

$$i + I_b = i_1 + i_{c1} = i_2 + i_{c2} \quad \dots\dots\dots\dots \quad (1)$$

For the three capacitances,

$$i_{c1} = C_1\,(dv_1/dt) \quad \dots\dots\dots\dots \quad (2)$$

$$i_{c2} = C_2\,(dv_2/dt) \quad \dots\dots\dots\dots \quad (3)$$

$$i = C\,\frac{d}{dt}\,(v_i - iR - v_1 - v_2) \quad \dots\dots\dots \quad (4)$$

The input $v_i(t)$ is a symmetrical pulse of the type shown in Fig. 8(c); so that

$$\frac{d}{dt}\,[v_i(t)] = k \quad \dots\dots\dots\dots \quad (5)$$

where $k = \Delta v_i/t_r$ for $0 < t < t_1$

$= 0$ for $t < 0$, $t_1 < t < t_2$, and $t_3 < t$

$= -\Delta v_i/t_r$ for $t_2 < t < t_3$.

On making the appropriate substitutions, equations (2), (3) and (4), respectively, may be rewritten:

$$dv_1/dt = [i - i_1 + I_b]/C_1 \quad \dots\dots\dots\dots \quad (6)$$

$$dv_2/dt = [i - i_2 + I_b]/C_2 \quad \dots\dots\dots\dots \quad (7)$$

$$di/dt = [k - (1/C + 1/C_1 + 1/C_2)i + (i_1/C_1 + i_2/C_2) - (1/C_1 + 1/C_2)I_b]/R \quad \dots \quad (8)$$

The nonlinear differential equations (6), (7) and (8) describe the response of the tunnel-diode chain to an input pulse with equal rise and fall times. These equations are too complex for a general analytic solution to be obtained, and it is necessary to resort to numerical methods. Solutions for $v_1(t)$ and $v_2(t)$ may be obtained by using the Runge-Kutta[10] method of time incrementation.

An examination of equations (6), (7) and (8) indicates that the following variable parameters affect the response of the chain:

amplitude of the input pulse	Δv_i
risetime of input pulse	t_r
input coupling capacitance	C
input series resistance	R
bias current	I_b
peak currents	I_{p1}, I_{p2}
valley capacitances	C_{v1}, C_{v2}

It is obvious from the number of parameters involved, that a systematic procedure of adjusting one parameter while keeping all the others constant is not feasible. By considering only certain realistic values for some of the parameters, selected on the basis of practical experience, the total amount of computation is greatly reduced.

Results of transient analysis

The results of the transient analysis are presented in terms of $v_o(t)$ response diagrams. $v_o(t)$ is the voltage across the whole chain, i.e. $v_o(t) = v_1(t) + v_2(t)$. Fig. 9 shows two sets (one theoretical and the other experimental) of six waveforms, which represent all the possible response modes ranging from the situation where neither tunnel diode switches to that where both tunnel diodes switch to their high-voltage states and remain switched at the termination of the input pulse. The results are set out in a series of tables. Each table indicates the varying responses of the chain as the values of two, and in some cases three, of the parameters are changed. Normally the tunnel diode with the smaller peak current switches first, but with anomalous switching the order is reversed. Anomalous switching is denoted by an asterisk beside the response diagram. The following tables contain a large amount of information condensesd from a substantial quantity of

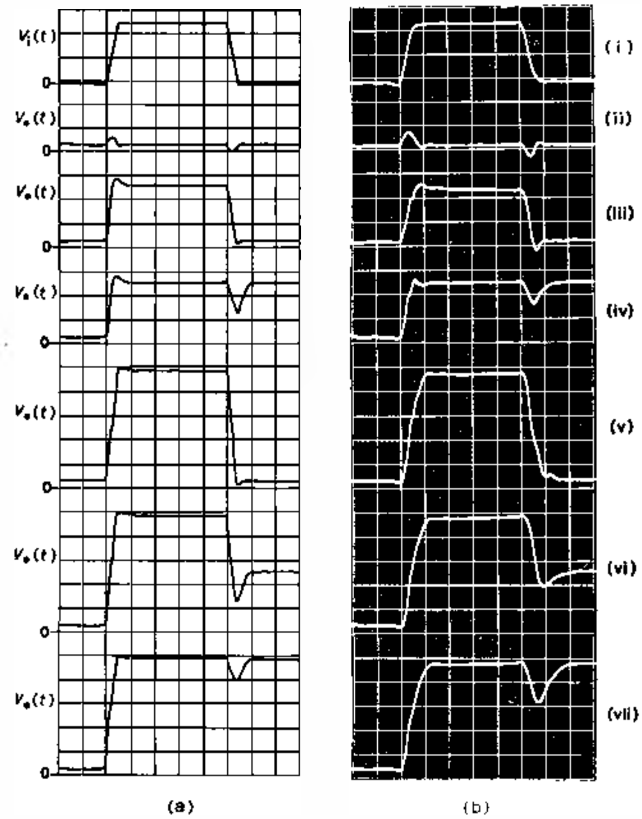

Fig. 9 Response waveforms for a chain of two tunnel diodes. Vertical: 0·2V/division; horizontal: 5ns/division (a) Theoretical (b) Experimental

(i) Input pulse; (ii) No switching; (iii) One diode forward switches and is then reverse switched by the trailing edge of the input pulse; (iv) One diode forward switches and remains forward switched; (v) Both diodes forward switch (double switching) and both are reverse switched; (vi) Both diodes forward switched, one is reverse switched and the other remains switched; (vii) Both forward switch and remain switched

computer output. It is not proposed to discuss all the results presented but instead to highlight a few features pertinent to the design of series-connected tunnel-diode scalers. It should be emphasized that the values in the tables are simply representative ones at which various types of responses occur. The range of various parameter values for a particular response are not shown here. However, a careful study of the detailed results of the switching calculations indicate that these ranges are small, and this is supported by practical experience.

Table 1 Variation in input capacitance C and bias current I_b

ΔV_i mV	t_r ns	C pF	R Ω	I_b mA	I_{p1} mA	I_{p2} mA	C_{v1} pF	C_{v2} pF	$V_o(t)$
500	2	5	20	2	5·0	5·5	10	20	
		5		3					
		5		4					
		10		2					
		10		3					
		10		4					
		15		2					
		15		3					
		15		4					
		20		2					
		20		3					
		20		4					

VARIATION IN INPUT CAPACITANCE C AND BIAS CURRENT I_b

The results presented in Table 1 clearly show the occurrence of all the possible modes set out in Fig. 9. The $v_o(t)$ waveforms indicate that the number of tunnel diodes which are forward switched by the leading edge of the input pulse increases with both C and I_b (see changes in the leading edge of the $v_o(t)$ waveform as C is increased from 5 to 20pF for a fixed value of $I_b = 2$mA, and as I_b is increased from 2 to 4mA for a fixed value of $C = 10$pF). The number of tunnel diodes which are reverse-switched by the trailing edge of the input pulse increases with C but decreases with I_b (forward switching must have taken place before the tunnel diodes may be reverse-switched). This observation is inferred from the results presented.

Clearly, forward and reverse switching are governed by the total current supplied to the chain. For the leading edge of a given input pulse, this current increases with both C and I_b, and, in this case, the tendency for either one or both of the tunnel diodes to forward switch also increases. For the trailing edge, the transient component of this current is negative and as C increases the total current decreases. This decrease in the total current increases the tendency for either one or both of the tunnel diodes to reverse switch.

VARIATION IN INPUT RESISTANCE R

Table 2 shows the responses of the chain for various values of R. In the range considered (i.e. R = 10 to 50Ω), the value of R has no significant effect on the response.

Table 2 Variation in input resistance R

ΔV_i	t_r	C	R	I_b	I_{p1}	I_{p2}	C_{v1}	C_{v2}	$V_o(t)$
500	2	10	10	3	5·0	5·5	10	20	
		10	20						
		10	50						
		20	10						
		20	20						
		20	50						

VARIATION IN PEAK CURRENTS I_{p1}, I_{p3} AND VALLEY CAPACITANCES C_{v1}, C_{v2}

From an inspection of the results presented in Table 3, the order of switching of the tunnel diodes is governed not only by the peak currents but also by the valley capacitances of the tunnel diodes. The valley capacitances control the rates at which currents i_1 and i_2 [Fig. 8(a)] increase initially. For equal valley capacitances the initial rates of increase of i_1 and i_2 are approximately equal and the lower peak current is exceeded first. However, if the tunnel diode with the lower peak current has the higher valley capacitance, anomalous switching may occur, as illustrated by the following case:

$$C = 10\text{pF}: I_{p1} = 5\text{mA}, \; I_{p3} = 5{\cdot}05\text{mA}$$
$$C_{v1} = 20\text{pF}, \; C_{v2} = 10\text{pF}$$

The dependence of the order of switching on the valley capacitance is, however, not as great as the dependence on the peak currents, because considerable differences in the valley capacitances (of the order of 100%) are required to cause any significant difference in the initial rate of increase of i_1 and i_2. This is borne out by the following case:

$$C = 10\text{pF}: I_{p1} = 5\text{mA}, \; I_{p2} = 5{\cdot}25\text{mA}$$
$$C_{v1} = 20\text{pF}, \; C_{v2} = 10\text{pF}$$

Here, when the difference in the peak currents is increased from 1% to 5%, the difference in the valley capacitance of 100% is now insufficient to reverse the normal order of switching. The results for the larger input capacitance of 20pF supports these observations.

Table 3 Variation in peak currents I_{p1}, I_{p2} and valley capacitances C_{v1}, C_{v2}

ΔV_i	t_r	C	R	I_b	I_{p1}	I_{p2}	C_{v1}	C_{v2}	$V_o(t)$
500	2	10	20	3	5·00	5·00	20	10	*
		10				5·00		20	
		10				5·00		40	
		10				5·05		10	*
		10				5·05		20	
		10				5·05		40	
		10				5·25		10	
		10				5·25		20	
		10				5·25		40	
		10				5·50		10	
		10				5·50		20	
		10				5·50		40	
		20				5·00		10	*
		20				5·00		20	
		20				5·00		40	
		20				5·05		10	*
		20				5·05		20	
		20				5·05		40	
		20				5·25		10	*
		20				5·25		20	
		20				5·25		40	
		20				5·50		10	
		20				5·50		20	
		20				5·50		40	

It is clear that, if such a chain is to be utilized for scaling, the tunnel diodes should ideally be selected not only according to their peak currents but also according to their valley capacitances. This double selection requirement is a very undesirable and somewhat impracticable design feature, particularly for a chain containing a number of tunnel diodes (say five or more).

VARIATION IN AMPLITUDE ΔV_i OF INPUT PULSE

In a practical scaler, some standardization of the input pulses is necessary, and a convenient means of achieving this is to use a tunnel diode to shape it. An input amplitude of 500mV would then by typical. In practice, owing to resistive and capacitive loading, the input amplitude may be somewhat less than 500mV. Table 4 demonstrates the effect of possible reductions in the input amplitude. The input amplitude governs the magnitude of the transient current supplied to the chain and observations similar to those of the variation in the input capacitance can be similarly explained.

Table 4 Variation in input amplitude ΔV_i

ΔV_i	t_r	C	R	I_b	I_{p1}	I_{p2}	C_{v1}	C_{v2}	$V_o(t)$
300	2	10	20	3	5·0	5·5	10	20	
400		10							
500		10							
300		20							
400		20							
300		20							

VARIATION IN RISETIME t_r OF INPUT PULSE

To complete the investigations, responses for risetimes differing from the nominal 2ns (a 5mA germanium tunnel

Table 5 Variation in input risetime t_r

ΔV_i	t_r	C	R	I_b	I_{p1}	I_{p2}	C_{v1}	C_{v2}	$V_o(t)$
500	1	10	20	3	50	5·5	10	20	
	2	10							
	4	10							
	1	20							
	2	20							
	4	20							

diode with a γ of 5 and valley capacitance of 20pF has a nominal risetime of about 2ns) by a factor of 2 are shown in Table 5. The risetime controls the initial surge of current into the chain. When the risetime is reduced to 1ns, the initial current is sufficient to cause double switching; while, with a 4ns risetime, the initial current is not even sufficient to switch one of the tunnel diodes.

Conclusions

The apparent simplicity of the static composite characteristic curve displayed by conventional curve tracers [Fig. 2(a)] is often misleading. Not only is this curve generally incomplete (because closed-loops and convoluted sections are often not displayed[1]), but in addition it is invalid at normal tunnel-diode switching speeds. Under certain limitations, it may be used to explain on a qualitative basis the operation of a chain of series-connected tunnel diodes, but such an explanation cannot accurately predict the occurrence of double switching nor account for the phenomenon of anomalous switching. The static composite characteristic therefore should not be used as a basis for design considerations for devices employing tunnel-diode chains.

It is necessary to resort to the transient characteristics to describe the operation of a tunnel-diode chain under practical conditions. These transient characteristics depend not only on the static and dynamic parameters of the individual tunnel diodes, but also on the parameters of the external circuit. The derivation of the transient characteristics is not straightforward, since it involves the solution of many simultaneous nonlinear differential equations containing many variable parameters.

In view of the results obtained for only two series-connected tunnel diodes, the design of scalers employing five and possibly ten tunnel diodes is far more complex than it appears at first sight. The large number of parameters involved makes the design of this type of scaler very difficult indeed, and the design conditions are further complicated by the small operating margins for some of the parameters, which become even more critical when attempts to increase the speed of operation are made. Although scalers of this type have been made to operate (Figs. 2 and 6) with critically selected components, their design does not appear to be a feasible proposition from an engineering standpoint.

Acknowledgments

The authors would like to acknowledge the generous financial support provided by the New Zealand Universities Research Grants Committee for their current research programme. The provision of suitable research facilities in the Physics Department at the University of Auckland is also very much appreciated.

REFERENCES

1 Earnshaw, J. B., and Tan, Z. C.: Composite characteristics of series-connected tunnel diodes, *Electronic Engng.*, *38*, 242 (April 1966)
2 Spiegel, P.: High-speed scalers using tunnel diodes, *Rev. Sci. Instrum.*, *31*, 754 (July 1960)
3 Aleksander, I., and Scarr, R. W. A.: Tunnel devices as switching elements, *J. Brit. I.R.E.*, *23*, 177 (March 1962)
4 Rabinovici, B.: Tunnel-diode decade counter, *Rev. Sci. Instrum.*, *33*, 1391 (Dec. 1962)
5 Foote, R. S., and Johnson, D.: High-speed decade pulse counting, *ibid.*, *35*, 1126 (Sept. 1964)
6 Swamy, M. N. S.: A high-speed tunnel-diode scaler, *Electronic Engng.*, *37*, 225 (April 1965)
7 Zinov'ev, G. S., and Rozhkov, V. M.: Timer with decatrons using semiconductor devices, Instruments and Experimental Techniques (USA), No. 2 (Oct. 1965)
8 Tan, Z. C.: *A study of some of the switching characteristics of tunnel diodes and their application in the design of a high speed scaler* M.Sc. Thesis, University of Auckland, December 1964
9 Foote, R. S., and Johnson, D.: Private communication
10 Singer, J.: *Elements of numerical analysis*. Academic Press (1964)

Demonstration model for a simple learning situation

by **P. C. van Soest,** *Technological University of Eindhoven, Netherlands; formerly with the Laboratory for Information Theory, Technological University, Delft, Netherlands*

In order to demonstrate some of the properties of a learning system based on the linear model by Bush and Mosteller, a simple technical realization of such a system will be described. In this, the probability vector assigned to the response classes is modified as required by the linear model. The act of forgetting, not taken into account in the linear model, is introduced. A circuit diagram of the final set-up is given.

(Voir page 664 pour le résumé en français: Zusammenfassung in deutscher Sprache auf Seite 666)

THE mathematical model for studying learning, proposed by Bush and Mosteller[1] in 1955, has since been widely adopted by psychologists and engineers for the explanation and prediction of the learning behaviour of certain animals. The scope of this linear model, however, does not seem to be restricted to that field. In engineering, many of the ideas concerning the linear model for learning are applicable in artificial learning systems[2,3]. In order to demonstrate some of the fundamental properties of a learning device based on the linear model by Bush and Mosteller, a model was developed using electronic components. In this model, there are two response classes; these classes are represented by red and green lamps. The operator of the device acts as ' environment ' for the learning model. The action taken by the learning device (e.g. lighting one of the lamps on a neutral stimulus) can be approved or disapproved by him ('reward' or 'punishment').

If the operator approves of the action of the device he presses the button RIGHT, if not, he presses the button WRONG. The device interprets the action taken by the operator in such a way that, after a certain number of experiments, the learning device gives the response endorsed by the operator with a larger probability. If no action is taken by the operator, the probability of a green or red light being lit remains unchanged. The transformation of the probability vector in each experiment takes place exactly as described by the mathematical model. The rate of learning and the final probability vector $\underline{\lambda}$ can be adjusted in a simple way by two potentiometers. A notion immediately associated with learning is that of forgetting. In the mathematical model by Bush and Mosteller, this aspect is not taken into account. In this device, forgetting has been introduced. Interesting cases, for instance, arise when the buttons RIGHT and WRONG are pressed alternately, regardless of the response of the system. Other important cases arise when the operator is not consistent in his reactions; the environment then becomes more or less stochastic.

Description of the model

The probabilities used in the model are realized with the aid of a noise generator. In principle, this generator should give noise with a uniform probability-density function. Such a generator will, in general, not be available, and a generator giving Gaussian noise can be used without seriously affecting the operation of the device. The noise signal x' is compared with a signal x. This d.c. signal x is influenced by the actions taken by the operator (e.g. pressing the buttons RIGHT/WRONG).

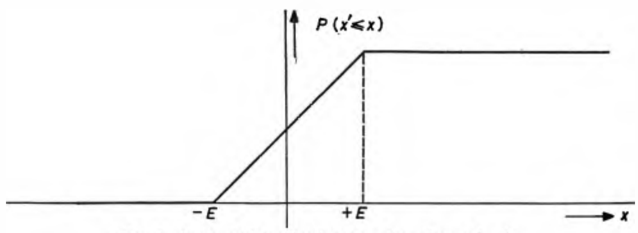

Fig. 1 Probability distribution function of x'

The probability P (that red will light) $= P_r$ is made equal to the probability $P(x' \leqslant x)$. Correspondingly, P (that green will light) $= P_g$ is made equal to the probability $P(x' > x)$. From the probability-distribution function for x',

$$P_r = P(x' \leqslant x) = 1/2\left(\frac{x+E}{E}\right) \quad \ldots\ldots\ldots\ldots (1)$$

$$P_g = P(x' > x) = -1/2\left(\frac{x-E}{E}\right) \quad \ldots\ldots\ldots\ldots (2)$$

with $|x| \leqslant E$.

If P_r is required larger, the voltage x is raised. This can be accomplished using the circuit in Fig. 2, by connecting

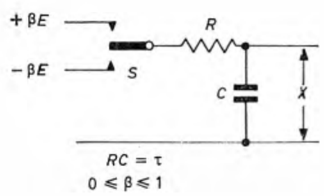

Fig. 2 Capacitor C acting as memory

C during a time interval $\triangle T$ to the voltage source $+\beta E$. Should P_r be required smaller, the capacitor can be connected to the source $-\beta E$ during an interval $\triangle T$. Of course, if P_r increases, P_g decreases, and *vice-versa*, as $P_r + P_g = 1$.

A time $\triangle T$ after the switch is closed in the nth experiment, the voltage across C will be:

$$x(n+1) = \beta(1 - e^{-\triangle T/\tau})E + e^{-\triangle T/\tau}x(n) \quad \ldots\ldots (3)$$

with $\tau = RC$. If $e^{-\triangle T/\tau} = \alpha$; equation (3) reduces to

$$x(n+1) = \beta(1-\alpha)E + \alpha x(n) \quad \ldots\ldots\ldots (4)$$

Substitution of equation (4) into equation (1) yields

$$\begin{aligned} P_r(n+1) &= 1/2\left[\frac{\beta(1-\alpha)E + \alpha x(n) + E}{E}\right] \\ &= 1/2\left[\alpha\frac{x(n)+E}{E} + \frac{(1-\alpha)(1+\beta)E}{E}\right] \\ &= \alpha P_r(n) + 1/2(1+\beta)(1-\alpha) \quad \ldots\ldots\ldots (5) \end{aligned}$$

Similarly

$$\begin{aligned} P_g(n+1) &= 1/2\left[\frac{-\beta(1-\alpha)E - \alpha x(n) + E}{E}\right] \\ &= 1/2\left[\alpha\frac{E - x(n)}{E} + \frac{E(1-\alpha)(1-\beta)}{E}\right] \\ &= \alpha P_g(n) + 1/2(1-\beta)(1-\alpha) \quad \ldots\ldots\ldots (6) \end{aligned}$$

Making $\quad 1/2(1+\beta) = \lambda_1 \;;\; 1/2(1-\beta) = \lambda_2\,;$

$\quad \lambda_1 + \lambda_2 = 1 \;;\; \underline{\lambda} = (\lambda_1, \lambda_2)$

we find that

$$P_r(n+1) = \alpha P_r(n) + \lambda_1(1-\alpha) \quad \ldots\ldots\ldots\ldots (7)$$

$$P_g(n+1) = \alpha P_g(n) + \lambda_2(1-\alpha) \quad \ldots\ldots\ldots\ldots (8)$$

This fixed-point operator is similar to that described by Bush and Mosteller in their mathematical model. In that model, the parameter α is inversely proportional to the rate of learning, having a value between 0 and 1. The parameters λ_1 and λ_2 are the limits of the probabilities P_r and P_g for n approaching infinity.

From the results in equations (7) and (8), the transformation matrix $\mathbf{T}$ of the probability vector $\mathbf{P}(n)$ can be obtained. Having

$$\mathbf{P}(n+1) = \begin{bmatrix} P_r(n+1) \\ P_g(n+1) \end{bmatrix} = \mathbf{T}\begin{bmatrix} P_r(n) \\ P_g(n) \end{bmatrix} = \mathbf{TP}(n)$$

we find

$$\mathbf{T} = \begin{bmatrix} 1-(1-\alpha)\lambda_2 & (1-\alpha)\lambda_1 \\ (1-\alpha)\lambda_2 & 1-(1-\alpha)\lambda_1 \end{bmatrix} \quad \ldots\ldots\ldots (9)$$

For the special case $\lambda_1 = 1$ (the red light will light with probability one after a large number of experiments), the transformation matrix turns out to be

$$\mathbf{T}' = \begin{bmatrix} 1 & 1-\alpha \\ 0 & \alpha \end{bmatrix}$$

or, expressed in the time constant of the RC network (Fig. 2),

$$\mathbf{T}' = \begin{bmatrix} 1 & 1-\exp(-\triangle T/\tau) \\ 0 & \exp(-\triangle T/\tau) \end{bmatrix}$$

Although it is possible to extend this model to more than two response classes, the complications involved are such that the advantage of simplicity is lost. In the next section, we will show how the parameters α and $\underline{\lambda}$ can be adjusted.

Technical realization of the model

The electronic circuit diagram is shown in Fig. 3; the green and red bulbs shown at the right of the diagram, together with the pressbuttons RESET, STIM, RIGHT,

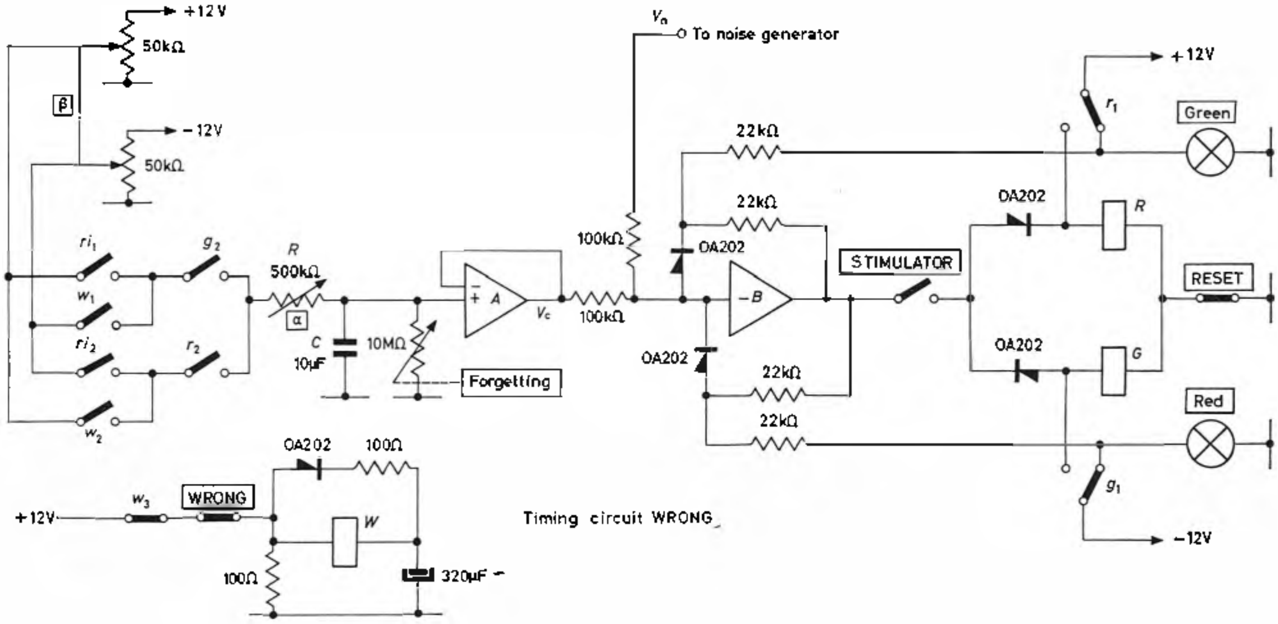

Fig. 3 Circuit diagram of demonstration model (timing circuit 'right' identical except for pushbutton and relay)

WRONG and the potentiometers α and β and FORGETTING are located on the front panel of the device. At the bottom left of the diagram, two timing circuits are shown for obtaining the time interval of ΔT. The main part of the device consists of two operational amplifiers. In this model integrated-circuit operational amplifiers are used, but the choice is rather arbitrary, provided that the operational amplifier B is able to actuate relays R and G. The circuit configuration round amplifier B enables the use of this amplifier as an amplitude discriminator[4]. Provided that $V_n + V_c < 0$, the output voltage of amplifier B will be +12V. As soon as $V_n + V_c$ becomes larger than zero, the output voltage of amplifier B will switch to −12V. The probability of finding a positive voltage at the output of the amplifier is in this way made equal to the probability $V_n + V_c < 0$. The probability of finding a negative voltage at the output will be equal to the probability $V_n + V_c > 0$. When one presses the STIM button relay R or relay G will be actuated with a probability depending on voltage V_c. Amplifier A is used acting as impedance transformer. The same voltage exists at the input and output of this circuit. The input impedance of the circuit, however, is very high, owing to negative feedback[4]. The uncontrollable discharge of capacitor C, acting as memory, is prevented in this way. Explaining briefly how the device operates, if the RESET button is pressed, relays R and G are deactuated. The green and red lamps will both light, as r_1 is a contact of relay R and g_1 is a contact of G. All contacts in Fig. 3 are shown with relays deactuated. When the STIM button is pressed, only the red or the green lamp will light, depending on whether the output voltage of amplifier B is positive or negative. The probability of the red or the green lamp lighting depends on V_c, as explained. Suppose that relay R is actuated; this relay will then be held by contact r_1 and the green lamp will extinguish.

If the response of the device is favourable for the environment, the RIGHT button will be pressed; otherwise it will be the WRONG button. When the RIGHT button is pressed, contacts ri_1 and ri_2, to the left of the diagram, will be closed during a time interval ΔT. This action is accomplished by the circuits at the bottom left of Fig. 3. With the red lamp alight, the voltage on C decreases and so does V_c. A decrease in V_c will result in a larger probability that the red lamp will be lit in the next experiment. This is how it should be, as the response of the device is approved by the environment. If the WRONG button had been pressed instead of the RIGHT button, the voltage on C would have been increased. The result would have been a smaller probability that the red lamp would be lit in the next experiment.

The final probability vector $\bar{\lambda}$ can be adjusted by the potentiometer β. The rate of learning is inversely proportional to α. The value of α can be adjusted by the variable resistor R. An increase in R results in a slower learning rate, as is readily seen from the diagram. Forgetting is introduced by a variable resistor connected across C. After a time interval depending on the setting of this resistor, the device lights the red or green lamp with equal probability as the capacitor C is discharged.

Experimental results

For these demonstrations, a noise generator producing Gaussian noise and a generator giving noise with a uniform distribution function were employed. No noticeable difference in performance was noticed between one or other generator. In order to avoid correlation between the subsequent trials, the noise generator should generate noise of a sufficient large bandwidth. On the other hand, the bandwidth should not be too large, as the relays require some time to become actuated. In this experiment, noise with a bandwidth of about 200Hz was used.

Acknowledgments

The author wishes to express his thanks to Prof. Y. Boxma for his stimulating interest and valuable suggestions made in the course of the project.

REFERENCES

1 BUSH, R., and MOSTELLER, F.: *Stochastic models for learning*. Wiley (1955).
2 FU, K. S., and MCLAREN, A. W.: *An application of stochastic automata to the synthesis of learning systems*. Purdue University, Lafayette, Indiana (Sept. 1965).
3 VAN SOEST, P. C.: *Learning systems based on a linear model*. Master thesis, Technological University, Delft, Netherlands (1966).
4 JACKSON, A. S.: *Analog computation*. McGraw-Hill (1960).

Analysis of repeated systems of transmission lines with matched loads

by **J. N. Saha**, M.Tech., M.Sc., *University of Manchester Institute of Science and Technology*

Very high-frequency transmission lines are often supported by a large number of short-circuited shunt stubs over long distances of their run between the transmitter and the aerial. It is most desirable for such a line to transmit as wide a band of frequency as possible, keeping the reflection in the passband at a minimum. This article determines the effect of a large number of stubs on the match and bandwidth. Scattering-matrix methods have been adopted in deriving the formula for the forward transmission coefficient for symmetrical stubbed sections constituting the line. Several combinations of stub lengths and their spacings have been considered in a digital-computer program, and the frequency response has been plotted to show that many such combinations result in random variations of the transmission coefficient with frequency. In order to achieve maximum bandwidth and yet keep the transmission coefficient at a high value, it has been shown that, for a matched load, λ/8 short-circuited shunt stubs spaced at λ/4 constitute the best design. The validity of the procedure has been confirmed by experimental observations.

(Voir page 664 pour le résumé en français: Zusammenfassung in deutscher Sprache auf Seite 666)

THE scattering-matrix method is a very powerful tool in solving transmission-line problems. Formulas derived by this technique are convenient for programming a digital computer, where it is possible to cycle a large number of line variables and choose the best result for practical application. In a previous article[1], the scattering-matrix method on a digital computer has been used in determining the frequency response of a line matched by a single stub. In this article, the scattering-matrix method has been extended to determine the forward transmission coefficient of a long line supported by many stubs. A lossless line has been considered as consisting of a number of symmetrical reversible 4-terminal networks. The effect of their dimensions on the forward transmission of power obtained by programming an Atlas digital computer is studied, and, on comparing the plotted curves, it is found that λ/8 short-circuited stubs spaced λ/4 apart constitute the best line. Experiments carried out in the laboratory testify to the validity of the theory adopted.

Lossless reciprocal symmetrical networks

It has been shown that, for a 2-port network[2],

$$\begin{bmatrix} b_i \\ b_o \end{bmatrix} = \begin{bmatrix} s_{11} & s_{12} \\ s_{21} & s_{22} \end{bmatrix} \begin{bmatrix} a_i \\ a_o \end{bmatrix} \quad \ldots\ldots\ldots\ldots (1)$$

where a_i and b_i are the incident and reflected parameters at the input and a_o and b_o those at the output, respectively, and the matrix

$$\begin{bmatrix} s_{11} & s_{12} \\ s_{21} & s_{22} \end{bmatrix} = \mathbf{S} \quad \ldots\ldots\ldots\ldots (2)$$

is the scattering matrix of the 2-port network; s_{11} is called the input reflection coefficient, s_{21} the forward transmission coefficient, s_{12} the reverse transmission coefficient, and s_{22} the output reflection coefficient.

Equation (1) can be written as

$$\begin{bmatrix} a_i \\ b_i \end{bmatrix} = \begin{bmatrix} \dfrac{1}{s_{12}} & \dfrac{-s_{22}}{s_{12}} \\ \dfrac{s_{11}}{s_{12}} & \dfrac{-|S|}{s_{12}} \end{bmatrix} \begin{bmatrix} b_o \\ a_o \end{bmatrix} = \mathbf{T} \begin{bmatrix} b_o \\ a_o \end{bmatrix} \quad \ldots\ldots (3)$$

where $|S|$ is the determinant of the matrix $\mathbf{S}$ defined by equation (2), and

$$\mathbf{T} = \begin{bmatrix} \dfrac{1}{s_{12}} & \dfrac{-s_{22}}{s_{12}} \\ \dfrac{s_{11}}{s_{12}} & \dfrac{-|S|}{s_{12}} \end{bmatrix} \quad \ldots\ldots\ldots\ldots (4)$$

The relation between the forward transmission coefficient s_{21} and the input reflection coefficient s_{11} is such that the sum of the squares of their magnitudes is unity, which necessarily implies that their phase difference is $\pi/2$. If θ is the phase angle of s_{21}, it can be shown that, for a lossless symmetrical network, equation (4) takes the form

$$\mathbf{T} = \begin{bmatrix} \dfrac{\exp(-j\theta)}{\sqrt{(1-|s_{11}|^2)}} & \dfrac{-j\,|s_{11}|}{\sqrt{(1-|s_{11}|^2)}} \\ \dfrac{j\,|s_{11}|}{\sqrt{(1-|s_{11}|^2)}} & \dfrac{\exp(j\theta)}{\sqrt{(1-|s_{11}|^2)}} \end{bmatrix} = \begin{bmatrix} A & B \\ C & D \end{bmatrix} \text{(say)} \quad \ldots (5)$$

SYMBOLS

λ = wavelength
a = incident parameter
b = reflected parameter
S = scattering matrix of the 2-port network
s_{11} = input reflection coefficient
s_{21} = forward transmission coefficient
s_{12} = reverse transmission coefficient
s_{22} = output reflection coefficient
θ = phase angle of s_{21}
n = number of sections
f = frequency
f_o = centre frequency
β = phase-change coefficient
l_s = length of a short-circuited stub
l_o = length of an open-circuited stub
l = half of the spacing between two consecutive stubs
α_1, α_2 = eigenvalues
Q = eigenvector
j = imaginary quantity

Fig. 1 shows a reversible symmetrical lossless four-terminal network, the input and output parameters of which are related as described in Reference 1:

$$\begin{bmatrix} a_i \\ b_i \end{bmatrix} = \begin{bmatrix} \exp(j\beta l) & 0 \\ 0 & \exp(-j\beta l) \end{bmatrix} \frac{1}{2\rho + 2} \begin{bmatrix} 3+\rho & 1-\rho \\ \rho - 1 & 1 + 3\rho \end{bmatrix} \begin{bmatrix} \exp(j\beta l) & 0 \\ 0 & \exp(-j\beta l) \end{bmatrix} \begin{bmatrix} b_o \\ a_o \end{bmatrix}$$

$$= \begin{bmatrix} \frac{3+\rho}{2\rho+2}\exp(j2\beta l) & \frac{1-\rho}{2\rho+2} \\ \frac{\rho-1}{2\rho+2} & \frac{1+3\rho}{2\rho+2}\exp(-j2\beta l) \end{bmatrix} \begin{bmatrix} b_o \\ a_o \end{bmatrix} \quad \ldots (6)$$

where ρ is the stub reflection coefficient.

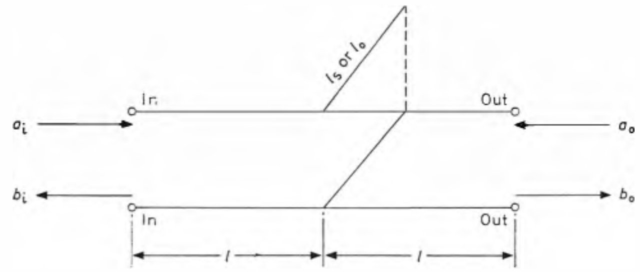

Fig. 1 Lossless symmetrical network

Thus, for the network shown in Fig. 1,

$$\mathbf{T} = \begin{bmatrix} \frac{1}{s_{21}} & \frac{-s_{22}}{s_{21}} \\ \frac{s_{11}}{s_{21}} & \frac{-|S|}{s_{21}} \end{bmatrix} = \begin{bmatrix} \frac{3+\rho}{2\rho+2}\exp(j2\beta l) & \frac{1-\rho}{2\rho+2} \\ \frac{\rho+1}{2\rho+2} & \frac{1+3\rho}{2\rho+2}\exp(-j2\beta l) \end{bmatrix} \quad \ldots\ldots\ldots\ldots (7)$$

For n such networks connected in cascade, the matrix of the resultant network, worked out in the Appendix, is

$$\mathbf{T}^n = \begin{bmatrix} \frac{1}{s_{21c}} & \frac{-s_{22c}}{s_{21c}} \\ \frac{s_{11c}}{s_{21c}} & \frac{-|S_c|}{s_{21c}} \end{bmatrix}$$

$$= \frac{|s_{11}|}{2j\sqrt{p}} \begin{bmatrix} -\frac{\sin\theta}{|s_{11}|}(\alpha_1^n - \alpha_2^n) + \frac{j\sqrt{p}}{|s_{11}|}(\alpha_1^n + \alpha_2^n) & -(\alpha_1^n - \alpha_2^n) \\ (\alpha_1^n - \alpha_2^n) & \frac{\sin\theta}{|s_{11}|}(\alpha_1^n - \alpha_2^n) + \frac{j\sqrt{p}}{|s_{11}|}(\alpha_1^n + \alpha_2^n) \end{bmatrix} \quad \ldots\ldots (8)$$

where the suffix c indicates the overall parameters of the cascaded network, and p is given by equation (21).

Forward transmission coefficient

The forward transmission coefficient s_{21c} of a line comprising n sections terminated in a load equivalent to the characteristic impedance of the line is obtained from equation (8):

$$1/s_{21c} = \frac{|s_{11}|}{2j\sqrt{p}}\left\{-\frac{\sin\theta}{|s_{11}|}(\alpha_1^n - \alpha_2^n) + \frac{j\sqrt{p}}{|s_{11}|}(\alpha_1^n + \alpha_2^n)\right\}$$

$$= \frac{\alpha_1^n + \alpha_2^n}{2} + j\frac{(\alpha_1^n - \alpha_2^n)\sin\theta}{2\sqrt{(|s_{11}|^2 - \sin^2\theta)}} \quad \ldots\ldots\ldots\ldots (9)$$

Since $\rho = \exp(j\theta_S) = \cos\theta_S + j\sin\theta_S$, where $\theta_S = \pi - 2\beta l_s$ for a short-circuited stub of length l_s and $\theta_S = 2\pi - 2\beta l_o$ for an open-circuited stub of length l_o, we have, from equation (7),

$$s_{21} = |s_{21}|\angle\theta = \frac{2(\cos\theta_S + 1 + j\sin\theta_S)(\cos 2\beta l - j\sin 2\beta l)}{3 + \cos\theta_S + j\sin\theta_S}$$

from which

$$|s_{21}| = \sqrt{\left[\frac{4(1+\cos\theta_S)}{5 + 3\cos\theta_S}\right]} \quad \ldots\ldots\ldots (10)$$

and

$$\theta = \tan^{-1}\frac{3\sin(\theta_S - 2\beta l) - 4\sin 2\beta l - \sin(\theta_S + 2\beta l)}{3\cos(\theta_S - 2\beta l) + 4\cos 2\beta l + \cos(\theta_S + 2\beta l)} \quad \ldots\ldots (11)$$

Thus,

$$|s_{11}| = \sqrt{(1 - |s_{21}|^2)} = \sqrt{\left(\frac{1-\cos\theta_S}{5 + 3\cos\theta_S}\right)} \quad \ldots\ldots (12)$$

Once $|s_{11}|$ and θ are found, α_1 and α_2 can be determined from equation (15). The forward transmission coefficient of the cascaded network, s_{21c}, can then be evaluated by substituting the values in equation (9).

Effect of stubs shunted across a matched line

The formulas derived in the previous section were programmed on an Atlas digital computer to determine the effect of stubs of various lengths with different spacings on the transmission of power on a line feeding a matched load. The variation in magnitude of the forward transmission coefficient with frequency for $\lambda/8$ short-circuited stubs spaced at $\lambda/4$ (i.e. $l = \lambda/8$) intervals is shown in Fig. 2. All the curves start from zero at zero frequency, as expected, since no power reaches the load because of the short circuits. $|s_{21c}|$ remains at zero for a larger initial range of frequency for higher values of n, because then the input conductance remains at zero and the susceptance maintains a high value for that frequency range. The rise of $|s_{21c}|$ becomes steeper for higher values of n because the change in susceptance from a high value to zero, and that of the conductance from zero to unity, are accomplished in a shorter frequency span. For $n = 1$, the coefficient gradually rises with frequency and reaches unity at $f = 2f_0$. For a system consisting of many sections, the magnitude of ripples with the normalized frequency range 0 to 2 as many times as the number of sections involved, reaching unity at the peaks of the ripples. This is because the conductance part of the input admittance of the line reaches unity, and the susceptance becomes zero, in the frequency range as many times as the number of sections. The maximum depth of the ripple is found to increase with n, because between two consecutive peaks the line susceptance assumes a higher value for a large number of sections. Again, this value is greater in the lower-frequency range, and so causes maximum depth of the ripple to occur immediately after the first peak. The response beyond $2f_0$ can be shown to be the exact image replica of the corresponding curve below that frequency, suggesting that such a transmission line can be used as a bandpass filter.

Fig. 3 shows the frequency response for a line with $l = 3\lambda/8$ and $l_s = \lambda/8$. The magnitude of the ripples being very large throughout, a line consisting of such sections can hardly transmit any band of frequencies over it. Still less acceptable lines are those supported by $\lambda/8$ short-circuited stubs spaced at $5\lambda/4$, as may be seen from Fig. 4.

A large number of combinations of l, l_s and n were cycled in the computer, and it was found from the computed response curves that supporting a transmission line with stubs of random lengths and spacings renders the

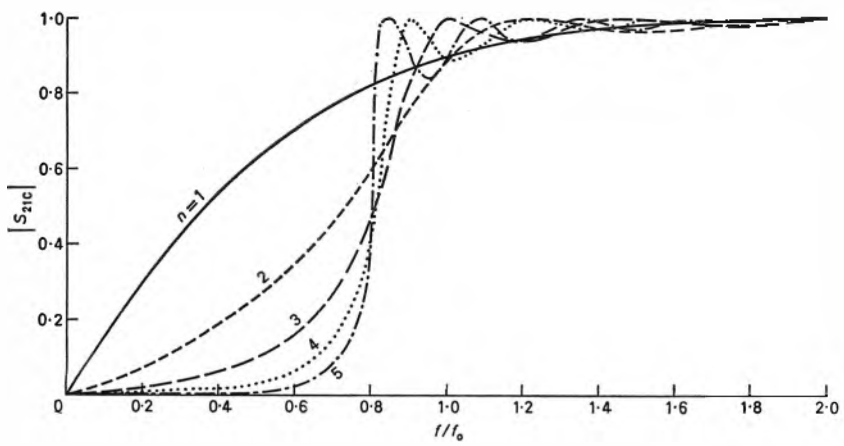

Fig. 2 Forward transmission coefficient with $l=\lambda/8$ and $l_s=\lambda/8$

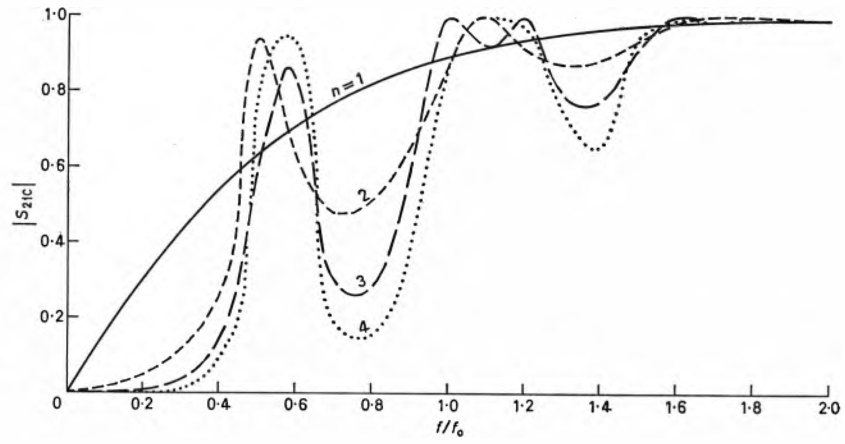

Fig. 3 Forward transmission coefficient with $l=3\lambda/8$ and $l_s=\lambda/8$

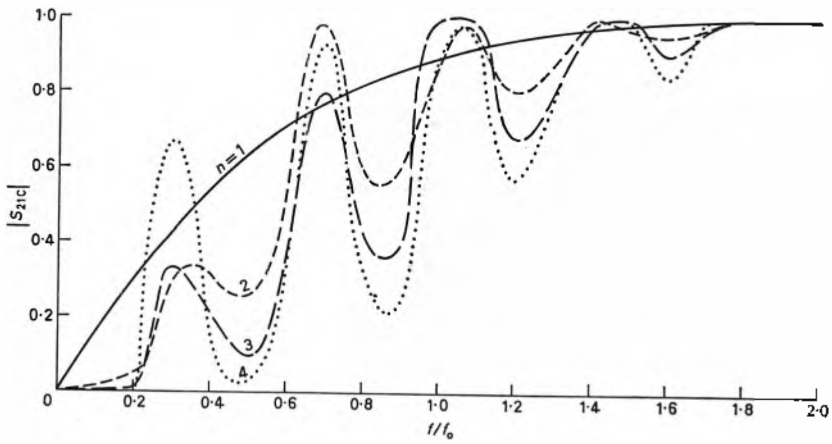

Fig. 4 Forward transmission coefficient with $l=5\lambda/8$ and $l_s=\lambda/8$

line unsuitable for carrying any considerable band of frequencies over it.

Optimum stubs

Having found how different lengths of stubs having different spacings affect the transmission of power on a long line terminated in a matched load, it was required to design the optimum line which could transmit the maximum bandwidth. In a program, the effect of the variation of stub spacing with stub lengths fixed at $\lambda/8$, for a line consisting of n sections, was determined. From the resulting curves (some shown in Fig. 5), it was found that $l=\lambda/8$ gives the best result. In another program keeping the spacings fixed at $\lambda/4$, the effect of different stub lengths was computed and $\lambda/8$ short-circuited stubs were found to be optimum (Fig. 6).

Thus, for a matched load, $\lambda/8$ short-circuited stubs spaced $\lambda/4$ apart constitute a line that can transmit the widest possible bandwidth. This conclusion, although based on $n=4$, holds for $n=20$ and more.

Practical observations

It was intended to verify experimentally the performance of a transmission line expected from the analysis carried out in this article. The experiment was carried out in the frequency range 65-900MHz on an air line of charac-

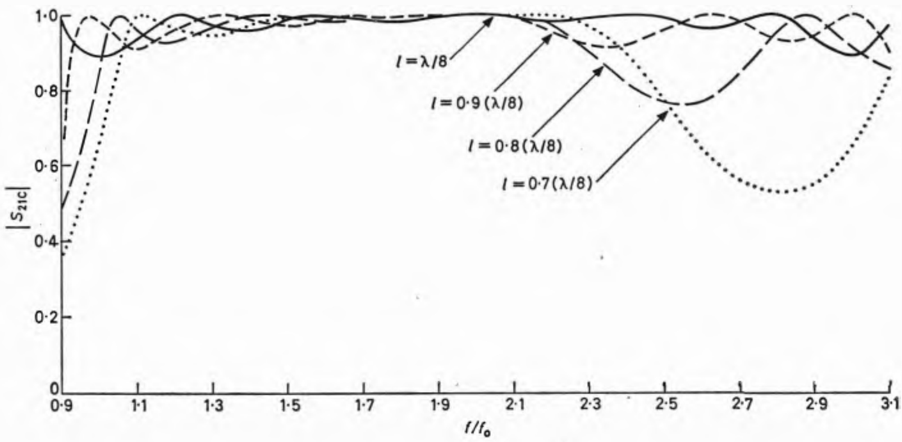

Fig. 5. Forward transmission coefficient with $l_s=\lambda/8$ and l varying ($n=4$)

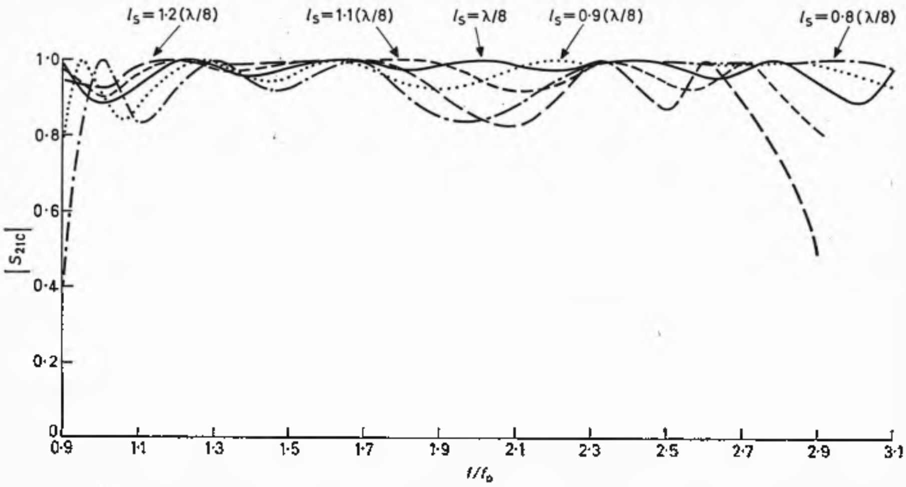

Fig. 6. Forward transmsision coefficient with $l=\lambda/8$ and l_s varying ($n=4$)

teristic impedance 50Ω terminated also in a 50Ω load for one, two, three and four symmetrical sections, two such being shown in Fig. 7(a). The lengths of the air lines, T-connectors, and stubs were measured on a slotted line, and the signal generators and local oscillators shown in Fig. 7(b) were calibrated beforehand; x-x' in Fig. 7(b) shows the point of insertion of the line sections.

The frequency responses of the sections measured by the substitution method were plotted against the corresponding curves obtained theoretically using the computer; Fig. 8 shows one such plot. The dimensions indicated in Fig. 7(a) were based on the slotted-line measurements with a 400MHz signal, for convenience. The effective stub separation of 27·6cm was taken as a quarter-wavelength, for which the centre frequency was 272MHz. If, however, the measurements could be carried out with a signal of 272MHz, the stub separation was likely to have a different value; this explains a slight tilt in the experimental curve in Fig. 8.

Ignoring the difference between the theoretical and the practical observations in the maximum depth of the ripple in the passband, due possibly to the crudeness of measurements, it may be observed that the passband patterns in the two cases are similar, in that they have almost the same outlines and exactly the same number of ripples.

Conclusions

The scattering matrix and the concept of symmetrical sections forming a transmission line have been asserted as convenient tools in designing a lossless line with the aid of a digital computer. Mental calculation with the

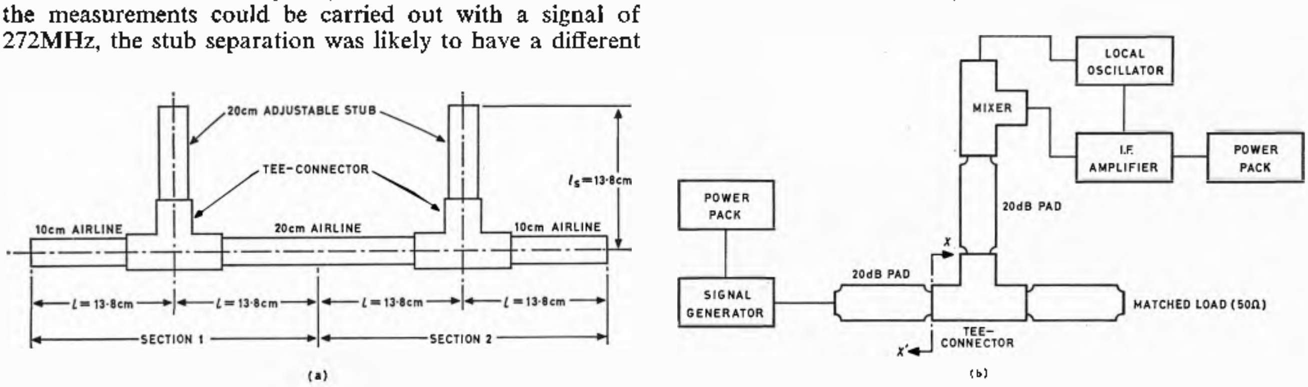

Fig. 7 Apparatus for the measurement of forward transmission coefficient

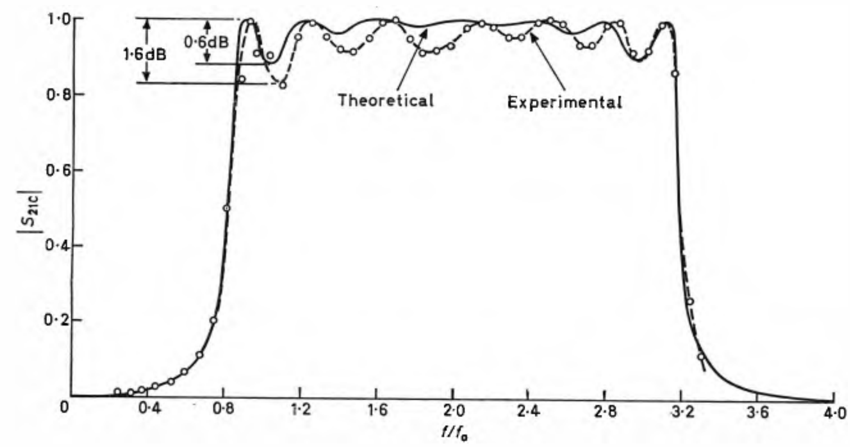

Fig. 8. Forward transmission coefficient with $l = \lambda/8$ and $l_s = \lambda/8$ for $n = 4$

Smith chart and the human effort involved in arriving at the best design would have been extremely laborious, if not impossible, for longer lines. Laboratory experiments carried out on 50Ω air lines in the frequency range 65-900MHz have revealed that the performance of these lines is very nearly similar to that expected from the theory developed and the computation undertaken. The computed results have been occasionally checked by the Smith chart to ensure their accuracy. The theory developed in this article can be extended to cover the design aspects of stub-supported long lines terminated in any unmatched loads.

Acknowledgements

The author is grateful to the Government of India for financing the project and to Prof. C. Adamson for providing research facilities in the Department of Electrical Engineering and Electronics, the University of Manchester Institute of Science and Technology. Sincere thanks are due to C. S. Gledhill for supervising the work, and to O. P. D. Cutteridge, of the University of Leicester, for helpful discussions. Finally, the author is grateful to the University of Manchester Institute of Science and Technology for permission to submit the article.

REFERENCES

1 SAHA, J. N.: Analysis of stub matching by scattering-matrix methods. *Electronic Engng.* 39, 571-575 (1967)
2 KUO, F. F.: *Network analysis and synthesis*. Wiley (1964)
3 PURCELL, E. M., MONTGOMERY, C. G., and DICKE, R. H.: *Principles of microwave circuits*. McGraw-Hill (1948)
4 TROPPER, A. M.: *Matrix theory for electrical engineering students*. Harrap (1962).

APPENDIX

Cascaded connexion of symmetrical networks

If a number of the networks shown in Fig. 1 were connected in cascade, the output parameters of a network would be the input parameters of the next section. It has been shown[3] that the resultant network of n sections has a matrix $\mathbf{T}^n$, where $\mathbf{T}$ is the matrix of an individual network given by equation (7). The eigenvalues of the matrix in equation (5) are the roots of the equation

$$\begin{vmatrix} (A-\alpha) & B \\ C & (D-\alpha) \end{vmatrix} = 0 \quad \ldots\ldots\ldots\ldots \quad (13)$$

It may be seen from equation (5) that

$$AD - BC = 1$$

so that, from equation (13),

$$\alpha^2 - \alpha(A+D) + 1 = 0 \quad \ldots\ldots\ldots\ldots \quad (14)$$

which gives

$$\alpha = \frac{A+D \pm \sqrt{[(A+D)^2-4]}}{2} = \frac{\cos\theta \pm \sqrt{(|s_{11}|^2 - \sin^2\theta)}}{\sqrt{(1-|s_{11}|^2)}} \quad (15)$$

The two values of α are α_1 with the addition and α_2 with the subtraction.

The diagonal matrix Δ is given by

$$\Delta = \begin{bmatrix} \alpha_1 & 0 \\ 0 & \alpha_2 \end{bmatrix} \quad \ldots\ldots\ldots\ldots\ldots\ldots \quad (16)$$

Let $\begin{bmatrix} q \\ 1 \end{bmatrix}$ be an eigenvector corresponding to the eigenvalue α:

$$(A-\alpha)q + B = 0$$

$$Cq + D - \alpha = 0$$

Eliminating α,

$$Cq^2 + (D-A)q - B = 0$$

which gives

$$q = \frac{-\sin\theta \pm j\sqrt{(|s_{11}|^2 - \sin^2\theta)}}{|s_{11}|} \quad \ldots\ldots\ldots \quad (17)$$

The matrix with $\begin{bmatrix} q_1 \\ 1 \end{bmatrix}$ and $\begin{bmatrix} q_2 \\ 1 \end{bmatrix}$ as the column vectors is given by

$$\mathbf{Q} = \begin{bmatrix} q_1 & q_2 \\ 1 & 1 \end{bmatrix} \quad \ldots\ldots\ldots\ldots\ldots\ldots \quad (18)$$

From matrix theory[4],

$$\mathbf{T}^n = \mathbf{Q}\Delta^n\mathbf{Q}^{-1} \quad \ldots\ldots\ldots\ldots\ldots \quad 19)$$

Substituting the values,

$$\mathbf{T}^n = \frac{|s_{11}|}{2j\sqrt{p}} \begin{bmatrix} -\frac{\sin\theta}{|s_{11}|}(\alpha_1^n - \alpha_2^n) + \frac{j\sqrt{p}}{|s_{11}|}(\alpha_1^n - \alpha_2^n) & -(\alpha_1^n - \alpha_2^n) \\ \alpha_1^n - \alpha_2^n & \frac{\sin\theta}{|s_{11}|}(\alpha_1^n - \alpha_2^n) + j\frac{\sqrt{p}}{|s_{11}|}(\alpha_1^n + \alpha_2^n) \end{bmatrix} \quad \ldots\ldots\ldots \quad (20)$$

where $\quad p = |s_{11}|^2 - \sin^2\theta \quad \ldots\ldots\ldots\ldots\ldots \quad (21)$

Thermistor powermeter

by **S. M. Bozic,** Ph.D., and **J. R. Whitbread,** B.Sc.

The powermeter described here uses, as a sensing element, a thermistor whose heating power is kept almost constant by means of a feedback system. The circuit is analysed and its main features are discussed. A fully transistorized practical circuit is also given. It exhibits a true power law up to 10mW over the frequency range 100Hz to 10MHz. The effects of ambient-temperature variations have been considered and made negligible over the range 0 to +55°C. The circuit time-constant of 18s is defined by the thermistor.

(Voir page 664 pour le résumé en français: Zusammenfassung in deutscher Sprache auf Seite 665)

THE power content of both random and nonrandom waveforms is an important quantity which often needs to be measured. It has a particular significance for noise, where it represents the second moment (or mean square) of a statistical distribution, and fully describes it if the process is Gaussian. Power measurement consists essentially in squaring and integration or smoothing operations. The latter is usually achieved by an *RC* smoothing network or by a moving-coil meter. The integration time is an important quantity which affects the accuracy of filtered-noise measurements; this is usually expressed in terms of the filter-bandwidth observation-time product[1]. When the filter bandwidth is very narrow, special integrating circuits are required which amplify the *RC* time constant.

The squaring operation is often approximated by means of a nonlinear element, such as a diode operated in a suitable region of its characteristic, but the signal is restricted to low levels[2,3]. The thermocouple is an alternative device for power measurement, but it has the disadvantage of being slow and easily damaged by overload. A true mean-square voltmeter has been developed by Campbell[4], using a feedback circuit. The sensing element in this circuit is a thermionic diode, and valves are used in the associated d.c. amplifier. A modification of this circuit, using a transistorized a.c. amplifier, has been made[5]. Both instruments require high-voltage d.c. stabilized supplies.

The authors have developed a further version of Campbell's circuit, in which a thermistor is used as the sensing element and the associated d.c. amplifier is fully transistorized. A 20V power supply is used for this instrument. The principle of operation, practical realization of the circuit and its performance are described.

Principle of the circuit

The basic circuit of the powermeter is shown in Fig. 1; the essential parts for power measurement are on the left-hand side. An indirectly heated thermistor TH_1, is connected *via* the resistor $R_1 \gg R_t$ to a supply direct voltage V. The voltage developed across R_t is applied to the input of amplifier A. The output current I_f from terminal 3 of the amplifier is fed back to the heater resistance R_h *via* the resistor R; the input waveform is applied *via* the capacitor C to the same heater. This capacitor prevents direct-current flow into the signal source and the resistor $R \gg R_h$ prevents a.c. current loss into the feedback path. The circuit is arranged in such a manner that the heater power remains very nearly constant. This property will be proved by means of a simple analysis. The thermistor has two heating sources, one constant derived from the current I_1 in R_t, and another from the currents i and I_f in the heater resistance R_h. If the heating power remains almost constant, a linear approximation for the thermistor characteristic can be written as

$$r_t = R_t - R_{t0} = -a(\overline{P_h - P_{h0}}) = -a\overline{p_h} \;\ldots\ldots\; (1)$$

where r_t is the change in the thermistor resistance from the value R_{t0} to R_t, due to application of an external current i causing a heater-power change from P_{h0} to P_h. The parameter a is the slope of the thermistor characteristic $R_t(P)$ at the operating point defined by P_{h0} and I_1.

The thermistor performs both squaring and smoothing operations by virtue of its thermal properties; therefore

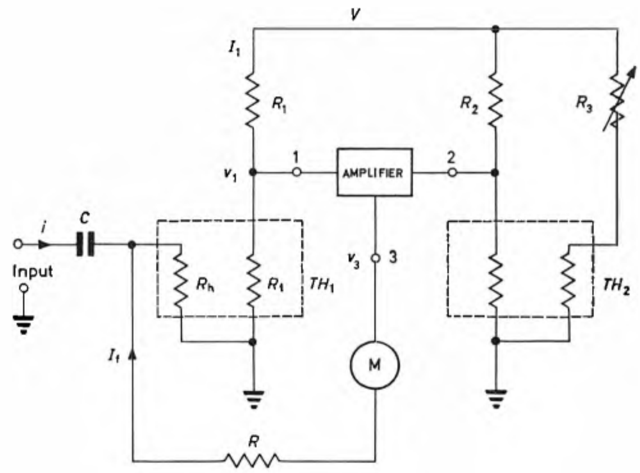

Fig. 1 Basic circuit

the change in heating power represents the mean power, which can be expressed as

$$\overline{p_h} = \overline{P_h - P_{h0}} = \overline{R_h[(I_f+i)^2 - I_{f0}^2]}$$
$$= R_h(i_f^2 - 2I_{f0}i_f + \overline{i^2}) \;\ldots\ldots\; (2)$$

where $I_f = I_{f0} - i_f$; i_f is the feedback-current change due to application of the external current i. It should be noticed here that the current i is a relatively fast varying function of time with zero mean value, i.e. $\bar{i} = 0$. However, the feedback current I_f is a very slowly varying quantity, practically constant due to smoothing action of the circuit; therefore the term

$$2\overline{I_f i} = 2I_f\bar{i} = 0 \;\ldots\ldots\ldots\ldots\ldots\; (3)$$

in expression (2).

The voltage change at the input of the amplifier due to change in thermistor resistance is

$$v_1 \simeq (V/R_1)r_t = -aI_1\overline{p_h} \;\ldots\ldots\ldots\; (4)$$

where the approximation $R_1 \gg R_t$ has been used and I_1 represents the current through the resistor R_1.

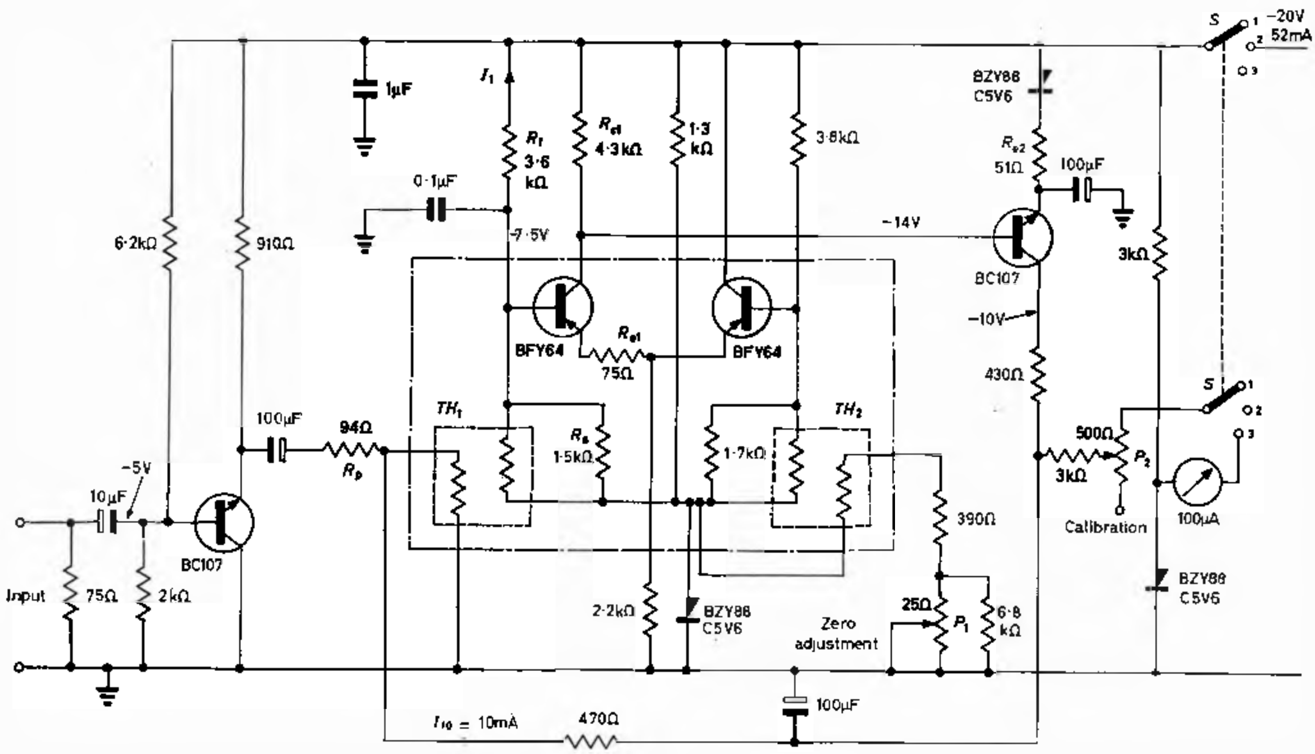

Fig. 2 Thermistor-powermeter circuit

The feedback current can be written directly as

$$i_f = \frac{v_3}{R + R_h} = \frac{Av_1}{R + R_h}$$

$$= -\frac{aI_1AR_h}{R + R_h}\,(i_f^2 - 2I_{f0}i_f + \overline{i^2}) \quad \ldots\ldots\ldots\ (5)$$

where A represents voltage gain between terminals 1 and 3, and v_1 has been substituted from equations (4) and (2). From equation (5), the change in the feedback current satisfies the quadratic equation

$$i_f^2 - 2I_{f0}[1-(1/L)]i_f + \overline{i^2} = 0 \quad \ldots\ldots\ (6)$$

where

$$L = 2aI_1I_{f0}A\,\frac{R_h}{R + R_h} \quad \ldots\ldots\ (7)$$

It is shown in Appendix 1 that the quantity L represents the loop gain of the circuit. The solution of equation (6) is

$$i_f = I_{f0}[1-(1/L)]\left\{1 - \left[1 - \frac{\overline{i^2}}{I_{f0}^2[1-(1/L)]^2}\right]^{\frac{1}{2}}\right\} \quad \ldots\ (8)$$

which, for large loop gain L, simplifies to

$$I_f^2 + \overline{i^2} = I_{f0}^2 \quad \ldots\ldots\ldots\ (9)$$

where $I_f = I_{f0} - i_f$ has been used. Equation (9) shows that, when the loop gain is large, the circuit keeps the thermistor-heater power constant. This is usually taken as a starting point in describing this type of circuit. Further, from equation (9),

$$i_f \simeq \overline{i^2}/2I_{f0} \quad \ldots\ldots\ldots\ (10)$$

where it has been assumed that $\overline{i^2} \ll I_{f0}^2$. The resulting equation (10) shows that the change in feedback current i_f is directly proportional to the mean-square current of the applied signal.

The above analysis is simplified, and the effects of ambient-temperature variations on the circuit, and particularly the thermistor, have not been considered. In order to compensate for these, the input part of the amplifier has been arranged in a balanced structure, in which another thermistor TH_2 has been added, Fig. 1. The characteristics of the thermistors TH_1 and TH_2 should be identical ideally; however, in practice, a reasonable degree of equalization can be achieved by shunting the thermistors, as will be seen later. The variable resistor R_3 in Fig. 1 can be used for the initial zero adjustments.

Practical circuit and results

Realization of a practical circuit is shown in Fig. 2, where the basic elements from Fig. 1, discussed in the previous section, may be recognized. The thermistors are type B24 (STC), having a heater resistance $R_h = 100\Omega$. The amplifier consists of a balanced emitter-coupled pair followed by a common-emitter stage. The a.c. input waveform is fed into the heater of TH_1 through a buffer common-collector stage and resistor R_p. This stage allows a high input impedance if required (removing the 75Ω termination). The meter is arranged in a bridge circuit and can be balanced to zero for $i = 0$, by means of the potentiometer P_1. Full-scale deflection (f.s.d.) or sensitivity can be set up by means of the potentiometer P_2. One of the 100μF capacitors is used to prevent oscillations. The expression for the loop gain of the circuit in Fig. 2 is given in Appendix 2, and it is shown that it is typically 390.

The zero-signal feedback current $I_{f0} = 10$mA has been chosen as a convenient value, since maximum transistor dissipation is 40mW. The instrument has been designed to have f.s.d. for an input power of 10mW (into 75Ω). In this case, with a value of $R_p \simeq 100\Omega$, the heater a.c. power is 1·6mW while $P_{h0} = 10$mW (therefore $\overline{i^2}/I_{f0}^2 \simeq 0{\cdot}16$ for f.s.d.). The power law has been checked by measuring the input power of a sinusoidal signal ($f = 120$kHz) in a calibrated powermeter (GEC) and comparing the meter reading (P_m). The result is shown in Fig. 3 for $P_{in} \leqslant 10$mW

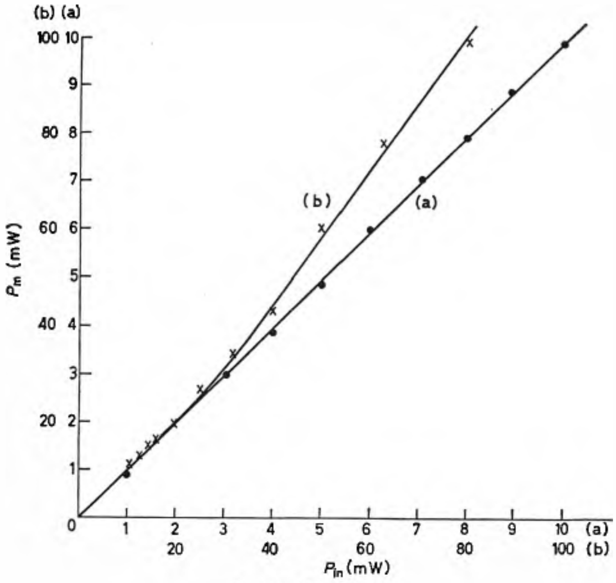

Fig. 3 Power law

(curve 1) and also for $P_{in} \leqslant 100$mW (curve 2). For $P_{in} > 10$mW, the meter was shunted, to decrease its sensitivity by a factor of 10. It is interesting to note that the power law breaks down for $P_{in} \simeq 20$mW, i.e. $I^2/I_{f0}^2 = 0{\cdot}32$. However, it can be extended by increasing the value of the resistor R_p. The time constant of the circuit ($T \simeq 18$s) is defined by the thermistors. The frequency response is flat, and falls by 0·3dB at 100Hz and 10MHz. The bandwidth is mainly controlled by the input stage and associated elements: the low frequencies by the coupling capacitors, and the high frequencies by the choice of transistor and its configuration, and also by the thermistor and general layout.

To minimize the effects of ambient-temperature changes, two thermistors are used as described in the previous section. However, it was found that the thermistors have to be enclosed in a metal can, shown in Fig. 2, with ¼in-thick polyurethane foam as a thermal insulation against the effects of the short-term ambient-temperature changes. The percentage zero drift, $\epsilon_0(T_A)$ for the temperature range 0 to +55°C, is shown in Fig. 4 (curve 1). The large error at low temperatures is due to greater thermistor differences at low temperatures. Considerable improvement has been obtained by shunting the thermistors with normal resistors, Fig. 4 (curve 2). This

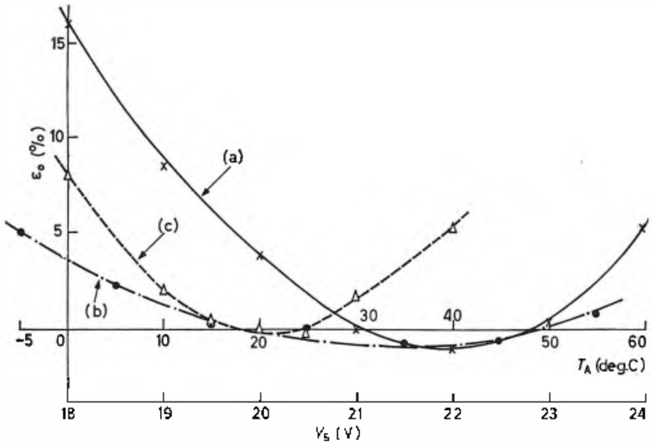

Fig. 4 Zero drift with temperature T_A and supply voltage V_s
(a), (b) $\epsilon_0(T_A)$ (c) $\epsilon_0(V_s)$

arrangement decreases the loop gain, as shown in Appendix 2: however, this is not serious since the loop gain is already large. Zero drift with respect to supply direct-voltage variations $\epsilon_0(V_s)$ is also shown in Fig. 4 (curve 3). It is seen that a $\pm 0{\cdot}5$V variation from 20V produces a zero drift of approximately 0·5%. For larger changes, it increases, but a simple supply stabilizer would be sufficient to prevent this. All relative changes in Fig. 4 are referred to the meter f.s.d. of 10mW.

It has been found that precautions should be taken to avoid d.c.-supply transients damaging the meter while switching on or off. The switch in Fig. 2 is so arranged that, in position 2, the d.c. supply is on, but the meter is still disconnected. There should be a delay of about 15s, to allow for the transients to die out, before switching to position 3. Similarly the switch should be always turned to the position 1 before disconnecting the external d.c. supply.

Acknowledgments

The authors wish to thank G.E.C. (Telecommunications) Ltd for the permission to publish this article. Thanks are also due to T. Goodison for the experimental work.

REFERENCES

1 MIDDLETON, D.: *Introduction to statistical theory of communication*, Chap. 16. McGraw-Hill (1960)
2 BULL, C. S.: The diode as an a.c. voltmeter, *J. Sci. Instrum.* 24, 254-256 (1947)
3 BURGESS, R. E.: The measurement of fluctuation noise by diode and anode-bend voltmeters. *Proc. Phys. Soc. B.*, 508-518 (1951)
4 CAMPBELL, R. D.: Diotron—an aid to r.m.s. instrumentation, *Electronics*, 93-95 (July 1950)
5 BOZIC, S. M.: Mean-square voltmeter, *J. Sci. Instrum.*, 210-213 (May 1962)

APPENDIX 1

To determine the open-loop gain, the loop is broken at the input of the amplifier and a voltage ΔV_0 is injected. The incremental quantities used in this analysis are very slow time varying, i.e. their time-constants are much

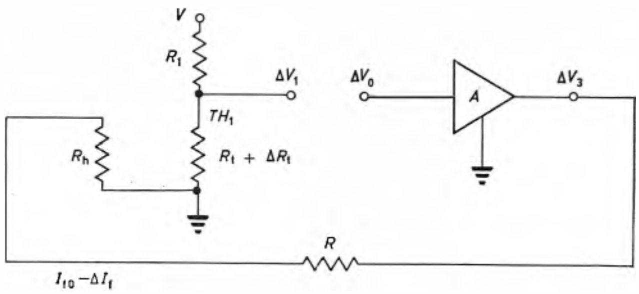

Fig. 5 Open loop

greater than that of the thermistors. Therefore no averaging or smoothing by the thermistor takes place. Starting with ΔV_0,

$$\Delta I_f = \frac{A}{R + R_h} \Delta V_0$$

The power increment in the thermistor is

$$\Delta P_h = P_h - P_{h0} = R_h[(I_{f0} - \Delta I_f)^2 - I_{f0}^2]$$
$$\simeq -2R_h I_{f0} \Delta I_f$$

since ΔI_f can be made very small. The power increment ΔP_h causes change of the thermistor resistance $\Delta R_t = -a\Delta P_h$ producing the voltage

$$\Delta V_1 \simeq (V/R_1)\Delta R_t = I_1 \Delta R_t = -aI_1 \Delta P_h$$

where $R_1 \gg R_t$ has been assumed. Substituting for ΔI_f in ΔP_h and further for ΔP_h in the above,

$$L = \frac{\Delta V_1}{\Delta V_0} = 2aI_1 I_{f0} A \frac{R_h}{R + R_h}$$

which proves that the quantity in expression (7) represents the loop gain of the circuit.

APPENDIX 2

In order to evaluate the loop gain of the circuit in Fig. 2, the voltage gain A and the effect of the shunt resistor R_s on the thermistor TH_1 must be determined. The voltage gain follows directly from Fig. 2:

$$A \simeq \frac{\beta R_{c1}(R+R_b)}{R_{e1}(R_{c1}+\beta R_{e2})}$$

where β is the current gain of the output transistor. The effect of R_s can be found from

$$r_{ts} = \frac{R_t R_s}{R_t + R_s} - \frac{R_{t0} R_s}{R_{t0}+R_s} = \frac{r_t}{1 + (R_{t0}/R_s)^2}$$

This can be expressed more conveniently as a modified value of the slope:

$$a_s = \frac{a}{1 + (R_{t0}/R_s)^2}$$

Substituting A and a_s into expression (7), the approximate loop gain in Fig. 2 becomes

$$L \simeq \frac{2aI_1I_{t0}}{1 + (R_{t0}/R_s)^2} \frac{\beta R_{c1} R_b}{R_{e1}(R_{c1}+\beta R_{e2})}$$

Note that L does not depend on the feedback-path resistance, since the meter-circuit resistance is so much greater.

The value of a is found from the manufacturer's data, $R_t(P)$, for P = 14mW, to be 130Ω/mW, and R_{t0} = 1kΩ. A typical numerical value of the loop gain, for the circuit in Fig. 2, is L = 390 for β = 100.

Analysis of the capacitance error of a m.i.s.f.e.t. chopper modulator

by **J. Dostál**, *Research Institute for Mathematical Machines, Prague*

The article discusses and analyses the interelectrode capacitance as a source of error in the metal-insulator-semiconductor field-effect transistor when used as a chopper modulator.

(Voir page 664 pour le résumé en français: Zusammenfassung in deutscher Sprache auf Seite 666)

THE dominant error source of the metal-insulator-semiconductor field-effect transistor (m.i.s.f.e.t.) as a solid-state chopper is the interelectrode capacitance of its drive and switching electrodes. In general, this depends on properties of the whole cascade modulator, amplifier and demodulator. The following considerations relate to the most common configuration, shown in Fig. 1. The modulator consists of a series resistor R and a shunt chopper transistor VT with grounded source and substrate. The transistor is driven by the square-wave voltage v_G [Fig. 2(a)] with a mark/space ratio $k = T_{off}/T_{on}$, where T_{on} and T_{off} are durations of the ON and OFF states, respectively. The corresponding values of its differential resistance are r_{on} and r_{off}, and the instantaneous value is r. The amplifier A has a d.c. gain A_0, a dominant time constant τ, an input resistance R_i, and zero output resistance. The demodulator switch S is operated synchronously with the modulator switch; its ON and OFF resistances are

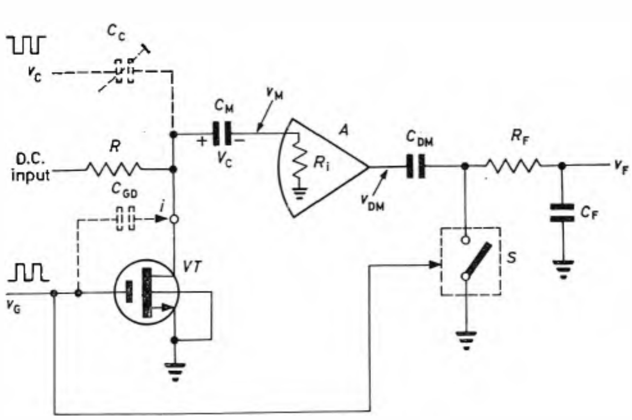

Fig. 1 Basic arrangement of chopper amplifier

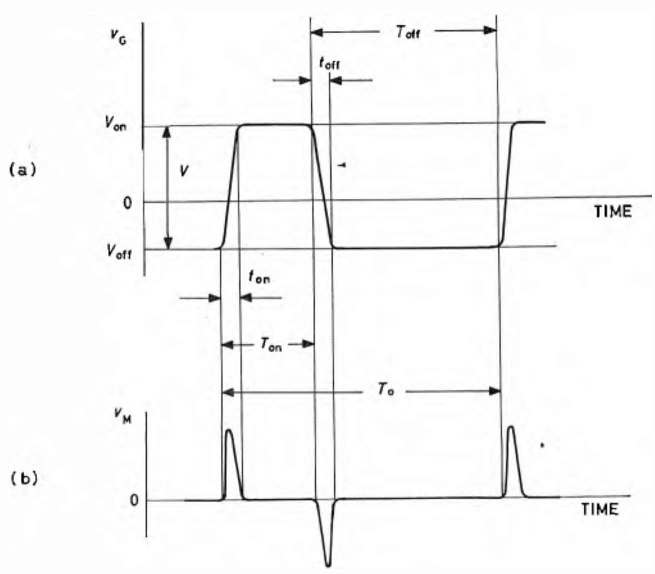

Fig. 2 Waveforms of (a) the drive voltage and (b) the induced spikes

zero and infinity. The coupling capacitors are large enough to neglect their discharge within T_{on} and T_{off} (C_M) or within T_{off} (C_{DM}); the time constant of the output filter is $C_F R_F \gg T_0 = T_{on} + T_{off}$.

The presence of an interelectrode gate-drain capacitance of VT gives rise to voltage spikes v_M [Fig. 2(b)] superimposed on the regular squarewave modulator output voltage. Even if overloading of the end stages of the amplifier by these spikes were prevented, the capacitance could result in modulator drift in the following ways. An inflowing capacitive current could charge C_M, the steady voltage of which is then evaluated as corresponding d.c. input voltage; as will be shown, this does not occur in the modulator under consideration. The second way depends on transmission of the spikes by the amplifier and evaluating their area by the demodulator.

Compared with the drive-voltage peak-to-peak value V, the amplitude of the induced spikes is very small, and hence $i = c_{GD}(dv_G/dt)$, where c_{GD} is the differential gate-drain capacitance. With grounded modulator input, the instantaneous magnitude of v_M is therefore

$$v_M = R\|R_i\left[c_{GD}\frac{\rho}{\rho+1}dv_G/dt - V_C/R\left(1 + \frac{R}{R_i(\rho+1)}\right)\right] \quad \ldots\ldots\ldots\ldots (1)$$

where V_C is the steady voltage on C_M and $\rho = r/R\|R_i$ is the relative resistance of the chopper. In the steady state, the following equation is satisfied:

$$\int\limits_{T_0} c_{GD}\frac{\rho}{\rho+1}dv_G/dt\ dt - V_C/R\int\limits_{T_0}\left(1 + \frac{R}{R_i(\rho+1)}\right)dt = 0$$

Assuming that ρ and c_{GD} follow the changes in v_G without delay, the value of the first integral is zero, and hence

$$V_C = 0 \quad \ldots\ldots\ldots\ldots\ldots\ldots\ldots (2)$$

The areas of the positive and negative spikes cancel each other, and outside the turn-on and turn-off times t_{on} and t_{off}, the output voltage v_M is zero, as shown in Fig. 2(b). This fact is conditioned by the assumption made which is fulfilled by m.i.s.f.e.t.s provided that the times t_{on} and t_{off} are of the order of $1\mu s$ (i.e. much greater than the time-constant of forming the channel), which, however, need not be accomplished in those cases where the dependence of ρ and/or c_{GD} on v_G is associated with a considerable time-lag of linear or delay character, as for example in bipolar transistors.

During the transmission of v_M by the amplifier, its instantaneous output voltage v_{DM} is given by $\tau\dot{v}_{DM} + v_{DM} = A_0 v_M$. Provided that τ, t_{on}, $t_{off} \ll T_0$ (with respect to the overall gain, the opposite case is inconvenient), it is possible to assume that the transients at the amplifier output will finish within T_{on} and T_{off}. Consequently, it is in the OFF state and

$$\int\limits_{(T_{off})}(\tau\dot{v}_{DM} + v_{DM})\,dt = \int\limits_{(T_{off})} v_{DM}\,dt = A_0\int\limits_{(t_{off})} v_M\,dt \ldots (3)$$

regardless of $\tau \ll T_0$. The output filter produces a voltage

$$v_F = 1/T_0\int\limits_{(T_{off})} v_{DM}\,dt = A_0 f_0\int\limits_{(t_{off})} v_M\,dt =$$

$$A_0 f_0 R\|R_i\int\limits_{V_{on}}^{V_{off}}\frac{c_{GD}}{1+1/\rho}dv_G$$

in accordance with equation (1), (2) and (3). The last integral will be solved using an approximation of the voltage-dependent differential capacitance c_{GD} by its average value C_{GD} in the range $V_{off} \leqslant v_G \leqslant V_{on}$, on the assumption of a control characteristic in the form[1]

$$1/r = g_0 + K(v_G - V_T) \quad \ldots\ldots\ldots\ldots (4)$$

and for optimum driving conditions $V_{off} = V_T$, $V_{on} = V_T + V$. [In equation (4), g_0 is the conductance of a possible uncontrolled channel and that of the drain junction, K is the control factor and V_T is the threshold voltage]. Accordingly

$$v_F = -\frac{A_0 f_0 C_{GD}}{K}\ \ln\ \frac{\rho_{off}(\rho_{on}+1)}{\rho_{on}(\rho_{off}+1)},$$

where $\rho_{on} = r_{on}/R\|R_i = 1/[(g_0 + KV)R\|R_i]$, and

$$\rho_{off} = r_{off}/R\|R_i = 1/(g_0 R\|R_i).$$

The corresponding equivalent input-voltage drift is then given by

$$v_{eq} = -\frac{f_0 C_{GD}}{KA_M A_{DM}}\ \ln\ \frac{\rho_{off}(\rho_{on}+1)}{\rho_{on}(\rho_{off}+1)} \quad \ldots. (5)$$

or by

$$v_{eq} \simeq -\frac{f_0 C_{GD} R}{kKR_i}\ \ln\ 1/\rho_{on} \quad \ldots\ldots\ldots\ldots (6)$$

for sufficiently large drive $\rho_{off} > 10$, $\rho_{on} < 0{\cdot}1$, and for $R_i \ll R$. In equations (5) and (6), $f_0 = 1/T_0$ is the conversion frequency and A_M and A_{DM} are the transmission coefficients of the modulator and demodulator, given by[2]

$$\left.\begin{aligned} A_M &= \frac{\rho_{off} - \rho_{on}}{(\rho_{on}+1)(\rho_{off}+1) + \dfrac{k(\rho_{on}+1) + \rho_{off}+1}{(k+1)R_i/R}} \\ A_{DM} &= \frac{k}{k+1}\end{aligned}\right\} \quad \ldots (7)$$

It is remarkable that, under the conditions shown, the magnitude of v_{eq} is independent of the duration of the drive-voltage edges; their slope influences the amplitude of induced spikes only.

As expected, in order to reduce the drift, the conversion frequency should be as low as possible (limitation is by the acceptable magnitudes of C_M and C_{DM}); usually $f_0 <$ 1kHz. The unsymmetrical switching $k > 1$ is advantageous in respect of increasing A_M and A_{DM}. The upper limitation of k is given by the bandwidth of the amplifier; in practice $k < 5$. In accordance with equation (4), the magnitude of V appears in equations (5) and (6) through ρ_{on}, the optimum value of which is given by compromise between the dynamic error and the transmission coefficient A_M. The most suitable drive corresponds to ρ_{on} of the order of 0·1.

By neglecting $g_0 \ll 1/R\|R_i$, the transistor itself is represented through a quality coefficient K/C_{GD} characterizing its suitability for this application. The relation of C_{GD} to the physical structure of the transistor is difficult; nevertheless, it is possible to use an obvious fact that, for a symmetrical device, C_{GD} increases with an increasing gate capacitance C_0. According to Sah[1], however, $K/C_0 = \mu/L^2$. Consequently, the first limitation of the quality coefficient is given by the mobility μ of carriers in the channel, which is always lower than that in the bulk. The second one is conditioned by the limited resolution ability of known technological processes, which prevents reducing the channel length L below several micrometers. Breaking the symmetry, certain additional rise of K/C_{GD} is possible by geometrical displacement of the gate towards the source.

The spikes could be partially compensated[3] by an opposite squarewave voltage v_C through a capacitor C_C (Fig. 1). Besides the voltage dependence of c_{GD}, perfect compensation is disturbed by temperature and time fluctuations of C_{GD}, both of them being caused mainly by corresponding fluctuations of the threshold voltage. For the Hitachi 3SK12 [m.o.s., n-channel, $V_T \simeq -5$V, $K \simeq 50\mu A/V^2$ (an effective value in the knee region), $g_0 < 0{\cdot}01\mu A/V$, $C_{GD} \simeq 0{\cdot}06$pF] $\partial C_{GD}/\partial T \simeq +0{\cdot}001$pF/degC and $\partial C_{GD}/\partial t \simeq -0{\cdot}01$pF/day was measured, which, in accordance with equation (5) and for $f_0 = 1$kHz, $k = 3$, $R = R_i = 100$kΩ, $\rho_{on} = 0{\cdot}1$ and $\rho_{off} = 10$, gives a temperature coefficient of the input drift $\partial v_{eq}/\partial T \simeq -0{\cdot}1\mu V$/degC and a short-term input drift $\partial v_{eq}/\partial t \simeq +1\mu V$/day.

REFERENCES

1 SAH, C. T.: Characteristics of the m.o.s. transistors. *IEEE Trans. ED-11*, 324-345 (July 1964)
2 DOSTAL, J.: Spínací modulátor s tranzistorem řízeným polem. Slaboproudý obzor (to be published)
3 KORN, G. A., and KORN, T. M.: *Electronic analog and hybrid computers* McGraw-Hill (1964)

Transistorized 100MHz binary counter

by **R. J. Hood**, A.M.I.E.E., *University of Salford*

Two transistorized binary counters are described: a 50MHz circuit based on the current-mode switch and a unit capable of operating at frequencies above 100MHz. A 3-stage 100MHz counter is shown.

(Voir page 665 pour le résumé en français: Zusammenfassung in deutscher Sprache auf Seite 666)

THE maximum gain-bandwidth product of modern transistors is in excess of 1000MHz. Hence it is possible to make transistor switching circuits capable of operating at repetition rates above 100MHz. However, effects that are insignificant at lower frequencies then become important; the operating speed is limited by components and circuit configuration. It has been suggested that the current-mode switch should be used when minimum switching times are required.

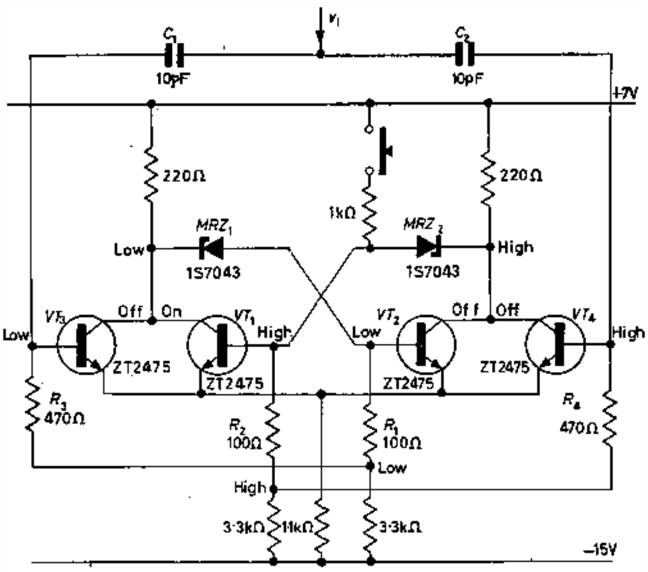

Fig. 1 50MHz current-mode binary counter

A high-speed binary counter† is shown in Fig. 1. Transistors VT_1 and VT_2 form a basic current-mode switch crosscoupled by the Zener diodes MRZ_1, MRZ_2 for voltage-level transference. By operating the diodes in the Zener mode, carrier-storage effects are avoided. The transistors VT_3 and VT_4, together with C_1, C_2, R_1, R_2, R_3 and R_4 form a steering and triggering circuit. This circuit has been found to function satisfactorily up to about 50 to 60MHz, with the limitation imposed by the steering and triggering network. The duration of the triggering pulse should be approximately equal to the circuit switching time. However, when the steering-network components are chosen to give the correct duration, quite a high attenuation of the input voltage results before it reaches the bases of VT_3 and VT_4. Furthermore, the input is applied to both sides of the bistable circuit simultaneously, tending to slow down the change of state. Consider the circuit of Fig. 1, where the various voltage levels are indicated for VT_1 nonconducting. The base of VT_4 is at a higher potential than that of VT_3, so that a positive input applied to both cases simultaneously causes VT_4 to conduct. This produces a lowering of the collector potential of VT_2 which is transferred by MRZ_2 to the base of VT_1. The normal regenerative action that occurs in bistable circuits then takes place. However, the input is also applied to the base of VT_1, *via* the resistors R_4 and R_2. Although it is attenuated, it is positive-going and thus tends to counteract the decrease of the base potential of VT_1 described above. This hinders the change of state.

† Based on a design in Texas Instrument Application Note 7: *Millimicrosecond switches*

Modified current-mode binary counter

Fig. 2 shows a binary counter based on the current-mode switch that is capable of operating at repetition rates above 100MHz. However, the output available from the circuit is incapable of driving similar circuits; so that, if stages are used in cascade, interstage amplifiers are required. A 100MHz 3-stage counter was constructed using the circuits of Figs. 1 and 2. The complete circuit is shown in Fig. 3, and the various circuit waveforms are shown in Figs. 4, 5 and 6.

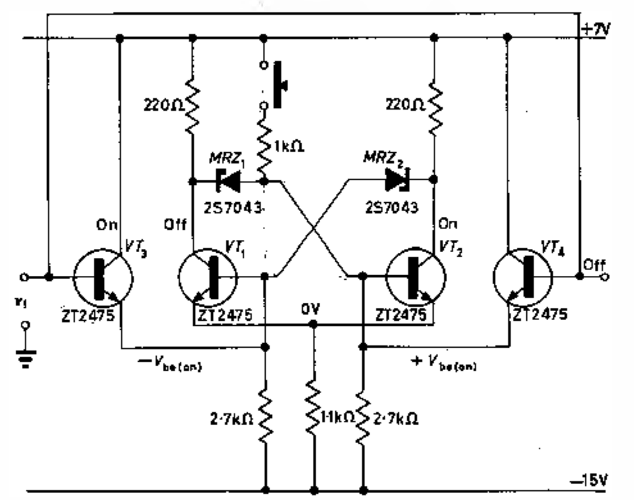

Fig. 2 Modified current-mode bistable circuit for operation at frequencies above 100MHz (potentials are with respect to earth)

Circuit operation and design

In Fig. 2, VT_1 is assumed to be switched off, while VT_2 is conducting. The potentials with respect to earth for this condition are shown. With the bases of VT_3 and VT_4 at earth potential, their emitters are at $-V_{be}$(on) and $+V_{be}$(on) respectively. Hence VT_3 is conducting while VT_4 is biased off. A positive input voltage applied to the bases of VT_3 and VT_4 is blocked by VT_4 and transmitted by VT_3. This voltage arrives at the base of VT_1, turning it on and thus changing the state of the bistable circuit. The input is also transferred to the collector of VT_2 by MRZ_2;

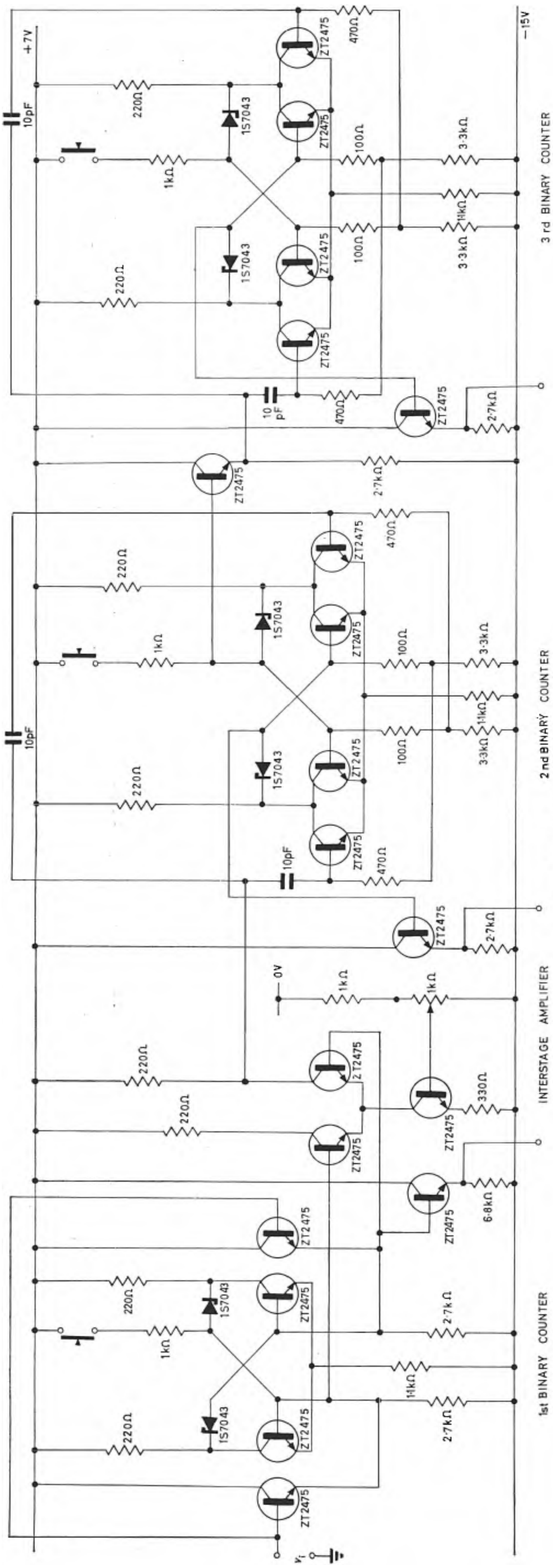

Fig. 3 100MHz 3-stage counter

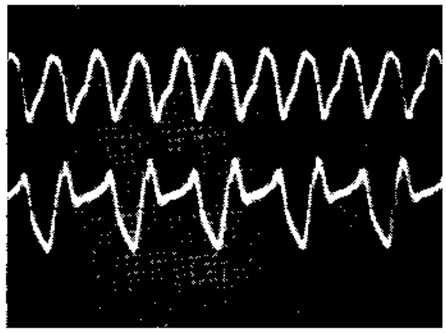

Fig. 4 Top: 100MHz clock signal
Bottom: Output from first binary counter (2V/square; 10ns/square)

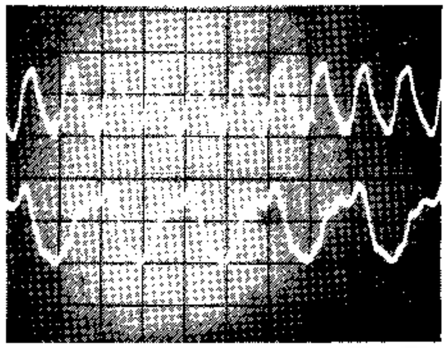

Fig. 5 Top: Output from interstage amplifier
Bottom: Output from second binary counter (2V/square; 20ns/square)

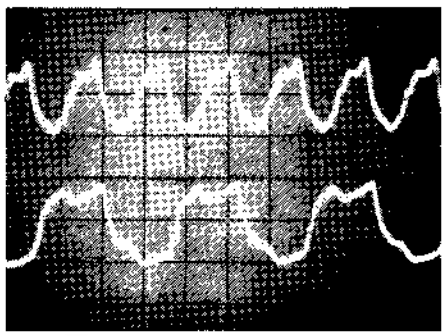

Fig. 6 Top: Output from second binary counter
Bottom: Output from third binary counter (2V/square; 25ns/square)

and so the input voltage is transmitted to the output with very little delay or obstruction. However, when the circuit changes state, the collector potential of VT_3 goes positive; so that the transference from input to output actually assists the change of state.

The circuit constructed as shown in Fig. 2 operated at frequencies of about 150MHz. It can be seen from Fig. 2 that the output voltage available is only $2V_{be}$(on) and that the input voltage required is also $2V_{be}$(on). The duration of the input voltage is important, and if one stage is to drive another the desired duration may be obtained by using a differentiating network. The attenuation introduced by this network makes interstage amplifiers necessary.

The circuit design consists in obtaining the desired d.c. levels, while attempting to select bias conditions conducive to high-speed operation. The collector current is selected to give the maximum transistor gain-bandwidth product, and the collector-to-base voltage is selected to give a small collector capacitance.

Voltage/current-characteristic tracer providing calibrated axes

by **Min Wei Li** and **G. Hoffmann de Visme**

This article describes an instrument, based on very simple principles, for tracing the current/voltage characteristics of both normal and negative-resistance diodes, and providing calibrated axes. The same principles can be applied when tracing the current/voltage characteristics of any device. A feature of the circuit is the use of the electronic equivalent of a rotary switch which is voltage-operated and has an almost-zero contact potential. The article also includes a statement of the exact conditions governing the stability of tunnel diodes in particular and of voltage-controlled negative-resistance 2-terminal networks in general.

(Voir page 664 pour le résumé en français: Zusammenfassung in deutscher Sprache auf Seite 665)

Displaying the voltage/current characteristics of a device on a c.r.o. together with axes and scale markers raises interesting problems of circuit design which are also useful from the point of view of teaching. Gooder and Potok* have described a method of displaying characteristics confined to the first quadrant, together with axes, calibration being by what amounts to moveable horizontal and vertical cursors. Their method depends on time-sharing between a sinusoidal and a sawtooth waveform, the former being used to generate the characteristic and the latter the axes.

The present method differs in a number of fundamental respects. Both characteristic and axis generation are accomplished using a single sinewave. The frequency of this wave is not critical, and 50Hz is convenient. Furthermore, characteristics are not confined to the first quadrant: in its present form, the instrument displays the characteristics of diodes, including the tunnel diode, but it is simple to extend the circuit to allow the display of families of characteristics of 3-terminal devices, such as transistors. Calibration is provided in the form of brightened spots along the axes, which may, if desired, be displaced at right angles to the axes to resemble scales. The whole instrument is transistorized, and the complementary properties of *n-p-n* and *p-n-p* transistors are exploited in the realization of the electronic analogue of a rotary switch.

Principle of characteristic and axis display

The basic characteristic tracer is shown in Fig. 1, in which the range of v_s is sufficient to cover the required voltage range of the characteristic but the form of the v_s variation is to a large extent irrelevant.

The voltage at X is the voltage across the device, and the voltage at Y is proportional to the current through R. If this is the same as the current through the device, v_Y is proportional to the device current. An inverting amplifier is required in either X or Y output to present the characteristic the right way up. Axis generation may be included by using the circuit in Fig. 2. The characteristic is traced when the switch is in position 1, the Y-axis when it is in position 2, and the X-axis when it is in position 3. To avoid spurious arcs on the display, the switch position must be changed when v_s is instantaneously zero. It is convenient to divide the switching sequence into four equal times, with the switch in position 1 for two cycles of v_s, and in positions 2 and 3 for one cycle each. In this way, the display of the characteristic is brighter than that of the axes.

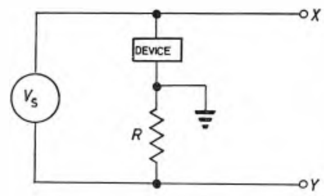

Fig. 1 Basic characteristic tracer

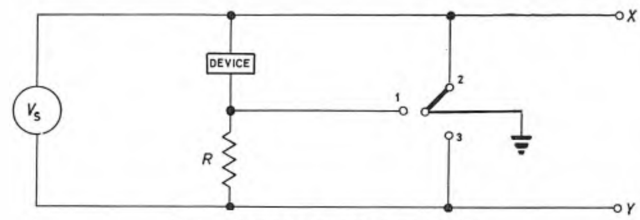

Fig. 2 Circuit for axis generation

Tracing the tunnel-diode characteristic

If current is driven through a tunnel diode by a source of alternating voltage having an internal resistance, two forms of instability can occur, depending on the source resistance; these are shown in Figs. 3(a) and (b). In each case, part of the diode static characteristic (shown dotted in the diagrams) is not revealed.

The first instability, known as splitting, occurs if the source resistance exceeds R_1, the magnitude of dv/di at its least negative value, while the second occurs if the

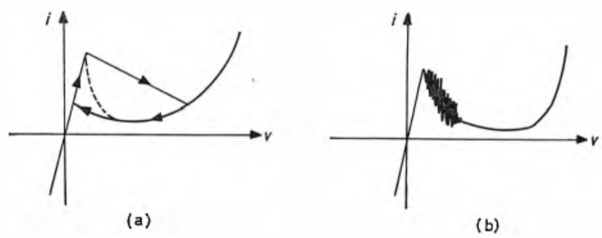

Fig. 3 Possible forms of instability

* Gooder and Potok: A valve and transistor characteristic tracer. *Electronic Engng.* *35* (Nov. 1963).

source resistance is less than R_2, the magnitude of the diode dynamic resistance at its most negative value. Thus stability is ensured if $R_1 > R_s > R_2$. Normally there is a positive interval between R_1 and R_2, allowing the choice of a suitable source resistance. If R_2 exceeds R_1, however, the source resistance must have two different components R_{dc} and R_{rf}, where $R_{dc} < R_1$ and $R_{rf} > R_2$. For low-current tunnel diodes, it has been found that a resistance of the order of 100Ω across the diode leads to stable operation.

Bridge circuit for characteristic and axis tracing

When a resistance S shunts the device of Figs. 1 and 2, the current through R no longer equals the current flowing in the device, and the bridge circuit of Fig. 4 is required to produce a Y-output proportional to the device current. With $R/S = R_1/R_2$, $v_Y = SR/(S + R)$ multiplied by the device current. In this condition, the maximum voltage that can appear across the device is $Sv_{s(peak)}/(S + R)$, the

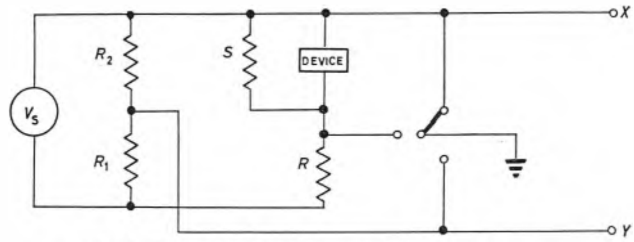

Fig. 4 Bridge circuit for characteristic and axis tracing

maximum current which can flow through the device is $v_{s(peak)}/R$, and the peak axis-generating voltage is $R_2v_{s(peak)}/(R_1 + R_2) = Sv_{s(peak)}/(S + R)$. These formulas enable suitable values of the circuit parameters to be chosen in terms of the device under test. As far as a tunnel diode is concerned, the effective shunting resistance in this configuration is $SR/(S + R)$.

In both Figs 2 and 4, provided that the device itself contains no source of voltage, the trace of its characteristic is exactly contained inside the quadrilateral formed by joining the extremities of the axis traces, as shown in Fig. 5; and since $(v_X + v_Y)$ and the instantaneous axis-generating voltages are at all times equal to $S/(S + R)$ multiplied by the instantaneous source voltage, the speed at which any part of the characteristic is traced depends on the gradient of the characteristic as well as on the rate of change of the source voltage. A feature of the

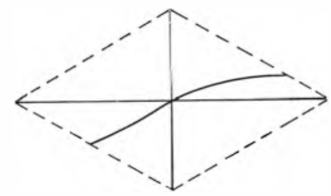

Fig. 5 Quadrilateral joining extremities of the trace axes

bridge circuit, which follows from the principle of superposition, is that v_Y remains proportional to the device current during the characteristic-tracing phase, even if the Y-output is shunted to earth through a resistance; and so an inverting amplifier with finite input resistance may be connected to this output without upsetting the accuracy. Provided that any resistances shunting X and Y to earth are not too small, the property of Fig. 5 still holds.

Application of marker pulses to axes and general description of system

X-marker pulses are applied to the c.r.o. Y-terminal and as bright-up during the X-axis trace, and Y-marker pulses are applied to the c.r.o. X-terminal and as bright-up during the Y-axis trace. A diagram of the whole system is shown in Fig. 6. Six X-pulses and four Y-pulses are produced during each cycle by the X- and Y-marker-pulse generators (XP and YP), their positions in the cycle being adjustable to cover the whole range of the applied waveform B. The X- and Y-marker-pulse gates (XG and YG), controlled by waveforms F and G, allow the X-pulses to pass (to the Y-plates and bright-up terminal of the c.r.o.) while the X-axis is being traced. and the Y-pulses to pass (to the X-plates and bright-up terminal) while the Y-axis

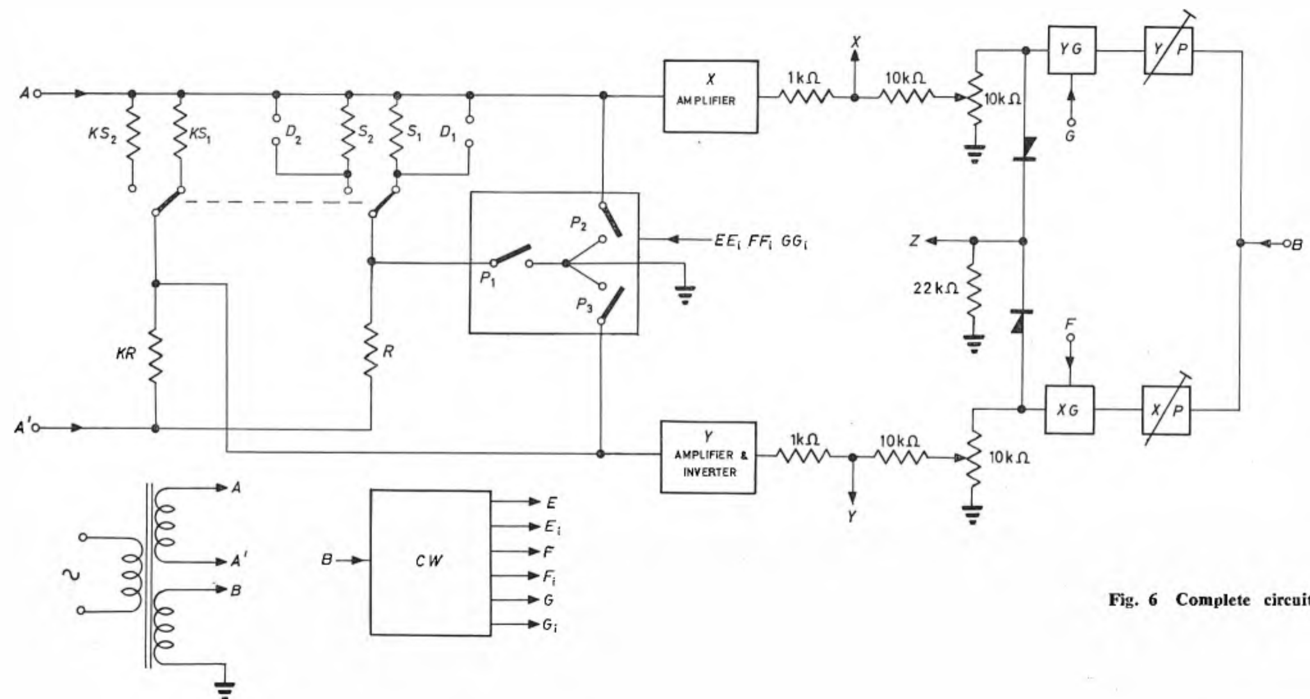

Fig. 6 Complete circuit

is being traced. The X and Y deflexions produced by these pulses are controlled by the 10kΩ potentiometers. The output voltage of the gates is zero between pulses. The bridge circuit providing the axis and characteristic traces is the same as that in Fig. 4, modified to accommodate normal and tunnel diodes. The source waveform AA' is similar to, though not necessarily of the same amplitude as, waveform B. The switches P_1, P_2 and P_3 comprise three similar electronic switches (see below) controlled, respectively, by waveform pairs EEi, FFi, and GG_i. The range of input voltages to the two amplifiers is symmetrical about zero, and so the d.c. supplies to these are chosen accordingly (HT+ is +12V and HT− is −12V).

The control-waveform generator (CW) produces a series of rectangular waveforms from the input wave B whose edges all occur when the instantaneous value of B is zero. Waveforms E, F and G lie between 0 and +6V, and waveforms E_i, F_i and G_i are the images of E, F and G, respectively, and lie between 0 and −6V. These waveforms close the switches P_1, P_2 and P_3, respectively, during the appropriate cycles of the AA' wave, while waveforms F and G close the gates XG and YG, respectively, during the appropriate cycles of the B wave.

Circuit details

The X-marker-pulse generator consists of six conventional trip circuits, one for each marker, whose trip levels are manually adjustable. These feed into a common load, the resulting voltage across which is differentiated to yield six short positive-going pulses per cycle. The Y-marker pulses (four per cycle) are generated in the same way. The gates XG and YG, the two amplifiers and the control-waveform generator CW are all conventional. The circuit of each of the switches P_1, P_2 and P_3 is shown in Fig. 7.

Waveforms E, F or G and their images are applied

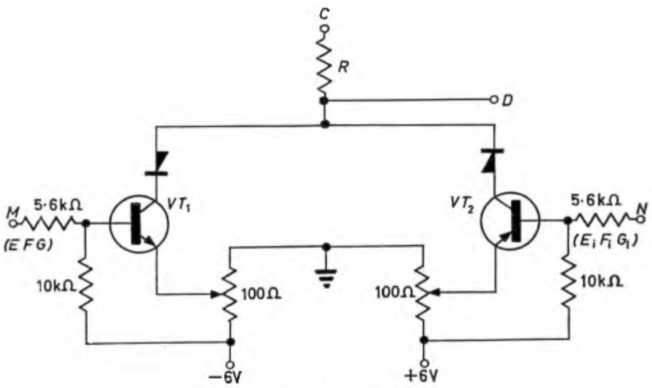

Fig. 7 Switch circuit

to M and N, respectively. When M is at +6V and N is at −6V, if the voltage at C is made positive, VT_1 conducts, and if negative VT_2 conducts. Suitable adjustment of the 100Ω backing-off potentiometers then ensures that the voltage at D remains substantially zero, as long as R is not less than about 500Ω. When the potentials of M and N are both zero, both transistors are open-circuited, and so the voltage at C appears unchanged at D. Thus the circuit behaves like a mechanical switch which is opened and closed by a voltage. Provided that the excursions of the voltage at C are not too large, one can dispense with the two diodes. This has the advantage of both reducing and making more constant the voltages which have to be backed off.

Voltage and current calibration

By tripping the X- and Y-marker-pulse generators with the independent supply B instead of the axis-generating voltages appearing at the inputs of the two amplifiers (Fig. 6), the potentiometers controlling the trip levels can be calibrated directly in voltage and current, respectively. Changing the setting of the diode selector switch does not alter the values of current represented by the Y-markers, while the values of S_1 and S_2 can be so chosen in terms of R as to make the voltages represented by the X-markers change by some convenient factor, say, 10. The gains of the X and Y amplifiers (both those of Fig. 6 and those on the c.r.o. itself) and the setting of the marker-pulse-amplitude controls do not affect the relative positions of marker pulses and characteristic trace. Suppose $R = 1\text{k}\Omega$, $S_1 = 10\text{k}\Omega$, $S_2 = 100\Omega$ and the amplitudes of the A and B waves are 16 and 12V, respectively; to obtain an X-marker at 5V with S_1 and D_1 in circuit, it would be necessary to adjust the X-marker-generator trip level to $5 \times (12/16) \times (10 + 1)/10 = 4{\cdot}125\text{V}$. This setting would be marked '5' on the trip-level control. With S_2 and D_2 in circuit, the same setting would produce a marker pulse at $4{\cdot}125 \times (16/12) \times 0{\cdot}1/(0{\cdot}1 + 1)$ or 0·5V, the factor of 10 arising since $R = 9S_1S_2/(S_1 - 10S_2)$.

Suppose that a Y-marker is required at 5mA with S_1 and D_1 in circuit; when the device passes 5mA, the voltage applied to the Y-amplifier of Fig. 6 during the characteristic trace is $(10 \times 1)/(10 + 1) \times 5 = 50/11\text{V}$. Thus the Y-marker generator trip level must be set at $(50/11) \times (12/16) \times (10+1)/10 = 3{\cdot}75\text{V}$. This setting is then called '5mA'. With S_2 and D_2 in circuit, 5mA in the device corresponds to a Y-voltage of $(0{\cdot}1\times1)/(0{\cdot}1+1) \times 5 = 5/11\text{V}$; thus the trip level must be set to $(5/11) \times (12/16) \times (0{\cdot}1 + 1)/0{\cdot}1 = 3{\cdot}75\text{V}$, as before.

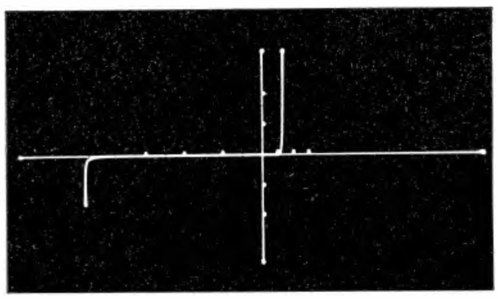

Fig. 8 Zener-diode characteristic

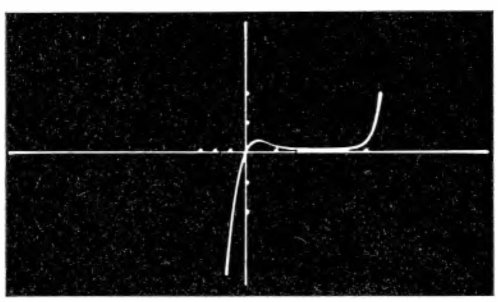

Fig. 9 Tunnel-diode characteristic

Fig. 8 is a photograph of a Zener-diode characteristic with voltage markers at −1·5, −1, −0·5, 0·2, 0·4, and 0·6V, and current markers at −6, −3, 3 and 6mA; while Fig. 9 is a tunnel-diode characteristic with voltage markers at −0·15, −0·1, −0·5, 0·1, 0·2 (hardly visible) and 0·4V, and current markers at −4, −2, 2 and 4mA.

Television in the BBC engineering division

Survey of BBC2 reception

To obtain reliable information on the standard of BBC2 reception in viewers' homes and to supplement the information on u.h.f. transmitter service areas provided by the extensive field-strength measurements which have been made, the BBC Engineering Division has carried out a wide-ranging reception survey in the service areas of the Crystal Palace, Sutton Coldfield and Winter Hill u.h.f. transmitters. Where possible, a comparison with reception of BBC1 and ITV was also made.

Some 40 technical staff were employed in this operation; they visited and checked receiver installations at over 1500 households. The sample of households was provided by the BBC Audience Research Department after a preliminary investigation to determine at which homes there were BBC2 receivers. It was selected from areas within the 70dB (reference $1\mu V/m$) field-strength contours of the transmitters, avoiding known major pockets of poor reception which will be served by BBC2 relay stations now under consideration or being planned. The contour corresponding to a median field strength of 70dB above $1\mu V/m$ represents the approximate limit of the service area of a u.h.f. transmitter.

The main results of the survey and conclusions are summarized as follows:

(i) More than 90% of viewers in the sample of households investigated would assess their BBC2 reception as being satisfactory provided that they have a properly installed aerial of the correct type and a correctly adjusted receiver with a reasonable performance.

(ii) A further and more detailed investigation at homes in the Crystal Palace service area where reception was found to be unsatisfactory during the survey indicated that some 98% of the total households in the Crystal Palace sample could obtain satisfactory BBC2 reception with suitable aerial installations and fault-free receivers. This does not involve the use of aerials of more than 10 elements.

(iii) In those households where BBC2 reception was found to be unsatisfactory, the major cause in more than 50% of the cases investigated is the use of inadequate or badly installed aerials. Of the total sample, 24% of the households were using aerials for BBC2 which were not designed for u.h.f. reception, and only 31% had outside aerials. Because of this and other factors, e.g. incorrectly adjusted receivers, the percentages of viewers in the survey sample assessing their reception as satisfactory is reduced to 64%.

(iv) Unsatisfactory BBC2 reception also resulted from the failure of viewers to adjust their receivers for best results. This difficulty appears to be mainly concerned with receivers having continuous tuning over the u.h.f. band but some receivers with push-button preset tuning were also giving trouble, owing to mechanical instability.

(v) Where outside aerials are used, BBC2 reception was technically assessed as being as good as or better than BBC1 and ITV reception at 59% and 60%, respectively, of the total households investigated. In a further 24% of the households, BBC2 reception was only marginally worse than BBC1 and ITV. The fact of BBC2 reception being worse than BBC1 and ITV reception does not necessarily mean it is unsatisfactory.

(vi) The survey results confirmed that multipath propagation causing 'ghosting' which is frequently troublesome in the v.h.f. bands, is not a serious problem with BBC2 reception on u.h.f.

(vii) The sample included early-type u.h.f. receivers having a lower performance than current models which have higher sensitivity and better noise factors. As more of these later models come into use, a higher percentage of BBC2 viewers getting satisfactory reception can be expected.

Electronic field-store colour-television converter

The BBC Engineering Division recently demonstrated the world's first purely electronic standards converter capable of converting colour-television pictures instantaneously from the 525-line 60-field NTSC system used in America and other countries, to the 625-line 50-field Pal system used in Europe; if required, the converter can be arranged to provide pictures on the 625-line 50-field Secam system used in France.

The principle on which the new electronic converter operates is best illustrated by considering any 1/10th of a second. If the two systems start scanning simultaneously, the first American field will have been completed slightly before the first European field, and thus the information can be transferred directly as regards time. The second American field will, however, begin slightly before the second European field, 16·6ms after the start as opposed to 20ms. Thus American field 2 is delayed until European field 2 is starting, and so on with increasing delays until American 5 becomes European 5. As the line-scanning rate has not been altered by the introduction of the delay, the height of the delayed 525-line picture will be reduced and the picture geometry will be wrong at this stage in the conversion; thus there will be a space at the top and bottom of the screen.

To rectify the geometry and also to deal with the colour content of the picture, further stages are necessary to complete the conversion. The output from the delay section of the converter is fed to an American-type NTSC decoder which separates the luminance and chrominance components of the delayed incoming signal. An extra unit in the decoder breaks down the chrominance signal into the I and Q signals which together form the coded NTSC colour signal. All these components are fed through line-store converters and emerge as 625-line signals. The luminance and chrominance components, all three now at 625-line standard, are fed into a PAL colour coder, the output of which is a European 625-line 50-field PAL colour signal. In correcting the picture geometry, the line-store converters compress the picture in a horizontal direction and the fully converted picture therefore has a small space on the right- and left-hand edges as well as at the top and bottom.

It will be noticed that field 6 of the incoming 525-line picture appears to be discarded; if this were really the case, movement in the picture, particularly of fast moving objects, would appear to be jerky, as every 6th field would be completely missing in the converted picture. To overcome this disadvantage, a further delay is introduced between field 6 of one series and field 1 of the following series, so that these two are superimposed as far as the delay-section output is concerned. The result of this technique is to mitigate the jerky effect to an extent to which is barely noticeable.

LETTERS TO THE EDITOR

(We do not hold ourselves responsible for the opinions of our correspondents)

A junction transistor electrometer circuit

SIR,—The excellent article by T. K. Cowell in the June issue on his simple and effective circuits almost leaves nothing more to be said on the subject of direct-coupled amplifiers with very high input resistance using bipolar junction transistors. There is, however, a different approach to the design of such amplifiers which it may be of value to describe.

RAISING THE INPUT RESISTANCE

The emitter-follower (or common-collector) connexion is a simple example of series feedback, which raises the input resistance of an amplifier at the expense of a reduction in gain. Series feedback can be applied not only to a single transistor but also to a multistage amplifier (see diagram). As is well known, the input resistance is raised according to the formula

$$R_{in} = R_{in}'(1 + A\beta) \quad \ldots\ldots (1)$$

$$\text{where } \beta = \frac{R_1}{R_1 + R_2}$$

assuming R_2 is small in comparison with R_{in}'. If unity voltage gain is satisfactory, $\beta = 1$ (i.e. $R_2 = 0$) and the circuit is then the multistage equivalent of the emitter-follower connexion.

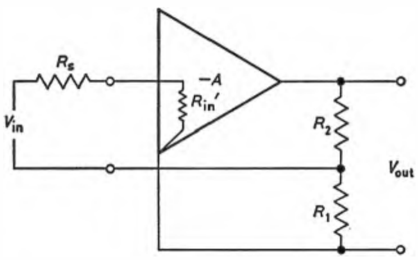

When we are interested in d.c. (i.e. virtually zero-frequency) measurements the zero-frequency value of A applies. This can be increased almost without limit, and so R_{in} can be raised to whatever value may be desired. It should be noted that this increase is effected (in one fell swoop, as it were) by the feedback connexion, which, when the loop gain is high, by itself causes the input stage to work under almost static conditions: no additional connexions, bootstrapping or the like, are needed.

OBTAINING A LOW VALUE OF I_{in}

Errors in measuring the e.m.f. of a high-resistance source can be caused by (a) the shunting effect of R_{in} across R_s, and (b) the flow through the input terminals, and hence through R_s, of any zero-point current (which means in practice the out-of-balance between the standing base current of the input transistor and the bias current supplied through the input base-leak resistor). In order not to put too much reliance on accurate balancing, therefore, it is desirable that the standing base current of the input transistor should be very low, and in a comparable application the working currents of the input transistor can well be approximately the same as in Mr. Cowell's circuits.

A useful technique, which is easily applied and which can greatly reduce the drift of standing input current with temperature, is to connect the base-leak resistor to a temperature-dependent voltage with a magnitude/temperature law matched to that of the standing base current of the input transistor. This may be done by having an auxiliary feedback amplifier whose output voltage varies in sympathy with the base current of a similar transistor, or by using a thermistor etc. It should be noted that the base-leak resistor is one of the components making up R_{in}', and so is subject to the effect of the feedback connexion as described by equation (1). This may make possible the use of a much smaller resistance than would otherwise be allowable.

Apart from the very low working currents of the input stage, the amplifier can be of normal direct-coupled design. Voltage zero drift can be reduced to very low values by the established technique of using matched pairs of transistors at the input. In this way voltage ranges with full-scale values of a few millivolts can be used with good accuracy.

A feature which arises from the application of series feedback to a multistage direct-coupled amplifier is that the lower output terminal (to which will be connected the power supply) is not commoned with the lower (i.e. the normally earthed) input terminal. This has been found to give no trouble in practice, partly, it may be assumed, because the indicating devices used (moving-coil meter or pen recorder) have an effective bandwidth up to only one or two hertz, and partly because the two terminals are connected by R_1 in parallel with R_2 and R_{out} in series (where R_{out} is the output impedance of the amplifier), which in practice make up a low-impedance path.

E. F. GOOD,
Malvern, Worcs.

Simple recorder integrator using a unijunction transistor

SIR,—In the article 'A simple recorder integrator using a unijunction transistor' by A. R. Atkins (July issue), the author gives an explanation of the operation of his integrator which is not clear and may be misinterpreted.

The author claims that the voltage V_o across the capacitor C is the integral of the input voltage V_i. This is true but is not sufficient, because there is no direct connection between the digital output of the integrator and the integral of the variable input voltage. Actually, for a constant value of the input voltage V_i, the voltage V_o will change linearly with time: $V_o = (1/C)\, kV_it$. Reaching the value V_s at the time $t = t_s$, the voltage across the capacitor C becomes zero and the cycle reinitiates. The repetition frequency of the cycle is (neglecting the discharging time) $f_s = V_ik/VC$. If V_s, k and C are constant, the repetition frequency depends linearly on the input voltage. In a given interval of time t, the total number of counted pulses N will be the integral of the time-varying frequency (supposing the input voltage changes):

$$N = \int_0^t f(t)\,dt$$

and consequently

$$N = [k/(V_sC)] \int_0^t V_i(t)\,dt$$

which had to be demonstrated.

C. PETRESCU
Institute for Atomic Physics,
Cluj, Romania

Precision peak-reading circuit

SIR,—A recent laboratory requirement involved the capture of the peak value of a positive pulse of varying duration. The standard method of doing this is by charging a capacitor *via* a diode and sensing the voltage across the capacitor with a high-input-impedance device, such as a valve. Disadvantages of such a system are primarily due to the diode. On applying a pulse, this has initially a low forward resistance but as the voltage across the storage capacitor rises the diode forward resistance increases. In a test the following results were obtained from an SGS Fairchild EC402 diode:

Forward current, mA,	Forward voltage, V	Forward resistance, Ω
1·0	0·65	650
0·52	0·62	1200
0·25	0·59	2360
0·10	0·55	5500
0·05	0·53	10600
0·025	0·51	20400
0·0125	0·485	38800
0·006	0·46	76700
0·003	0·435	145000
0·0015	0·41	274000
0·0005	0·365	730000
0·00025	0·345	1380000

The diode forward characteristic causes the peak-reading circuit to be sensitive to pulse duration, a short pulse giving a lower reading than a long pulse of the same amplitude. The diode characteristic also necessitates a meter with a nonlinear scale, particularly at the low end.

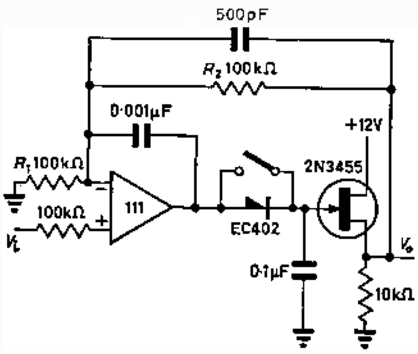

The illustrated circuit overcomes the above disadvantages, giving, for pulses of 2 to 300ms, an output that is not a function of pulselength and providing a linear V_o/V_i relationship. Performance was not investigated beyond these limits or for V_i greater than 4V. The graph shows the linearity and independence of pulselength that was achieved.

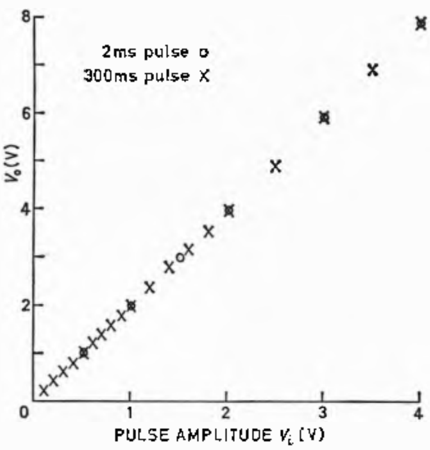

The gain of the circuit is given by $(R_1+R_2)/R_1$. The 500pF feedback capacitor brings results from 2ms pulses into line with those from 300ms pulses. The operational amplifier is an Analog 111, the diode is a low-reverse-leakage type and the field-effect transistor is by Amelco. The circuit will hold the peak value of an applied pulse for an hour or more if due attention is paid to insulation. Closing the switch resets the system to zero. A 20 000Ω/V meter was used to record V_o, but in the final application an emitter follower is connected to the field-effect transistor and the feedback loop taken from the emitter-follower output.

E. E. Wheeler
PIRA
(The Research Association for the Paper & Board, Printing & Packaging Industries) Leatherhead, Surrey.

Frequency stability in oscillators

Sir,—In response to the letter by U. S. Ganguly ('Null networks and frequency stability of null-network oscillators', March issue, page 186), I would like to point out that I have derived a general expression[1] for frequency stability of bridge feedback oscillators using any frequency-determining network (null network or otherwise). Although a specific reference was made to RC networks, it obviously applies to any selective network in such oscillators. Frequency stability of such oscillators is given by

$$S_F = A\frac{|d\gamma|}{|dx|_{x=1}} \quad \ldots\ldots\ldots\ldots (1)$$

where $x = \omega/\omega_0$, ω_0 is the resonant frequency, γ is the imaginary component of the transmission of the frequency-selective network and A is the gain of the amplifier section. For the null networks considered by Mr. Ganguly,

$$\gamma = \frac{Kbx\,(x^2-1)}{(x^2-1)^2+b^2x^2} = u/v, \text{ say.}$$

$$\therefore S_F = A\frac{|d\gamma|}{|dx|_{x=1}}$$

$$= A\left|\frac{du/dx}{v}\right|_{x=1} \quad \because u = 0 \text{ at } x = 1$$

$$= \frac{A2K}{b}$$

Equation (1) applies to any frequency-selective network (whether null or not) such as Wien, bridged-T (RC or RLC), twin-T, zero-phase[2], Meacham etc. employed in oscillators with dual feedback paths.

V. B. Mehta
Bombay 2, India

REFERENCES

1 Mehta, V. B.: 'Comparison of *RC* networks for frequency stability in oscillators,' *Proc. IEE*, *112*, 296 (1965)
2 Bernstein, S.: 'An improved *RC* bridge circuit with high selectivity,' *Electronic Engng*, *38*, 680 (1966)

Improved RC bridge circuit with high Selectivity

Sir,—The article 'An improved RC bridge circuit with high selectivity' by S. Bernstein (May 1966 issue) is interesting because of the widespread use of the CR-RC[1,2] and the Wien[3] networks in inductorless selective amplifiers and oscillators. However, in the sections dealing with the application of the various null networks in oscillators, the author seems to be guided by two completely erroneous ideas, as follows.

First, the phase characteristic of a true null network displays a jump discontinuity at the null frequency; and hence the normalised phaselope at this point is not defined in the strict mathematical sense. Hence, the 'selectivity factor' S_θ, defined by Mr. Bernstein as

$$S_\theta = \omega_0 \left.\frac{d\theta}{d\omega}\right|_{\omega=\omega_0}$$

after equation (15) in the Appendix does not exist.

Second, the frequency stability of an oscillator incorporating a null network having a voltage transfer function

$$\beta_N = E_o/E_i = \frac{K}{1 - j\,b/u} \quad \ldots\ldots\ldots\ldots (1)$$

where K and b are constants for the network,

$u = \omega/\omega_o - \omega_o/\omega = x - 1/x$

ω_o = null frequency

$x = \omega/\omega_0$

can be shown to be[4] $2KA/b$, where A is the gain of the maintaining amplifier. Hence, for a given amplifier gain, the figure of merit of a particular null network depends on $2K/b$ and not on $2/b$ as stated by the author. The K/b ratio for a CR-RC bridge with a buffering cathode follower ($n = \infty$) is 1/4 while that for the Wien network (n=1) is 1/9; and thus the former can be expected to provide 9/4 times the frequency stability attainable with the latter for the same maintaining amplifier. Hence the sensitivity factor S_T and not S_θ of these null networks is the relevant figure of merit in oscillator applications.

U. S. Ganguly
Javadpur University
Calcutta 32, India

REFERENCES

1 Nahin, P. J.: 'The two section *RC* phaseshift oscillator,' *Proc. Inst. Elec. Electronic Engrs.*, *52*, 198 (Feb. 1964)
2 Owens, J. H.: 'Audio oscillator uses new *RC* design,' *Electronics*, *27*, 176 (March 1954)
3 Reich, H. J.: '*Functional circuits and oscillators*,' pp. 384-391, Van Nostrand (1961).
4 Ganguly, U. S.: 'Null networks and frequency stability of null-network oscillators,' *Electronic Engineering*, *39*, 186 (March 1967)

Binary-to-decimal converter

Sir,—Without trying to labour the point, I would like to comment on the letters in the March and July issues on K. J. Dean's article (October 1966). Persuing Mr. Hanna's point, we must note that 6 should be added to a decade count both as a filler and to satisfy deficiency when a decade boundary is crossed. Note that these conditions can never exist simultaneously. The essence of the procedure, however, is timing, since the filler 6 is added *before* a shift, while a deficiency 6 is added *after* a shift. By adding 3 one shift earlier for the condition that the decade holds numbers 5, 6 or 7, we satisfy the filler requirements; by adding 3 when the decade holds 8 or 9, we have automatically waited one shift to satisfy the deficiency requirements (albeit one shift prematurely).

To convert a *bcd* number to pure binary, the converse process is simply to subtract 3 from a decade when a 1 is shifted across a decade boundary, the shifting being from the high to the low end of the register. Readers might be interested to know that a combined binary-decimal, decimal-binary convertor using this principle has been described by Couleur[1].

F. Raven
Rutherford College of Technology,
Newcastle upon Tyne 1

REFERENCE

1 Couleur, J. F.: 'A binary to decimal or decimal to binary converter,' *Trans. I.R.E.*, *EC-7*, 313-316 (Dec. 1958)

NEW BOOKS

Laplace transform theory and electrical transients

by S. Goldman. pp. 439. Demy 8vo. Constable and Co. Ltd. 1967. Price 24s (limp)

Laplace-transform theory for electrical-engineering students inevitably gives rise to an argument on depth of treatment. On the one hand, it can be offered superficially as a tool, with little attention being paid to existence and derivation; alternatively, a deeper mathematical approach may be given, although the students' facility may well be impaired. Prof. Goldman has attempted to bridge the gap between these two extremes. In Chapter 3 the 'tool' approach is given, only real parameters being used, and in Chapter 7 some of the gaps are adequately filled. Attempting to give a comprehensive and systematic treatment of transients in linear networks (nonlinear networks have not been considered), the author has included chapters on a number of related topics. In fact, the reviewer would not be surprised to find that students were purchasing this book for Chapters 5 and 6 alone, these giving a clear presentation of the theory of functions of a complex variable. The book also contains chapters on determinants; a brief review of the properties of electrical circuits, including node analysis, using the MKS-system units; gamma, error and Bessel functions; transmission-line equations; and solution of differential equations in series. Some useful appendixes follow and the Laplace transform is applied throughout where appropriate. Electrical engineers will find this book a useful one; it is claimed to have been written for mathematicians, although, in the reviewer's opinion, students of mathematics would do well to include this in their reading.

D. W. Porter

Laser light

By C. C. Eaglesfield. 192 pp. Demy 8vo. Macmillan & Co. Ltd. 1967. Price 30s.

The modern revolution in electronics started just after the last war, in fact with the invention of the transistor in 1948. Within two years, W. Shockley, one of the three co-inventors, wrote his classic 'Electrons and holes in semiconductors', which turned out to be the forerunner of a host of books on 'the solid state'. The situation is similar now, following the invention a few years ago of the laser, and the gates have now been opened on a flood of books on lasers. This book, however, is rather different. As its title implies, the emphasis is not so much on the generation of laser light and the modes of laser action, as on the unique properties of the radiation generated by lasers. The first half of the treatise deals with such topics as coherence of electromagnetic radiation, resonance and oscillations, with only 40 pages devoted to a description of the three major types, i.e. solid-state, gas and semiconductor lasers. Chapters 2 and 3 discuss in a clear and simple manner the coherence of light and the amplification of optical-frequency oscillations. Chapter 6 contains a useful and quantitative discussion of a topic which is frequently treated rather superficially in books on lasers, i.e. the calculation of the 'threshold' or minimum excitation power required for lasing. Though by no means rigorous, the calculation is sufficient for a quantitative appreciation of the main factors involved. The last few chapters of the book deal briefly with optical pipes, modulation etc. There is a delightful chapter on the visual effects of laser light, such as the 'granularity' of a surface under laser illumination, and on the remarkable stereoscopic effects which can be achieved with holography under coherent light. This book is true to the subject matter it covers—stimulating!

E. Billig

Lasers

By K. Paték. 288 pp. Demy 8vo. Iliffe Books Ltd. 1967. Price 45s.

This book is an early starter in the series of publications on lasers which is bound to follow soon on the rapid development of these and similar quantum devices and their applications in science and industry. Paték's book was first published in 1964 and translated into English in 1966. After a very readable introduction, there are four chapters on the major physical aspects of laser action, i.e. radiation, stimulated emission, optical-resonance cavities, coherence and noise. These are followed by a detailed account of the three major types of laser known at present, i.e. gas lasers, solid-state lasers (crystalline and glassy) and injection lasers (*p-n*-junction types in semiconductor crystals); finally there are four chapters on their application to scientific problems such as stimulated Raman radiation, harmonic generation etc., to communications, and to practical engineering applications (drilling, welding etc.) where use is made of the high energy concentration in laser beams. There is a very comprehensive list of references up to 1965 at the end of each chapter, covering about 600 relevant publications on both sides of the Iron Curtain. The book is obviously written by an expert, for the expert or anybody intending to become one. The reader is expected to be familiar with the basic ideas of wave mechanics and quantum mechanics: relevant formulas are stated without derivation and are used freely to discuss the problems on a quantitative basis, so essential to real understanding.

E. Billig

Microwave breakdown in gases

by A. D. MacDonald. pp. 201. Med 8vo. John Wiley and Sons. 1967. Price 64s.

This is the fourth book to appear in the Wiley series on plasma physics and it maintains the high standard set by the previous books in the series. As the loose cover states, it is the first self-contained and complete account of what is known about a subject which has become increasingly important in recent years. The introductory chapter emphasizes the difference between d.c. or low-frequency breakdown and high-frequency breakdown; it also contains a useful section on dimensional analysis to explain the combinations of experimental variables customarily used in describing breakdown phenomena. Chapter 2 is a condensed version of McDaniel's book in the same series, and reviews the electron processes relevant to microwave breakdown—elastic and inelastic collisions, diffusion, attachment and recombination. The Boltzmann equation for the electrons is treated in Chapter 3, initially ignoring second- and higher-order terms. Later in the chapter, the effect of higher-order terms is considered, together with the range of applicability of the simpler theory in practice. In Chapters 4 and 5, breakdown theory for constant collision frequency and for variable collision frequency is considered on the basis of the distribution functions of Chapter 3. The effects of nonuniform electric fields and of magnetic fields is considered in Chapter 6. There then follows a short chapter on experimental techniques, which indicates briefly how microwave measurements are made and describes a typical ultra-high-vacuum system. For those unfamiliar with microwave and vacuum techniques this chapter is, presumably intentionally, quite inadequate, but there are many references, including Heald and Wharton (another book in this series), to standard texts in these fields. The book concludes with a chapter on what is now a particularly important subject in the satellite- and missile-communications field—that of microwave breakdown in the atmosphere. The book is very well laid out, the diagrams are good and in themselves contain a considerable amount of experimental information. There are many references at the end of each chapter, a large number of which relate to work done between 1962 and 1964; there are two or three 1965 references. The book appears to be primarily aimed at people working directly in the field, but much of it could be read by interested physics and electrical-engineering graduates.

J. D. E. BEYNON

Fundamentals of electronics

By G. E. Owen and P. W. Keaton. 3 vols. Crown 4to. Harper and Row. 1967. Price 63s. per vol.

As the title suggests, the text throughout is devoted to fundamentals. Although the approach is indeed fundamental, it is not elementary—a significant difference. In fact, the level of treatment is very high, a laudible change from other texts bearing similar titles. Broadly, the three volumes are devoted to mathematical methods, physical electronics and circuits, respectively.

Volume 1 covers in a unified manner all the necessary mathematical background to the material introduced in subsequent volumes. As an example of its high level of treatment, the volume begins with the derivation of Kirchoff's laws from Maxwell's equations and their use in circuit analysis. Since only five pages are devoted to the derivation, these can be omitted by any reader who has already accepted Kirchhoff's laws and is not familiar with the DIV and CURL vector operators. The chapter on operational methods is devoted mainly to the solution of linear differential equations using the techniques of Fourier and Laplace transforms and Heaviside's expansion coefficients. This and the matrix solution of simultaneous differential equations in terms of eigenvalue and eigenvector solutions is given very good physical interpretation in the discussion of transfer functions, root loci and pole-zero diagrams of relatively elementary circuits. The techniques are used to advantage in the analysis of 2- and 3-port and 4-terminal networks. A chapter on special circuits includes amplitude, phase and null bridges, the ideal transformer, double tuned circuits, transmission lines and filters. Pertinent to the latter, amplitude, phase and maximal flatness are discussed for the non-ideal case. Asymptotic frequency and phase responses in piecewise-linear approximations are given where appropriate throughout the text. For the sake of completeness, the Z-transform for the analysis of discrete systems is given in an appendix.

Volume 2 is devoted entirely to physical electronics. The preliminaries, providing the basic background before discussion of devices, cover the fundamental electromagnetic equations, Maxwell-Boltzmann, Bose-Einstein and Fermi-Dirac statistics leading into the elements of quantum mechanics with a lucid derivation of Schroedinger's wave equation. Energy levels, wave functions and Fermi-levels are explained illustratively. The wave-particle duality of electron behaviour is discussed and the simplest representation used whenever it is appropriate. For example, in the chapter on charged-particle dynamics the classical representation is used where the region of partical localization is small compared with the distance between systems. After derivation of particle behaviour in electric, magnetic and cycloidal motion in crossed e.m. fields, the section on electron optics provides a useful course on focusing with aperture and cylindrical lenses. This is later extended to explain orbits in electron guns and trajectories in image tubes, including a section on quadruple focusing which appropriately follows a chapter on properties of vacuum tubes, commencing with thermionic emission, the Richard-Dushmann equation, triodes, tetrodes and pentodes, to the magnetron and the theory of modulated beams and plasma oscillations in klystrons.

A chapter on the free-electron theory of metals and the band theory of solids explains comprehensively the important role of energy gaps in the electrical behaviour of materials. This, of course, is used to advantage in a very clear description of semiconductor behaviour, including the development of the transport equations and the effect of fields and impurity states on concentrations and mobilities with both steady-state and pulsed excitations. A lengthy following chapter on *p-n* junctions will provide most engineers and students with all the material they are likely to require concerning semiconductor actions: the depletion layer, its dependent capacitance, the diode equation derived statistically, majority and minority carriers, injection, diffusion, its time-dependent characteristics and large-signal operation. The differences between the Zener, avalanche and tunnelling effects are explained with clarity in the discussion of Zener and tunnel diodes. The junction transistor naturally concludes this volume with a development of models, parameters for small and large signals, and the analysis of its behaviour for the three basic configurations with linear and nonlinear modes of operation. Descriptions only are given of other types, surface barrier, drift, epitaxial, planer etc., but the field-effect transistor is given the necessary additional analytical treatment. A useful appendix on noise properties is provided.

Volume 3 covers the operation of thermionic and semiconductor devices in circuit configurations, dealing principally with the latter. The basic responses of simple amplifying stages are analysed using the techniques covered in vol. 1 and the models developed in vol. 2. Degenerated operation with Miller capacitance etc., low-frequency and high-frequency cutoff, variation of gain, temperature compensation and simple biasing are discussed. A general consideration of multistage amplifiers follows with a discussion of feedback effects and configurations on stability and input/output parameters. Power amplifiers are included in all classes of operation (except D) with and without distortion effects. A.M., f.m. and p.m. introduce a section on selective amplification and filtering with single, double and stagger-tuned stages. Operational amplifiers, for the sparse coverage given, could well have been omitted. The limitations of the response of wide-band amplifiers, particularly with regard to risetime, are illustrated in the discussion of distributed amplifiers.

Operation of devices in the nonlinear region is covered in the chapter on timing circuits of the conventional kind: exponential, bootstrap, Miller with linear rundown etc. An excellent analysis is given of bistable, monostable and astable operation in both grounded-emitter and emitter-coupled configurations, where appropriate. Rise-time calculations of such circuits (omitted from most texts), triggering and current-steering networks are included. The analysis of the blocking oscillator and its difficulties concludes this section. A small chapter on negative-resistance devices, principally the tunnel diode, unijunction and 4-layer diode, discusses operation with both passive and active elements and their use as amplifiers. A discussion of the inherent property of negative resistance for the basis of an oscillator is the inevitable forerunner for a concluding chapter on such circuits utilizing phase shifting, bridges and resonant coupling. Detailed reading of these books provides a strong recommendation to students and engineers who require a refreshing yet thorough and fundamental approach to this subject. It will find a very wide use in both undergraduate and postgraduate courses and will benefit people in the disciplines of both physics and engineering.

E. T. POWNER

Elements of energy conversion

By C. R. Russell. 406 pp. Demy 8vo. Pergamon Press. 1967. Price 60s.

Once upon a time there was a tradition that prospective writers of technical or scientific books would first familiarize themselves with any prior books in the same field. In the case of the book under review, this would have saved the author — and the publisher — much trouble, as an excellent book on the same topic was published only four years ago ('Energy' by Bruce Chalmers, 1963), which was highly recommended by the reviewer to the 'educated layman and the sixth-form science student'. The statement on the wrapper of the present volume—that it is suitable for undergraduates—would certainly not apply to students in this country (there is unfortunately no indication about the status of the author or that of his 'undergraduates').

The preface makes strange reading: '. . . the author is neither responsible . . . for the safety of personnel following procedures described herein, nor for the losses and dangers that may arise as a result of errors and omissions in the presentation of material.' This is rather reminiscent of the attitude of a frightened official in some legal government department. The author has made extensive use of material published in some US Air Force documents.

E. BILLIG

Engineering Electronics

By J. D. Ryder. 690 pp. McGraw-Hill. 1967. Price £5.

This book is intended to cover the application of electronics in the fields of control, computation and instrumentation; radio, television and similar interests are not included. The first edition became available about a decade ago and the present edition shows a considerable updating of content. As may be expected, this updating takes the form of increased emphasis on semiconductor and digital aspects. The first two chapters, which account for some 65 pages, deal with the fundamentals of thermionic and semiconductor devices. The book then plunges into a discussion of transistor amplifiers in terms of h-parameters. The T-network low-frequency equivalent is then analysed and the method of transistor bias is explained. The material on linear transistor amplifiers occupies only 20 pages: it would seem to deserve more space. Thermionic-valve amplifiers are next dealt with and the factors affecting frequency response are evaluated. A chapter on feedback and one on low-frequency power amplifiers (both valve and transistor) complete rather more than one-third of the book. Up to this point, the material is of a type widely available elsewhere. The text then covers a group of low-power topics of a less widely known nature. These include direct-coupled amplifiers, switching circuits, analogue-digital conversion and coding systems. The final third of the book is concerned with power applications of electronics; here we have power rectification, power control, inversion, motor control and a final chapter on servomechanisms. The thyristor receives a reasonable amount of space and a number of examples of its use are given. This is a useful but by no means outstanding book. Its value to the engineer would have been enhanced by the wider use of practical circuit diagrams with component values, and by a less analytical approach.

V. H. ATTREE

Techniques of pulse-code modulation in communication networks

By G. C. Hartley, P. Mornet, F. Ralph and D. J. Tarran. 110 pp. Demy 8vo. Cambridge University Press. 1967. Price 30s.

The authors are to be congratulated on writing a very good book, the first of a series of monographs to be published jointly by the IEE and Cambridge University Press, and which is aimed at the practising engineer, graduate student and teacher with the purpose of bridging the gap between research papers and industrial application. The book deals with the present-day techniques and future requirements for transmitting digital data over line-communication circuits. After a brief introduction and historical review, the principles of p.c.m. are outlined and it is felt that someone meeting the subject for the first time would be well advised to consult other sources of reference for a more detailed account of time sampling and quantization, since these topics are covered without recourse to mathematics. The full potentialities of time-division multiplex (t.d.m.) operation are described in a chapter entitled 'Supplementary considerations', and it is shown that any future p.c.m. transmission system must be capable of handling general digital data, e.g. computer information. Having outlined the basic concepts, the book goes on to explain how these principles may be applied to communication networks. Present-day application involves a conversion from f.d.m. to t.d.m. for local-area use, in order to expand the capacity of existing networks approaching saturation. The conversion of long-haul circuits to t.d.m. operation has many problems yet to be solved; these are adequately detailed in the text. Whereas the major part of the book deals with the broad principles and techniques of p.c.m., the final chapter gives a more detailed account of a typical system, with an explanation of the terminal equipment and function of regenerative repeaters. In conclusion, it can be said that the book fulfils its purpose and is thoroughly recommended.

J. A. BETTS

Linear sequential circuits: analysis, synthesis and applications

By A. Gill. McGraw-Hill Book Co. 1966. 215 pp. £5 16s (in UK)

The circuits under discussion may have any finite number of input terminals, any finite number of output terminals, and any linear combination of instantaneous adders, instantaneous multipliers and delayers. Each delayer delays its input by the same time interval. The book is concerned with the mathematical methods and techniques required for handling such circuits, and with applications. It is not an easy book, because the essential algebra is not familiar to many practising engineers. It is mathematically fascinating, but it involves ideas which seem initially very odd to those familiar only with ordinary algebra, elementary calculus, and the impedance concept and related ideas like Heaviside's operational calculus or Laplace transforms. In ordinary algebra, we are usually concerned with equations, the difference between the two sides of which is zero. In the algebra of sequential circuits, the difference between the two sides of the corresponding expressions is a multiple of a fixed integer P (usually prime) and the coefficients of polynominals and the variables involved are integers. If $p = 2$, for example, $(1 + x)^2$ is equivalent to $1 + x^2$ because the difference is a multiple of 2. Thus squaring in this case becomes a linear process, whereas we have probably been taught to regard leaving out the middle term $2x$ as a heinous mathematical crime. Chapter I is called 'Mathematical prerequisites', and states without proofs the ideas required for use later. Four textbooks are given as references for 'more comprehensive coverage' and for proofs; all of these are American, and indeed the bibliography of 101 references at the end only contains one reference to a British paper by J. E. Meggitt of the IBM British Laboratory, Winchester, Hants. This is an unfortunate state of affairs: either not enough attention is being paid to circuits of this kind in Europe or else there is insufficient transatlantic knowledge of British work in this field.

All the ideas associated with linearity, such as the use of matrix techniques to reduce several relations between given inputs and unknown outputs to a set of relations expressing implicitly one output in terms of known quantities, the principle of superposition etc., remain just as valid for linear sequential circuits as for other linear circuits.

The majority of engineers might be 'warned off' this book as they may well find it too difficult. An enjoyment of mathematics as well as significant ability in the subject is needed to derive any benefit from it. But for those who can pass those stiff tests, the book is worth very careful attention. It has a great deal of useful information, and although it is in a highly condensed form, the author has taken unusual care to say which references form the basis of each chapter.

Possibly more attention should be paid in Britain by post-graduate students, and even by undergraduates having mathematical ability, to sequential circuits and to the unfamiliar algebra underlying them.

J. W. HEAD

SHORT NEWS ITEMS

Aircraft-identification-radar £1M orders
The new NATO defence-radar chain from northern Norway to eastern Turkey and the fixed and mobile defence-radar systems for the RAF are to be equipped with aircraft-identification-radar equipment SIF/SSR developed by Elliott-Automation; the orders for this equipment announced recently are together worth well over £1M. Elliott is to modernize existing identification-radar stations being incorporated into the great new NATO Air-Defence Ground Environment (NADGE) system and will be supplying the latest radar and identification equipment. In the RAF stations in Britain, the identification equipment will form part of the joint civil/military radar-traffic-control system. Identification involves the decoding by digital-computing techniques of coded radar signals returned automatically by aircraft transponders in reply to interrogations from the ground stations. Elliott has developed the digital techniques required to identify the thousands of information codes being introduced into service. Special 'de-fruiting' equipment has also been developed to suppress interference between neighbouring stations. A computer-controlled version of the decoder capable of operating without the usual primary radar is already being supplied to Eurocontrol at Bretigny, near Paris.

British telephone equipment for NZ
As part of the modernization and expansion of the New Zealand telephone system, Plessey has recently received orders to instal extensions to four of the country's exchanges. The orders, placed with Ericsson Telephones Ltd, part of the Plessey Telecommunications Group, are together worth more than £160 000, and the equipment, for improvements at Auckland, Wellington, Mount Roskill and Taradale, will be made at their Beeston, Nottingham, factory. The new orders follow an earlier substantial contract for the provision of a complete automatic exchange at Rotorua. This incorporates a number of specially developed features which will protect the equipment against the highly corrosive atmospheric conditions in this sulphur-springs area of New Zealand.

Radio and television disposals down
Although figures issued by the Economic and Statistical Division of the British Radio Equipment Manufacturers' Association indicate increases in home disposals to the trade of radio and television receivers during June, the position is not so optimistic for the total six months of this year compared with the same periods of 1966 and 1965. Government restrictions and nonrelaxation of rental and hire-purchase conditions are obviously continuing to have an adverse effect. Television receivers, at 545 000 for the first six months, show drops of 118 000 and 207 000 against 1966 and 1965 respectively, decreases of 18 and 28%. The story is exactly the same for radios, which, at 692 000 for the six months of this year, show deficits of 30 000 and 252 000 compared with 1966 and 1965.

I.Mech.E. to admit nonmembers to technical activities
The advance of technology is producing an increasing number of specialists who are not necessarily mechanical engineers but whose work brings them into contact with some aspect of mechanical engineering. To meet these interests, the Institution of Mechanical Engineers has introduced a scheme to enable individuals to take part in the activities of its 13 specialist groups and the automobile division; they will be described as group subscribers. Group subscribers will be able to join in the activities of one or more selected groups on payment of a small subscription; they will be permitted to use the library and will receive any papers issued in connection with the activities to which they subscribe. Being a group subscriber does not confer Institution membership. The scheme provides an opportunity for part-participation in Institution technical activities.

Colour-television-engineering course
A course of 26 lectures on colour-television-engineering will be given at the Northern Polytechnic, Holloway Road, London, N.7 on Monday evenings, commencing 9th October 1967, at 6.30 p.m. The course will cover the basic engineering requirements for colour television. A good fundamental knowledge of monochrome technique is required, and minimum entry qualifications are Final R.T.E.B. Certificate or Final C. & G. Telecommunications Technicians Certificate. Specialist lectures will be given by well known engineers from industry and the broadcasting organizations. The fee for the course is £2 plus a registration fee of 1s. (Lectures on 'Colour Television Servicing' intended for servicing technicians are also available and enrolment for these takes place at the Polytechnic on the general enrolment dates.

Leading semiconductor experts meeting at Manchester
The first major international scientific conference on solid-state devices in Britain was held at Manchester University on the 5th-8th September. Half of the 70 papers that were presented came from overseas, with particularly strong representation from America, including three outstanding papers from the Bell Telephone Laboratories. Nine papers were invited contributions by international authorities in the semiconductor field, four from America, one each from Russia, Germany and France and two from Britain. Other contributions came from as far afield as Hungary and Japan. The conference, which was run by the Institute of Physics and the Physical Society in collaboration with the IEE, IERE and IEEE, revealed some outstanding new technological advances in the field, with direct impact on the whole electronics industry, but particularly on such things as microelectronics, computers, radar and communications.

Mintech—the first three years
'The Ministry of Technology', a recently published memorandum, gives some idea of the scope of the work of Mintech and describes the various ways in which policy has evolved within the Department during its first three years. Referring to the electronics industry, the memorandum states that 'much of the ministry's work so far in electronics has been concentrated on microelectronics technology, which has great potential and significance, but in which the UK industry faces very severe problems. The American lead is vast, both in volume and in production technology and they could easily supply the entire world market. But because microelectronic technology seems likely to change greatly the traditional distinction between component and equipment producers and to require close vertical integration between them, the British (and indeed the European) electronics industry must be in a position to compete in microelectronics to remain in business. The Minister has announced

the department's willingness to support an industry r. and d. programme in the production technology of micro-electronics; the ministry has offered to contribute substantial sums to suitable projects, initiated by the industry itself. However, the crucial issue in micro-electronics is probably the industry's structure. It seems doubtful whether the UK market which can be foreseen for 1970 will support more than two or three viable enterprises manufacturing in this country.'

City & Guilds College open day
The work and new buildings of the City & Guilds College will be on view from 2.30 to 7.30 p.m. on the 25th October. The College comprises the five engineering departments of Imperial College—aeronautics, chemical engineering & chemical technology, civil, electrical and mechanical engineering—and visitors will also be able to see the equipment of the interdepartmental Centre for Computing and Automation which grew out of existing groups within the Department of Electrical Engineering. The City and Guilds College has been completely rebuilt and re-equipped during the past decade and it is in an unrivalled position to extend its activities further, both in the provision of undergraduate and postgraduate courses and in research.

British team develops power microcircuits
Prototype control modules small enough to fit into a matchbox, for the switching of mains voltages, have been developed by a team of applications engineers at the Lincoln plant of AEI-Thorn Semiconductors Ltd. Called power microcircuits, three versions have already been made and tested, and automated production methods will allow the devices to be sold for significantly less (about 30%) than the current electromechanical units needed for the control of washing machines, spin driers, food mixers and other equipment operated by fractional-horse-power units. Using a solid copper comb about 0·03in thick as a substrate, a specially developed series of high-voltage planar thyristors and diodes is put down with interconnexions to form a control circuit capable of withstanding surges up to 1000V. Each complete circuit is then encapsulated in an insulating block of resin plastic. The module—a power microcircuit—is completed by trimming the copper comb and forming the teeth into plug-in connexions which also serve as a highly effective heat sink capable of absorbing about 10W.

ITA contract for transmitters
The Independent Television Authority has signed with Pye TVT Ltd of Cambridge the largest single contract that it has ever placed. This contract, worth over £2M, is for 25 sets of transmitting equipment for the ITA's forthcoming duplicated 625-line u.h.f. service. Installation will begin in January 1969 and the first three stations to be equipped under this contract will start monochrome transmissions in the late summer of 1969, going over to colour as soon as possible. The remaining 22 stations will be brought into service successively up to the end of 1971. All this equipment will be used for the transmission of the ITA colour service, which is planned to open early in 1970. These transmitters will be automatically controlled and unmanned. For maximum reliability, transmitters will be installed in pairs connected in parallel.

344 classifications of engineering product at Olympia
The only international display of engineering components, materials, processes and finishes in the UK catering exclusively for engineering designers and technologists—the 5th Engineering Materials and Design Exhibition—was held at Olympia, London, on the 11th-15th September, 1967. More than 120 exhibitors participated in the show, including many from overseas—Belgium, Denmark, France, Germany, Holland, Norway, the Republic of Ireland, Sweden, Switzerland, South Africa and the USA. Exhibits on display represented the widest and most comprehensive range of engineering products and services ever presented at the show and encompassed the very latest materials and design developments in: electronics, transmission equipment, printed circuitry, automatic-control gear, insulators, mouldings, extruded products, plastics, resins, glass fibre, thermoplastic materials, corrosion-resistance materials, alloys, magnetic materials, electroplating, seals, adhesives, ceramics and every other type of component and product, process, finish and materials used in modern-day engineering. In all there were 344 separate classifications of product on show.

Music from electronics engineers
In the past decade dozens of new musical devices have been developed, all depending on electricity for motive power and/or amplification. This perhaps explains why the 6th British Musical Instruments Fair held at the Hotel Russell, London, on 20th-24th August, had on display more electrically operated instruments than ever before. Of the 35 firms exhibiting, over 25 displayed one or more instruments powered by electricity. From electric guitars and organs to the latest hi-fi gear, amplifiers, and sound-studio equipment, the Fair featured a wide range of electrical devices. Of particular interest were various automatic rhythm generators, particularly those shown by Rosetti and Severn Musical Instruments, which generate any of up to 16 dance rhythms (or combinations of them—sometimes with fascinating results) utilizing various combinations drawn from 10 different percussion-instrument sounds, some of which can be cancelled and added as required. These generators are not much larger than the average domestic radio receiver and contain no moving parts—the sounds all being spontaneously generated, thus allowing the user to start always on the first beat of the bar. Also of interest, albeit only in passing (at least to an observer), was an instrument which separates musical sounds into frequency bands, the outputs feeding special light panels to give visual effects which vary (predictably, after a few minutes' study) with the music.

British research on show in Poland
Some of Britain's latest scientific and technological achievements will be featured in the Scientific Achievements Exhibition which opens in Warsaw on the 7th October. The exhibition, being arranged by the Central Office of Information, is being produced in collaboration with the Polish Committee for Science and Technology whose members are co-operating in the arrangements being made. The exhibition's themes have been specially selected to interest Poland's research scientists, scientific and technical staff in industry and science students. Examples of British work being shown include projects and studies carried out by some of Britain's most distinguished scientists.

Pirate act becomes law
Since the 15th August, it is an offence to operate, work for, give assistance to or collaborate in any way with pirate radio stations. Severe penalties will be imposed on anyone who supplies records, staff, advertising, goods, services or apparatus for pirate broadcasters. The Marine Broadcasting (Offences) Act 1967 is designed to fulfil the international commitments of the United Kingdom under the European agreement for the prevention of broadcasting outside national territories. The object is to suppress *unauthorised* broadcasting from ships, aircraft and structures (such as the forts in the Thames estuary). The Act aims not only at the operating of unauthorized broadcasting stations, but also, and principally, at any form of deliberate assistance either in setting them up or helping them to carry on.

Second million for EMI colour television
EMI announced in April of this year that they had passed the million mark for colour-television-equipment orders. Since then they have received further substantial orders bringing the present total value to £2M in less than five months. These orders have been received mainly from Europe and the UK, and customers include the ABC, Anglia, BBC and Yorkshire television companies. Designed for both American and European television standards, using solid-state techniques throughout, the range includes the colour-camera channel, slide scanner, vision mixing and switching equipment, encoders, decoders, vertical aperture correctors and other ancillary equipment.

NEW EQUIPMENT

A description, compiled from information supplied by the manufacturers, of new components, accessories and test instruments.

COMPACT PACKAGED E.H.T.

The Marconi Co. Ltd. Chelmsford, Essex

A self-contained e.h.t. source about the size of a transistor radio is introduced by the Marconi Co. It is entirely solid-state and provides designers with a ready-to-use supply of up to 17500V for use in television and radar displays. Special attention has been given in the design to ensure that the unit conforms to all relevant military and ground specifications, and it will operate in extremes of temperature, humidity, gravitational forces, vibrations and other stresses. A test of impact has proved that the device will withstand 4000 shocks of 40*g*. An input supply of 15·5V is fed to the high-tension rail of a push-pull sinusoidal oscillator operating at an ultrasonic frequency in excess of 20kHz.

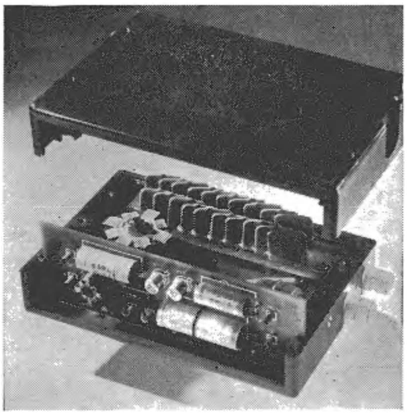

This output is transformer-coupled into a silicon-diode multiplier stack of the Cockroft-Walton type. An external corona stabilizer is employed at the output to provide a constant voltage over a wide range of currents up to 200μA. The unit will remain undamaged during short circuits of the output lasting a number of seconds, provided that there is a limitation on the supply input current to not greater than 0·70A. The output current can be monitored with an ordinary multimeter using a special output from the unit. The case of the unit consists of two identical open moulded boxes which fit together to form a compact rectangular box. A web across each section contains a silicone elastomer, which both insulates, and excludes moisture from, all the high-voltage components. The printed board which contains the oscillator circuits is separate from this encapsulated section and remains easily accessible for servicing.

For more information circle **No. 271**

NULL DETECTOR

Honeywell Controls Ltd. Brentford, Middlesex

A solid-state electronic null detector offering up to ten times the measurement resolution of comparably priced conventional galvanometers has been developed by Honeywell. This general-purpose laboratory instrument, which specifies 0·5μV measurement resolution, is available in two configurations. Model-3970 is designed to replace existing panel-mounted galvanometers; model-3792 is designed as a self-contained instrument for bench or field operation. Both models incorporate the same operational features. At the heart of the electronic direct-microvolt null detector is a stable wideband operational amplifier that permits fixed-gain amplifications over ranges of 10, 100, and 1000. Such gain capability allows full-scale voltage ranges of 25-0-25, 250-0-250, 2500-0-2500μV. The unit, which is battery-powered, is constructed so that the entire electronics is shielded and guarded to permit normal operation in environments subjected to stray fields and unwanted leakage paths. The unit is also designed to maintain zero null balance even though source impedance of related test instruments changes or is continually varied. The measured signal is displayed on a taut-band meter centred at zero. The following are typical uses associated with this new null detector: obtaining null balance between voltages and reference sources; measuring and adjusting for minimum residual voltages at the outputs of amplifiers and power supplies; recording d.c. stability of amplifiers or power supplies; recording low-frequency noise of amplifiers and power supplies; as a d.c. amplifier with fixed gains of 10, 100 and 1000; and detecting the balance of direct-current bridges.

For more information circle **No. 272**

CAMERA-VIEWFINDER TUBE

Thorn-AEI Radio Valves & Tubes Ltd, 7 Soho Square, London W1

The Brimar M17-15W is a 7in flat-face rectangular monitor tube with a 70° deflexion angle and a heater rated at 11·5V, 0·15A. Electrostatic focus and magnetic deflexion are used and the tube has an overall maximum length of 242mm with a 29·4mm maximum neck diameter. A clear glass face is used and

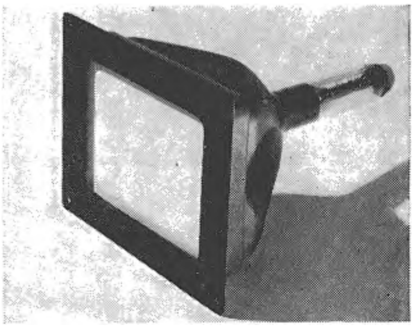

the screen is aluminized; an external conductive coating is also provided. This is a very-high-brightness tube, giving 850cd/m² for a final-anode voltage of 14kV and 170μA current, which gives excellent resolution under high-brightness conditions and can be used without a hood. This feature, coupled with the integral protection features and simplified mounting arrangements, makes this tube ideally suited to many small monitor and viewfinder applications. Implosion protection is given by the bonded-face-plate construction. In this system, the safety panel is bonded to the glass bulb of the tube by a transparent resin which sets to a tough rubbery consistency to give complete viewer protection. Flash-over protection for the supply circuits may be provided by the optional flash-over-protection base available for this tube. The specially moulded base incorporates accurately dimensioned spark gaps; simple connexions complete this safeguard. Tracking or surface-leakage problems are obviated by the application of a special moisture-repellent lacquer around to e.h.t. contact on the outside of the tube cone. The standard phosphor for the M17-15W is white, W(T4), but other phosphors can be supplied to special order.

For more information circle **No. 273**

H.V.-SUPPLY UNITS

Ekco Electronics Ltd, Southend-on-Sea, Essex

Ekco Electronics now market a range of high-voltage supply units for application where reliability under stringent environmental conditions is essential. Developed initially for use in airborne c.r.t. display systems, these units are now available to designers for similar airborne and ground applications. Transistor-oscillator circuitry is not included and designers therefore have complete freedom of layout when incorporating these units in equipment. The current range includes seven standard types with output voltages from 3 to 30kV. Special features are high efficiency, good regulation, high-altitude-operation capability, small size and low weight. The units are resin-encapsulated by a specially developed technique which gives particularly rugged construction and prevents voltage breakdown under low-pressure and humidity conditions; the temperature rating is −55 to +75°C. The rectifier diodes are mounted in cartridge form and are

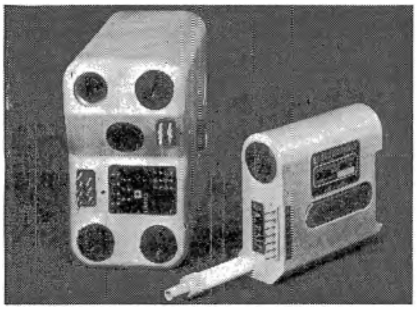

readily accessible for replacement purposes. The design and construction of these h.v. supply units have been tested by hundreds of thousands of hours of reliable service in civil and military airborne-radar systems. Currently, m.t.b.f.s in excess of 10 000 h are being achieved without any form of maintenance. Ancillary items available include a choke for use in the drive circuit and components to provide correct termination for the high-voltage outlets.

For more information circle **No. 274**

CIRCUIT-DEVELOPMENT BOARDS

Howard Electronic Industries Ltd, 77-79 Parkway, London NW1

Howard Electronic Industries have recently extended their range of circuit-development *Q*-boards to include the type - Q/IC/4001/Z/6 integrated - circuit board. It is designed to accommodate twelve integrated circuits of the dual-in-line type (type-TO5 and flat-packs can be used with suitable adaptors) together with any discrete components required.

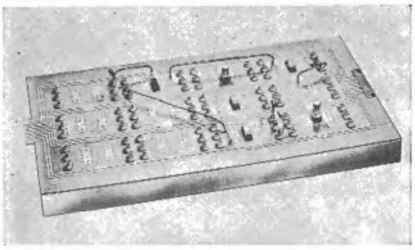

The integrated circuits are plugged into the board, effective electrical contact and location being achieved by means of individual spring-contact assemblies for each integrated - circuit termination. Similar contact assemblies are provided for the connexion of jumper leads, thereby completely eliminating the need to solder during circuit development. Bus-bars are provided for power supplies and are terminated at each end of the board by printed-circuit edge connectors, thereby allowing several boards to be interconnected.

For more information circle **No. 275**

PRINTED-CIRCUIT EDGE CONNECTORS

AMPindustrial, Terminal House, Stanmore, Middlesex

AMPindustrial have made a further addition to their range of printed-circuit connectors. This is the AMP-EDGE connector, featuring a contact which ensures excellent performance over a wide range of printed-circuit-board thicknesses. The contact-to-board pressure is almost constant for board thicknesses varying from 0·057 to 0·072in. The minimum pressure is reached with a spring deflexion as low as 0·0025in, while the upper limit will not be exceeded when a board of

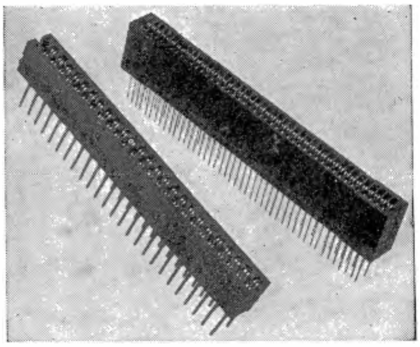

maximum thickness is used. The contacts are bifurcated for redundancy and are manufactured from phosphor bronze with selective gold-over-nickel plating. They are designed for manual or programmed wiring, using either miniature or standard Termi-point clips but are also suitable for wrap-type or soldering techniques. In addition to the wire-to-board type, a board-to-board version with short posts for soldering into a printed-circuit board is available. The connectors are available in 0·100, 0·150, 0·156 and 0·200in contact-to-contact spacings in a broad number of positions. Connectors can be ordered with contacts loaded on one or both sides for single or double-sided printed-circuit applications. The block material used is glass-filled polycarbonate. Connectors are available with either integrally moulded mounting holes or with snap-on fixing ears. The snap-on type are preassembled by AMP and the ears are designed to fit within the moulding cavities thus giving a performance equal to that of the fully moulded version.

For more information circle **No. 276**

MINIATURE H.V. SILICON RECTIFIERS

Bourns (Trimpot) Ltd, 17/27 High Street, Hounslow, Middlesex

A series of miniature multipurpose silicon power rectifiers, claimed to be the first series with peak inverse voltages ranging from 100 to 10000V, is now available. Manufactured by the Semtech Corporation, California, and marketed in the UK by Bourns, the new series, known as Sempac, have cylindrical insulated cases and axial leads, similar to a computer diode. Solid internal construction and pure silver leads provide mechanical strength and good thermal conductivity. Hermetically sealed, Sem-

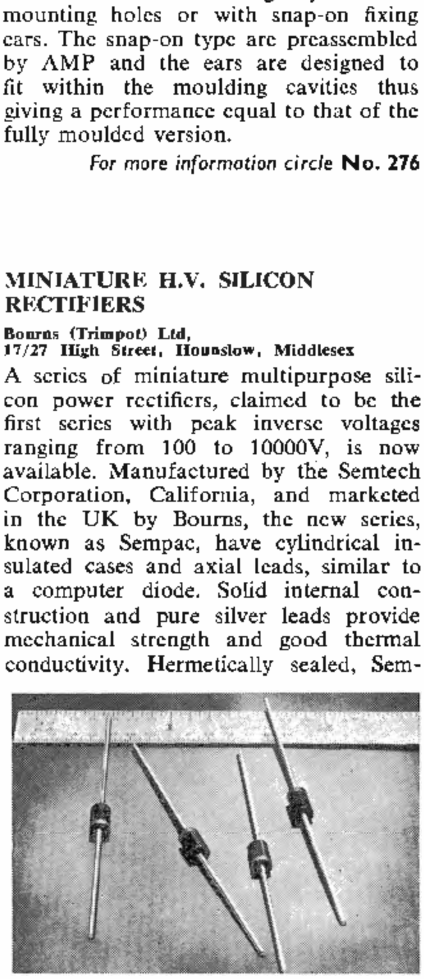

pac is designed to meet stringent temperature-cycling and humidity requirements.

Electrical and mechanical specification:

Types SCEL to SCEO:
100 to 1000V; 1A at 55°C (no heat sink); 3A to MIL STD750

Types SCEL5 to SCE30:
1500 to 3000V; 0·25A at 55°C (no heat sink)

Dimensions: length 0·235in, diameter 0·125in

Types SCE25A to SCE50A:
2500 to 5000V; 0·15A at 55°C (no heat sink)

Types SCE40 to SCE100:
400 to 10000V; 0·10A at 55°C (no heat sink)

Dimensions: length 0·410in, diameter 0·140in.

For more information circle **No. 277**

VERSATILE A.C.-D.C. VOLTMETER

Honeywell Controls Ltd, Brentford, Middlesex

A new multimeter designed to meet both a.c. and d.c. measuring requirements and, at the same time, function as a general-purpose laboratory unit is announced by Honeywell. The new instrument (model-1002) serves primarily as a differential voltmeter for measuring a.c. and d.c. signals but can also be used as a voltage-reference source, a ratiometer, a decade voltage divider and a null detector. Both alternating (r.m.s.) and direct voltages can be measured up to 1100V in four ranges by the model-1002, and d.c./d.c. ratios using external reference voltages up to ±100V. Full-scale measurement ranges for both operational modes (a.c. or d.c.) are 1, 10, 100 and 1000V, with 10% overranging for each range. The a.c. frequency range extends from 20 to 20 000Hz. The instrument's differential-input capability permits accurate measurements with high resolution in the presence of common-mode voltages and superimposed noise. Three basic elements make up to solid-state laboratory test unit: a Zener-regulated ±11V reference supply, an electronic null detector, and a 6-decade Kelvin-Varley voltage divider with numerical readout.

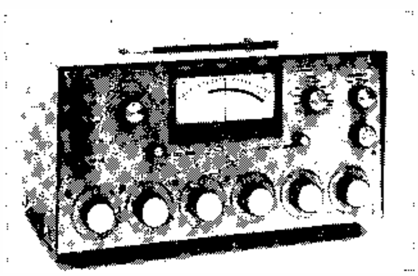

The voltmeter can be used as a standard laboratory unit for the following purposes: voltage-reference source for precision calibration of potentiometric instruments (voltage levels of 6-digit resolution, accurate to ±0·0025% and varying from 0 to 11V); null detection to provide highly sensitive indications of input changes as small as 100nV or input currents of 10^{-13}A; decade voltage divider to make accurate voltage-level divisions to ±0·001% using a 6-decade Kelvin-Varley divider network; ratiometer for precise d.c.-ratio measurements in full-scale voltage ranges of 1:1, 10:1 and 100:1 with ±0·001% accuracy.

For more information circle **No. 278**

SEMICONDUCTOR TEST SET

Dymar Electronics Ltd, Rembrandt House, Whippendell Road, Watford, Hertfordshire

The plug-in type-731 test set, available from Dymar Electronics evaluates the important parameters of semiconductors. Leakage currents (I_{co}) of diodes and transistors can be measured from 1μA to 3mA (1pA to 3mA when used in conjunction with the type-721 d.c. microvoltmeter) in either grounded-base or grounded-emitter configuration with a continuously adjustable bias voltage of 0-250V. The collector breakdown voltage of transistors and Zeners can be measured with currents of up to 30mA

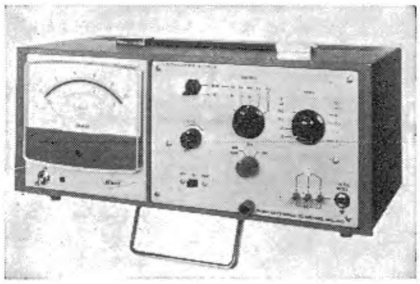

for collector voltages of 0-250V. The H_{fe} of transistors is measured at 1kHz (for bias collector currents up to 0·3A) and so is the input resistance and dynamic resistance of Zeners. The instrument is extremely simple to operate as all parameters are read directly on the meter and no balancing operations are required.

For more information circle **No. 279**

SIGNAL-CONVERTER SERIES

Mimic Diagrams & Electronics Ltd, Crayford, Kent

The Mimic series-SC300-B signal converters are inexpensive and versatile means of making most standard process-control instruments electrically compatible. The major manufacturers of process instruments use such a number of standard signal ranges that serious problems can arise when assembling a complete instrument system. The SC300 signal converters accept any one of the standard inputs and convert them to any standard output range. A typical application is a transmitter having a 1-5mA output which, by using the SC300, can drive a recorder requiring a 10-15mA input. The signal converter uses six silicon transistors and there are only two

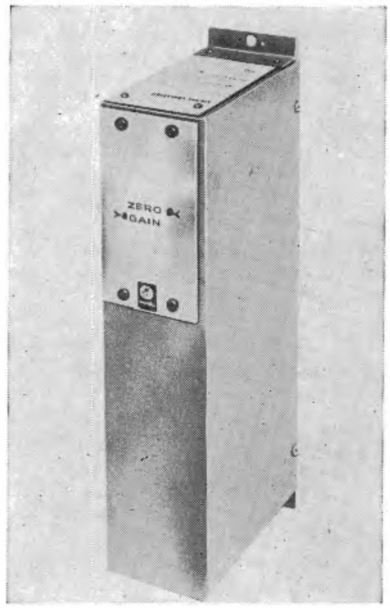

controls, each with 20 turns; the 'zero' potentiometer to adjust zero or minimum and the 'gain' potentiometer to adjust the full-scale output. Both controls are for fine adjustments only, as selection of terminal-strip connections determines the signal range covered. When desired, the signal converter may be easily re-adjusted to obtain another input- or output-range signal. Full technical details are given in a new brochure.

For more information circle **No. 280**

SOUND-LEVEL METER

Dawe Instruments Ltd, Western Avenue, London W3

A portable sound-level meter, now accepted as essential basic equipment for the determination and control of noise, has been developed by Dawe Instruments. The fully transistorized meter, designated type-1400G, incorporates the latest circuit techniques within a tough plastic case; so that, including micro-

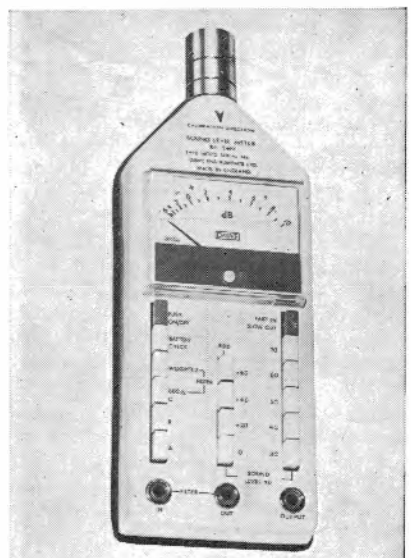

phone and battery, it weighs only 2lb 10oz (1·2kg). The type-1400G is an accurate and reliable instrument intended primarily for measuring sound levels from 24 to 140dB (or up to 200dB with a special microphone) over the entire audio range from 31·5Hz to 8kHz. The circuitry, which incorporates *A*, *B* and *C* weighting networks corresponding closely to the 40, 70 and 100phon equal-loudness contours, fully meets the IEC Publication 123: *Recommendations for sound-level meters* and BS 3489: *Specification for sound-level meters*. The very stable ceramic microphone is essentially nondirectional and can be detached for use up to 20ft away from the instrument on an extension cable. It is ruggedly constructed and capable of withstanding a wide range of temperature (−30 to +95°C) and humidity (0-100% rh). The ceramic microphone does not require a polarizing voltage nor a humidity-sensitive preamplifier. Jacks allow such equipment as a.f. analysers, variable for octave-band filters and statistical analysers to be used with the instrument. The impedance of the amplifier output to the filter jack is 600Ω. A selector provides load impedances of either 600Ω or 10kΩ. Overall dimensions are 12¼×4⅜×2½in (310×110×64mm).

For more information circle **No. 281**

DIFFERENTIAL D.C. VOLTMETER

Marconi Instruments Ltd, St. Albans, Hertfordshire

Marconi Instruments announces a new differential d.c. voltmeter, type-TF2606. It covers the ranges 0-11, 0-110 and 0-1100V, to an accuracy of 0·05% and with a measurement discrimination of 0·0001%; the discrimination is better than 0·1mV on the 11V range. The TF2606 is a manually operated voltage-measuring instrument with the full accuracy of a high-grade digital voltmeter. It comprises an accurate reference source, a five-decade potentiometer and a sensitive centre-zero electronic voltmeter. Voltages up to 11V are measured by comparing the unknown directly with the potentiometer output voltage. Above 11V, a high-impedance attenuator is introduced between the input terminal and measuring circuit. For many applications it has distinct advantages over a digital instrument. For example, below 11V it presents an almost infinite resistance to the unknown source when the potentiometer is set for a zero meter reading. It is very useful, therefore, for measurement of the output e.m.f. of high-resistance sources, and for other similar measurements where even the 1MΩ normally regarded as an acceptable digital-voltmeter input resistance can cause errors. Other important features of the instrument include: (a) provision for standardizing the reference voltage against a built-in standard cell; (b) the ability of the instrument to indicate small changes in voltage without the necessity to adjust the potentiometer setting manually, (c) the provision of an

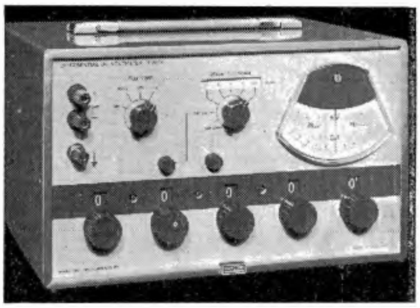

analogue output suitable for driving a chart recorder directly; furthermore, a true analogue-of-error voltage is available, free from the ±1 digit uncertainty. For applications where it is necessary to adjust the unknown voltage to a particular level, the differential voltmeter performs to considerable advantage. The potentiometer controls are simply set to the required voltage, and the device under test is adjusted to provide zero reading on the TF2606 panel meter. This capability is of particular value in production-line calibration and testing.

For more information circle **No. 282**

SOLID-STATE TRANSIENT SUPPRESSORS

Motorola Semiconductor Products Inc., Empire Way, Wembley, Middlesex

A series of solid-state transient suppressors, capable of protecting electronic equipment against damage from power surges up to 12kW, has been introduced by Motorola. The devices, utilizing a number of carefully matched silicon Zener diodes to achieve the required power ratings, are designed to be used individually in d.c. systems or as back-to-back pairs for applications up to 117V a.c. The transient suppressors are expected to find maximum use as external guardians of electronic systems composed of a number of individual equipments, such as aircraft systems, military automotive systems etc. In such applications, a single suppressor normally can protect the entire system against transients that could damage one or more equipments in the system. However, the devices may also be built into individual equipment during manufacture. Weighing less than 1oz and occupying less than 2in³ of space, they can be easily accommodated even in compact equipment. The Zener-diode suppressors have an impressive number of advantages over other types of suppressors in common use. These suppressors have predictable temperature sensitivity and maintain their Zener breakdown-voltage levels relatively constant over an operating range of −65 to +75°C; they do not change characteristics over long-term use. Ringing, associated with commonly used *RC*-type suppressor networks, is nonexistent. Also the large quiescent currents encountered with voltage-dependent resistors are reduced to 50μA in this suppressor. Other advantages include very fast reaction time and very low clamping factors (maximum breakdown voltage/minimum breakdown voltage) by comparison with the other types of suppressors.

For more information circle **No. 283**

D.C.-COUPLED WIDEBAND POWER AMPLIFIER

AIM Electronics Ltd, 71-73 Fitzroy Street, Cambridge

A low-distortion wideband power-amplifier module is the latest addition to the AIM modular instrumentation range; it completes a range of amplifiers built by AIM Electronics. This amplifier has a frequency response that is flat to within 3dB from d.c. to 100kHz. It contains its own power unit working from 105-117V or 195-260V supplies at 50-60Hz. The power output from the amplifier is greater than 25W, with less than 0·25% harmonic distortion. The circuit is proof against short circuits, open circuits and the most unpleasant capacitive or inductive loads. The input impedance is greater than 10kΩ, balanced or unbalanced, and the minimum output load impedance is 4Ω. Input level required for full output is greater than 100mV r.m.s. and the power response of the unit is flat to within 3dB from d.c. to 50kHz. The amplifier is an ideal high-fidelity loudspeaker driver for broadcast studio and auditorium work, because of its low distortion and wide bandwidth. It can also be used to drive a mechanical or optical chopper system from the reference channel of a coherent detector (AIM System 5.1), for driving shakers in vibratory transfer function analysis (AIM System 5.12) and for driving servomotors in servo-analysis systems. The amplifier is built as a standard 4in module and is complementary to other amplifiers in the modular range made by the same company. It is the last of the series of wideband amplifiers of which the first was the ultra-low-noise parametric amplifier.

For more information circle **No. 284**

GLASS-DIELECTRIC TRIMMER CAPACITORS

Steatite Insulations Ltd, Hagley Road, Birmingham 16

A new range of precision miniature glass-dielectric trimmer capacitors is now available from Steatite Insulations. The trimmers (type MSN) incorporate most of the features found on the highest-priced units, which are almost exclusively used in military and aerospace equipment, at less than 50% of the cost. Thus, apart from replacing high-cost units where a slight reduction in the capacitor characteristics is permissible, they are also likely to replace air-dielectric types in applications where higher stability and better resolution are required. The dielectric body is a silicate-glass (containing lead oxide) tube 4mm o.d. The air gap between the piston and the inner

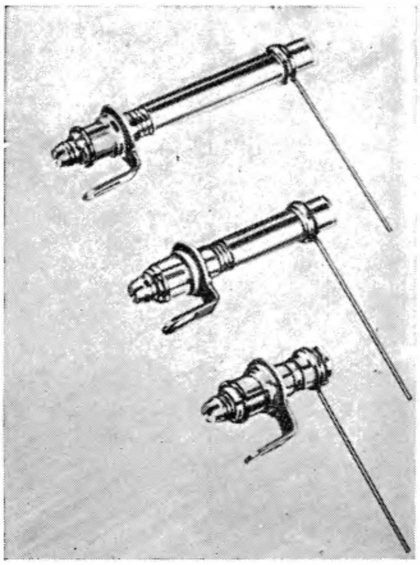

dielectric wall is less than 0·0002in. Three versions are available for chassis, printed-circuit and panel mounting. The capacitances available are 0·4-4, 0·4-6·3, 0·4-10, 0·4-16 and 0·4-25pF. Q-factors exceed 500 at 20MHz, with a capacitance resolution better than 0·01pF. The temperature coefficient is -50 ± 50 parts/10^6 per degC. The operating-temperature range is -55 to $+125$°C; working voltage 500V.

For more information circle **No. 285**

BINARY CAPACITOR BOX

Bi-Trinary Electrical Ltd,
Thirlmere Close, Frodham, Cheshire

A range of compact easily handled capacitor boxes has now been developed by Bi-Trinary Electrical to withstand a working voltage of over 250V, 50Hz or 600V d.c., with a maximum capacitance of 64μF. The equipment weighs between 10 and 15lb, dependent on capacitance, and measures 10 × 7 × 7in. By using the natural binary values of standard capacitors, it achieves its high power rating.

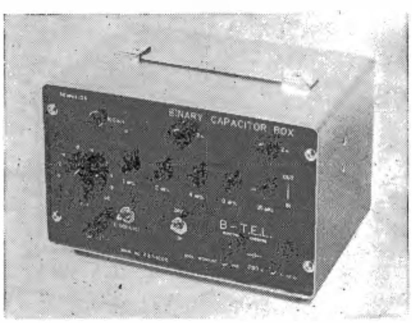

Two types of boxes have been produced: a 10%-tolerance model for use in colleges and industry for smoothing, power-factor correction, as a substitution box or as a capacitive load; and a 2%-tolerance model designed for engineers and laboratories as a standard capacitor or to determine capacitor tolerance in a system or prototype equipment. Both models are available with a capacitance of either 32μF or 64μF in 0·1μF steps. For ease of handling, storage or use in multiphase circuits, each piece of equipment is contained in a grey steel case fitted with a carrying handle and plastic feet.

For more information circle **No. 286**

INTEGRATED MEDIUM-POWER AMPLIFIER

SGS-Fairchild Ltd,
Planar House, Walton Street, Aylesbury, Buckinghamshire

A linear microcircuit, the μA716C, is announced by SGS-Fairchild. Designed primarily as a telephone-system channel amplifier, its characteristics make it also useful for audio, instrumentation, servo-control and mobile communication systems. This linear microcircuit is a monolithic fixed-gain medium-power amplifier, providing medium output current, low distortion, excellent gain stability and wide bandwidth (up to 5MHz). Voltage gains of 10, 20, 100 or 200 can be selected by the equipment designer, simply by connecting to the appropriate pins. Typical temperature stability of the gain at 0 to 70°C is $\pm$0·02dB. Minimum voltage swing is 10V peak-to-peak into a 150Ω load (15V peak-to-peak into loads of 5kΩ and above), allowing loudspeakers to be driven directly by the device. With a voltage gain of 100, total harmonic distortion of a typical amplifier is 0·01% making it attractive for audio applications. An output resistance of, typically, 1Ω provides constant-voltage output into varying loads; a large output-current capability of 100mA peak allows output stages supplying 5A to be driven directly; single-power-supply versatility is 18 to 24V.

For more information circle **No. 287**

ACCELEROMETER

Electro Mechanisms Ltd,
218-221 Bedford Avenue, Slough, Buckinghamshire

The type-QZR piezoelectric accelerometer available from Electro Mechanisms is designed to measure angular vibrations with a minimum response to linear acceleration. The QZR can be used for the measurement and remote indication of angular vibrations experienced on aircraft, vehicles and machinery. The QZR accelerometer employs the principle of bending a piezoelectric transducing element due to the effect of rotary acceleration. The rotary stress on the piezoelectric element produces an electrical charge proportional to the applied angular vibration. The patented construction techniques used in the QZR accelerometer allow production of a low-weight unit with high-sensitivity and a wide frequency range. The QZR accelerometer is intended for use with the Electro Mechanisms range of impedance-matching amplifier units.

For more information circle **No. 289**

THIN MICROSWITCH

Plessey Components Group,
Abbey Works, Titchfield, Fareham, Hampshire

The type-25 slim switch, made under licence from the Licon Division of Illinois Tool Works Inc., has been introduced by the Components Group of the Plessey Co. Ltd. The entire mechanism is packed into a case of high-temperature resistant plastic only 0·283in (7·2mm) thick, 1·5in (38·1mm) wide and 0·825in (21mm) high. With very long life at electrical ratings up to 12A resistive,

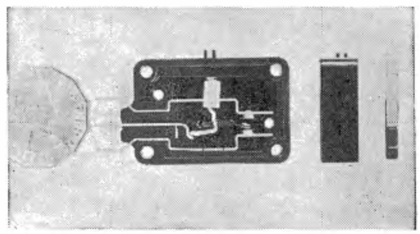

the type-25 uses a coil spring to operate the single-break mechanism as opposed to the stressed blades found in other units. Typical applications include vending machines, business machines, timing and control devices; the switches are available with a wide choice of actuators.

For more information circle **No. 289**

FREQUENCY COMPARATOR

Montronics Division of John Fluke Corporation,
PO Box 7428, Seattle, Washington 98133, USA

A frequency comparator (model-103A), which is capable of making 'stand-alone' relative-frequency comparisons, relative-phase measurements and short-term stability measurements without peripheral equipment is now available from the Montronics Division of John Fluke Corporation. The new comparator which is of all-silicon-semiconductor design to assure high reliability over a wide temperature range makes short-term frequency comparisons to 1 part in 10^{11}. Accuracy may be extended to 1 part in 10^{13} under controlled environmental conditions. The 103A accepts a range of test and reference frequencies of 100kHz to 5MHz in 14 discrete increments, acceptable for both inputs independently of one another and in any combination. Seven data channels out are available. Front-panel metering provides stand-alone operation with no other readout devices required for most measurements. This comparator can be used on the test bench as well as in the standards laboratory.

For more information circle **No. 290**

RADIO-FREQUENCY BRIDGE

General Radio Co. (UK) Ltd,
Bourne End, Buckinghamshire

General Radio has announced a new impedance bridge for accurate measurements in the 400kHz-60MHz range. The 1606-B radio-frequency bridge is adaptable to coaxial connectors, and in parti-

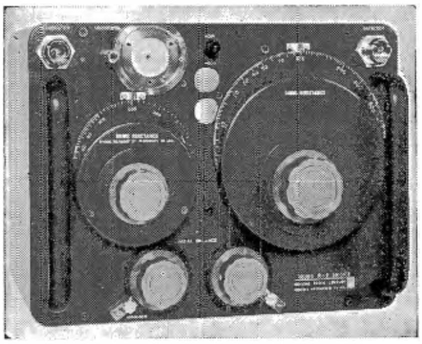

cular the GR900 precision coaxial connector, for convenience in making repeatable measurements on devices fitted with coaxial connectors. The GR900 coaxial connection also simplifies calibration of the bridge with precision resistance and capacitance standards. The screw-type terminals on the basic instrument can be adapted to GR900 coaxial connectors with the 1606-P2 adaptor kit, and to other coaxial systems with appropriate adaptors. The resistance range of the bridge is 0 to 1000Ω, and the reactance range is ±5000Ω at 1MHz (at other frequencies, the reactance reading must be divided by the frequency in megahertz).

For more information circle **No. 291**

POWER SUPPLIES

The Solartron Electronic Group Ltd, Farnborough, Hampshire

The Solartron AS1410 range of power supplies has been improved by the provision of current switch selection in 1% parameter increments and digital output-voltage selection with a continuously variable fine control. The new mark-2 range gives a choice of models providing voltages up to 60V and 5A maximum current. Completely isolated outputs allow these capabilities to be extended by series and/or parallel connection. All may operate as constant-voltage or constant-current supplies and incorporate fully automatic overload protection (which makes them virtually indestructible even under severe operating conditions). Remote programming, sensing

and mode indication with modulation facilities, fast transient response time and very low ripple and noise make the AS1410.2 series suitable for many specialized applications as well as for conventional laboratory use. The output voltage is adjusted digitally on three in-line selectors, the variable fine control covering the total range of 100mV between digits. This gives high setting resolution allowing full use to be made of the inherent stability; i.e. 0·01% line regulation; 0·005% load regulation and 0·01% per degC temperature coefficient. Current is indicated on a meter whose full scale is automatically adjusted to suit the load condition. Silicon semiconductors and glass-fibre printed-circuit boards are used throughout, and the specification is maintained from 0 to 50°C. Computer-grade electrolytic capacitors, high-grade transformers and cracked carbon resistors all contribute to the reliability of the basic design.

For more information circle **No. 292**

n-CHANNEL F.E.T.

Texas Instruments Ltd, Manton Lane, Bedford

To meet growing demands, a family of *n*-channel f.e.t.s. are being manufactured by Texas Instruments at Bedford. The 2N3821 family comprises five devices—2N3821-4 and T1S14—and perform v.h.f. amplification and mixing functions as well as high-speed chopping; the family is housed in TO-72 cases.

The 2N3821 and 2N3822 have leakage currents of less than 100μA, input capacitances of 6pF, and reverse transfer capacitances of 3pF. A feature of these devices is the high g_m of each—4mA/V and 6mA/V, respectively. These parameters render them suitable for a.f., r.f. and high-input-impedance applications. A further advantage of the 2N3822 is its 10Hz noise figure of better than 5dB. For v.h.f. applications the 2N3823 is recommended—it has a 2pF reverse transfer capacitance, a noise figure of 2·5dB at 100MHz and a g_m of 6mA/V. Since the 2N3823 has square-law transfer characteristics, crossmodulation is minimized. Chopping applications are satisfied by the 2N3824 which has an ON resistance of 250Ω maximum, and an $I_{D(off)}$ of 0·1nA. A low reverse transfer capacitance of 3pF allows a high chopping rate to be obtained. The TIS14 is a general-purpose device, suitable for most applications where an inexpensive unit is required, and where the circuit requirements are not stringent.

For more information circle **No. 293**

LOW-DRIFT HIGH-SPEED OPERATIONAL AMPLIFIER

Advance Electronics Ltd, Roebuck Road, Hainault, Ilford, Essex

Advance Electronics has introduced a new small chopper-stabilized operational amplifier sutiable for applications which demand very low drift and high speed of response such as digital-analogue conversion, precise integration and low-level amplification. Made under license from Zeltex of California, the new operational amplifier has a very low drift of 0·2μC/degC and an offset current of 30nA. The current drift is 0·2pA/degC. The amplifier model-145 has an exceptionally high slew rate of 250V/μs, corresponding to a full frequency output of 4MHz. A high gain-bandwidth product is also features (100MHz) together with an output current of 25mA. The chopper circuitry drive is internal, and the only power supply required is ±15V. The chopper drive is at 150Hz. The unit is housed in a diecast aluminium case which provides shielding in high noise environments.

For more information circle **No. 294**

WAVEGUIDE FREQUENCY METER

Microlab/FXR, Livingston, New Jersey, USA

A precision direct-reading reaction-type frequency meter for use with WR-75 waveguide is now available from Microlab/FXR. Covering a frequency range of 10 450 to 13 350GHz, the unit provides a 20% nominal absorption dip, with a loaded Q of greater than 7000. Accuracy is 0·06% of dial reading, or 0·01% with

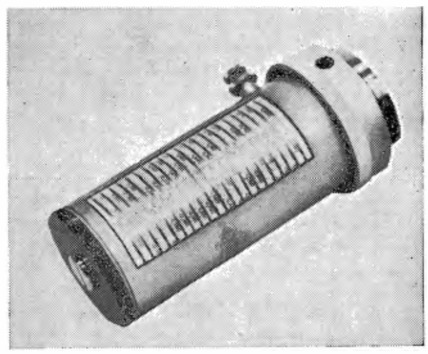

correction chart. Designated model 410-A12, the new frequency meter features full-scale visibility at all times for rapid reading, with scale markings of 2MHz/division. WR-75 waveguide frequency meters have application in broadcast, telephone and other communications fields.

For more information circle **No. 295**

ELECTRONIC THERMOMETER

Comark Electronics Ltd, Gloucester Road, Littlehampton, Sussex

Two instruments have been added to the range of electronic thermometers manufactured by Comark Electronics. The low-temperature range (−200°C to +30°C) is covered by the type 165CL, while the moderate-temperature range (−60°C to +170°C), which is ideal for all environmental-temperature testing, is covered by the type 165CM. Both instruments have 23 ranges, each spanning 10degC to give a resolution of 0·1degC at an accuracy better than 0·5degC. Temperature, measured by Cu/Con thermocouples, is read directly from the instrument without reference to calibration tables or charts; automatic compensation eliminates the need for cold-junction and lead-length corrections. Suitable Cu/Con

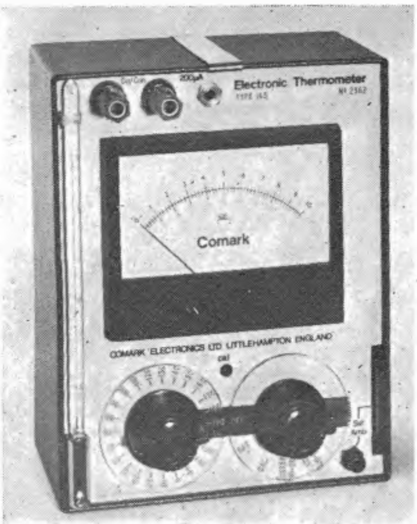

thermocouples are readily available from many sources. These instruments are battery powered and portable; they employ long-life Mallory mercury cells to give a minimum of 1500 operating hours between battery changes.

For more information circle **No. 296**

FIXED- OR ADJUSTABLE-TIME-DELAY RELAYS

Hi-Tek Corporation,
2220 South Anne Street, Santa Ana, California

A complete line of time-delay relays featuring solid-state timing networks for stable accuracy in preset or adjustable timing intervals and a choice of three operating modes is now available for military, industrial or commercial application from the Electronics Division of Hi-Tek Corporation. Units in the series feature highly reliable solid-state *RC* timing networks coupled to output relays to provide a large selection of output ratings. The timing circuit and the output relay are both sealed within one housing to afford the components complete protection from environmental extremes. The range includes the compact and the standard types. The compact units occupy approximately 30% less volume than standard units and are designed for delayed pull-in operation with 3 or 10A relay output ratings. Standard t.d.r.s. are available in three modes of operation: delayed pull-in; delayed drop-out maintained; and delayed drop-out one-shot. Output relays are rated at 2 or 10A. All units feature optional accuracies of $\pm 10\%$ or $\pm 5\%$, enhanced by the $\pm 2\%$ repeatability of the solid-state timing circuit. Accuracy remains constant and stable throughout the entire temperature and voltage range or any combination thereof as specified for each unit. Various can sizes, terminal types and optional mounting configurations, including studs, tabs and flanges, meet virtually all design requirements for efficient space utilization and interconnexion. Optional terminal types include solder hooks and plug-in pin terminals with mating sockets. Special application units may be supplied with 4PDT output capabilities, in larger or smaller units, with timing ranges beyond 600s.

For more information circle **No. 297**

PHOTOSENSITIVE SEMICONDUCTORS

Motorola Semiconductor Products Inc.,
Empire Way, Wembley, Middlesex

A photodetector type MRD200 and a phototransistor type MRD300, two light-activated sensing devices, mark Motorola's entry into the field of opto-electronics. The new devices are designed for applications such as punched-hole readers, lighting controls, counters, sorters, inspection and process controls, as well as activating low-level relays without using additional amplification. The MRD200 is a small (0·060in-diameter) 2-terminal device ideal for use where mechanical mounting requires high-density positioning, such as in high-speed tape- and card-readers and rotating-shaft information encoders. This photodetector exhibits a typical collector-emitter radiation sensitivity of 0·5mA per mW/cm^2, and displays linear characteristics over the dynamic range—ideal for reading film sound tracks. Maximum turn-on/turn-off time is only 6·5μs, allowing faster reading than any mechanical contacts. In addition, the MRD200 detector's narrow field of view minimizes crosstalk. The MRD300 transistor, with equally fast rise and fall times, utilizes a TO-18 case, with base external connection for added control. It has a higher sensitivity (1·6mA/mW per cm^2, typical S_{RCEO}) than the MRD200 detector and responds to modulation well above the audio spectrum, providing a useful means of information transfer from laser-light sources. Low leakage permits them to be used in direct-coupled circuitry, enabling them to operate at very low signal levels. Both devices operate from up to 50V power supplies and are compatible with most transistor circuitry.

For more information circle **No. 298**

MINIATURIZED MICROWAVES

Dale Electronics Ltd,
109 Jermyn Street, London SW1

A new generation of miniaturized co-axial devices has been announced by Microlab/FXR. These have been made possible by the type-MFM connector which allows microminiaturization beyond levels previously attainable and promises true TEM co-axial transmission up to 26·0GHz. Carefully compensated long-life stainless-steel connectors with interchangeable adaptors, launchers and other common parts have been developed and are available for any miniaturized co-axial requirements. Some of the microminiaturized hardware items now available to 18·0GHz are fixed attenuators, terminations, low pass filters, directional couplers, detectors, and power dividers. These devices are intended for installation in high density, miniaturized systems and experimental and laboratory use. The type-MFM connectors can also be incorporated in any Microlab/FXR co-axial component. This connector mates with most 0·141 line connectors such as OSM, BRM, NPN etc. The illustration shows three of these devices against a standard *N*-type microwave attenuator.

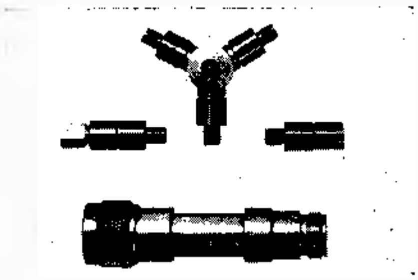

For more information circle **No. 299**

CALIBRATION RESISTANCE STANDARDS

Morganite Resistor Ltd,
Bede Industrial Estate, Jarrow, Co. Durham

A series of six transfer or secondary resistance standards for calibrating test instruments for measuring very low currents between 10^{-8} and 10^{-16}A is now available from Morganite Resistors. These standards are made with resistance values of every decade from 10^8 to $10^{13}\Omega$. They are based on the Megistor glass-enclosed resistor which over the past 15 years has proved its exceptional reliability and stability. Each standard is enclosed in a case 4·25in (10·8cm) long, on which the B.N.C. co-axial socket connectors are mounted. The complete set of six standards is supplied in a presentation and storage case. Individual standards can also be supplied.

For more information circle **No. 300**

EPOXY RESIN ADHESIVE/SEALANT

W. J. Furse and Co. Ltd,
Traffic Street, Nottingham

Hysol Epoxi-Patch kits are now available to industry through the sole distributors W. J. Furse and Co. Ltd. Applied cold, Hysol Epoxi-Patch offers the advantages of needing no critical weighting of its components, of having low toxicity, of requiring minimum preparation of surfaces to be bonded, and, since it is manufactured from 100% solids, minimal shrinkage after application (coefficient of linear thermal expansion at 30-90°C is approximately

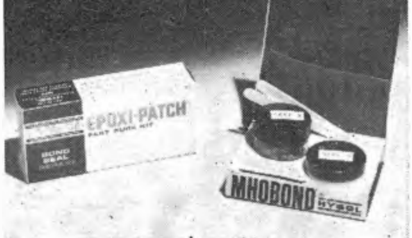

50×10^{-6}). In the basic kit, resin-sealant and hardener are packed in two tubes. Only amounts needed for a particular job need be mixed at one time so that wastage is eliminated. Once mixed, the adhesive is usable immediately, easy application being made by means of the spatula provided.

Hysol Epoxi-Patch kits have been tested and proved in use by leading manufacturers of precision instruments; permanent joins are possible between work-pieces of metal, wood, glass, concrete, ceramics and most plastics. Laboratory tests on aluminium to aluminium bonds with Hysol Epoxi-Patch have shown that the adhesive has a greater tensile shear strength than the joined metal. The kits provide industrial users with a fast, economcial method of effecting repairs in electrical connectors, circuit boards etc, and can be used to make oil- and water-proof seals.

It is available in nine different types which, apart from one general-purpose kit, are each specifically formulated for particular applications. Usable cure time varies from as low as 9min at room temperature for No. 309 to 24h for No. 0151 which is a special 'reading clear' formula for glass-to-glass bonds. Cure time can in every case be cut by heating to 60°C, by means of oven, lamp or blow-torch. Apart from two sizes of general-purpose kit, and the fast-cure and reading-clear formulas mentioned above, Hysol Epoxi-Patch mixes include iron-filled, bronze-filled, aluminium, shock-resistant and metal-to-metal. Tensile shear strengths, after full cure, vary between 1800 to 3280 lbf/in² at room temperature 25°C, and linear shrinkage and water absorption are in all cases negligible.

For more information circle **No. 301**

Data Sheets and Catalogues

CR test bridge
Nombrex Ltd, Exmouth, Devon

Details are given of the model-32 wide-range transistorized *CR* test bridge in this single-sheet leaflet.

For more information circle **No. 306**

Semiconductor-data summary
STC Semiconductors Ltd, Footscray, Sidcup, Kent

Over 70 new products are among the large number of semiconductor devices listed in the new STC data summary. A 28-page A4 booklet, it contains tabulated performance data on a broad range of silicon transistors, details of epoxy-encapsulated transistors and thyristors, increases to the range of 230 series DTL integrated circuits, stud-mounted Zeners etc.

For more information circle **No. 307**

Thick-film microcircuits
A.B. Metal Products Ltd, Dinas, Rhondda, Glam

This 4-page leaflet describes thick-film microcircuits, basic specifications for thick-film resistors, and microcircuit modules available.

For more information circle **No. 308**

Integrated-circuit-applications handbooks
Microelectronics Division, Electrosil Ltd, Lakeside Estate, Colnbrook Bypass, Slough, Bucks

'Designers' choice logic' is the title of a 46-page handbook on the series-8000 integrated-circuit elements. The booklet is in five parts, covering system design, electrical characteristics, a.c. testing, pin configuration, and life testing. Two other useful publications are a 32-page applications handbook on the company's Utilogic digital integrated circuits and a 12-page information pamphlet on design data and application of the Signetics 600 series of integrated DTL circuits.

For more information circle **No. 309**

Logic modules
West Hyde Developments Ltd, 30 High Street, Northwood, Middlesex

The 16 modules of the PIDAM (plug-in digital and analogue modules) system are described in detail and many examples of use are given in this 12p. 4to booklet.

For more information circle **No. 310**

Filters and networks
Barr and Stroud Ltd, Ammesland, Glasgow W3

The attenuation/frequency characteristics are given for examples from the manufacturer's range. Low-pass, bandpass, high-pass and bandstop frequency characteristics are shown.

For more information circle **No. 311**

Photofabrication
Kodak Ltd, Victoria Road, Ruislip, Middlesex

A new set of publications is introduced by Kodak, dealing with photofabrication—the process of producing metal parts by the use of photography and photosensitive resists. The literature consists of three booklets and five data sheets giving information on individual photoresists. The booklets cost 9s. each and the data sheets are free. Kodak is also offering the proceedings of its two seminars on microminiaturization held in the USA; each report costs 9s.

For more information circle **No. 312**

Statistical analysis
W. G. Pye and Co. Ltd, York Street, Cambridge

This 8-page leaflet describes the Datran classifier, an instrument produced by W. G. Pye and Datran Ltd which performs the major steps in statistical calculations—collection of successive measurements, division into categories, and totalling each category.

For more information circle **No. 313**

Plastics materials and products
Bakelite Xylonite Ltd, 27 Blandford Street, London W1

Bakelite Xylonite have published an 8-page leaflet: 'A concise guide to BXL plastics materials and products'. The materials are of particular significance in packaging, printing and electronics. Tables in the guide have been arranged to show the plastics available and the form in which they are supplied.

For more information circle **No. 314**

Silicon planar devices
Quarndon Electronics (Semiconductors) Ltd, Slack Lane, Derby

An 8-page booklet is available from Quarndon giving technical data on over 180 silicon planar transistors and digital and linear microcircuits manufactured by SGS-Fairchild, for whom Quarndon are distributors.

For more information circle **No. 315**

Ceramics for electronics applications
The Brush Beryllium Co., 17876 Street, Clair Avenue, Cleveland 10, Ohio

The Brush Beryllium Co. has made available the article 'Properties of ceramics for electronic applications', which appeared in the April 1967 issue of The Electronic Engineer. It is a comprehensive review of a number of technical ceramics and compares their properties relevant to electronic applications in a number of graphs and charts.

For more information circle **No. 316**

Semiconductor devices
AEI-Thorn Semiconductors Ltd, Carholme Road, Lincoln

The AEI-Thorn abridged catalogue lists the AEI range of semiconductor devices. If the user already holds a copy of the Thorn-AEI (Brimar) semiconductors handbook, a copy of the new AEI handbook in A4 size will soon be sent. In due course, all the Brimar data will be progressively transferred to this AEI handbook. New applicants will be charged a small fee for this service, while all existing holders of the Thorn-AEI handbook will receive the new publications free of charge.

For more information circle **No. 317**

Industrial cathode-ray tubes
Thorn-AEI Radio Valves & Tubes Ltd, 7 Soho Square, London W1

Brimar have published the 1967-68 edition of their abridged data brochure on industrial cathode-ray tubes. Since last year's edition, the number of available tube types shown had doubled to 80, covering the applications of radar, oscilloscopes, picture monitors and data display.

For more information circle **No. 318**

Batteries for electronics

Exide Batteries Division of Electric Power Storage Ltd, 50 Grosvenor Gardens, London SW1

A new edition of 'Exide batteries for light-electrical and electronic applications' has been published by Exide. Many new batteries are listed, designed to meet the needs of transistorized circuits and other electronic forms frequently for use under extreme conditions.

For more information circle **No. 319**

Controlled interception

Elliott-Automation Ltd, Portland Place, London W1

This is the latest in the series of booklets 'Automation in action' published by Elliotts. It describes interception control for supersonic speeds.

For more information circle **No. 320**

Arklone

Imperial Chemical Industries Ltd, PO Box 19, Weston Point, Runcorn, Cheshire

This booklet describes Arklone, ICI's latest cleaning solvent, which is ideal for cleaning components containing plastics, resins and elastomers.

For more information circle **No. 321**

DIARY OF THE MONTH

2 **Definition, realisation and use of time and frequency.** I.E.E. Colloquium. At Savoy Place, London, W.C.2, 9.30 a.m.

3 **The utilization of large telecommunications buildings** by T. J. Morgan. London Centre of Institution of Post Office Electrical Engineers. At I.E.E., Savoy Place, London, W.C.2, 5 p.m.

4 **Animal sonar** by David Pye. I.E.R.E. At 8/9 Bedford Square, London, W.C.1, 6 p.m.

Radiophonic workshop by F. C. Brooker. Society of Electronic and Radio Technicians. At London School of Hygiene and Tropical Medicine, Keppel Street, Gower Street, London, W.C.1, 7 p.m.

Colour television by D. G. Packham. Society of Electronic and Radio Technicians. At Charles Trevelyan Technical College, Maple Terrace, Newcastle upon Tyne, 7.15 p.m.

6 **The range of l.f. transmissions using digital modulation** by H. P. Williams and A. N. Ince. I.E.E. At Savoy Place, London, W.C.2, 5.30 p.m.

6–8 **Weekend course in colour television.** University of Bristol Department of Extra-Mural Studies. Lecturer: H. V. Sims. At Queen's Building, University Walk, Bristol. Details from 20a Berkeley Square, Bristol 6.

9 **Sources and uses of energy.** The Thomson lecture by Sir Henry Jones. Society of Instrument Technology. At the Royal Institution, 21 Albemarle Street, London, W.1, 6 p.m.

10 **Extending a narrow-band v.h.f. system to 230MHz** and **U.H.F. distribution at fundamental for large communal systems.** Society of Relay Engineers. At Conference Room, I.T.A., 70 Brompton Road, London, S.W.3, 2.30 p.m.

10–11 **Seminar on network techniques (for production planning).** Production Engineering Research Association. At P.E.R.A., Melton Mowbray, Leicester.

10–15 **Fourteenth international exhibition of electronics, telecommunications, automation and nucleonics.** At Ljubljana, Yugoslavia.

10–19 **Exhibition of scientific and industrial instruments.** Sponsored by Het Instrument. At Utrecht.

11 **Modern rodding and cabling methods** by M. Doherty and N. E. Fletcher. London Centre of the Institution of Post Office Electrical Engineers. At Conference Room, Fleet Building, Farringdon Street, London, E.C.4, 5 p.m.

The use of lasers in instrumentation by Dr. W. G. Townsend. West Wales Section of Society of Instrument Technology. At University College of Swansea, 7.15 p.m.

The automation of engineering design by R. J. Redding. Midland Section of the Society of Instrument Technology. At Birmingham Chamber of Commerce, 75 Harborne Road, Birmingham, 6.30 p.m.

Ultrasonics and medicine. I.E.E./I.E.R.E. Medical and Biological Electronics Group Colloquium. At Middlesex Hospital Medical School, Cleveland Street, London, W.1, 2.30 p.m. Tickets from I.E.R.E.

12–15 **Fifteenth international communications congress.** Istituto internazionale delle communicazioni. At Genoa.

13 **Recent advances in measurement circuits using semiconductor devices.** I.E.E. colloquium. At Savoy Place, London, W.C.2, 2.30 p.m.

The Ariel III satellite. I.E.E./I.E.R.E. joint symposium. At Middlesex Hospital Medical School, Cleveland Street, London, W.1. Registration forms from I.E.R.E.

13–22 **International fair for electronics, automation and instruments.** At Copenhagen.

16–21 **Electra '67:** fourth South African Electra exhibition. At Johannesburg.

17 **Education for the engineering mission** by Dr. W. G. Shepherd. I.E.E. At Savoy Place, London, W.C.2, 6 p.m.

17–19 **International symposium on antennas and propagation.** I.E.E.E. At the University of Michigan, Ann Arbor.

Fourth electronics in action exhibition. I.E.R.E. and I.E.E. At Napier College of Science and Technology, Edinburgh.

18 **Men, circuits and systems in telecommunications** by J. H. H. Merriman. I.E.E. Chairman's address. At Savoy Place, London, W.C.2, 5.30 p.m.

The impact of computers on business mathematics by Andrew Muir. British Computer Society. At the Renold Building, University of Manchester Institute of Science and Technology, 6.30 p.m.

19 **Printed-circuit group meeting,** Institute of Metal Finishing Annual Symposium. At the Palace Hotel, Buxton.

Thyristors. Society of Electronic and Radio Technicians. At Herbert Art Gallery and Museum, Early Street, Coventry, 7.30 p.m.

23 **Materials for ultrasonic delay lines.** I.E.E. discussion meeting opened by C. M. Van der Burgt. At Savoy Place, London, W.C.2, 5.30 p.m.

23–25 **National electronics conference.** I.E.E.E. and N.E.C. At Chicago, Illinois.

24 **Correction of linear distortion in wide-band links for multichannel telephony and waveform transmission** by J. M. Linke, I. F. McDiarmid, J. A. Taylor and D. A. Coles. I.E.E. At Savoy Place, London, W.C.2, 5.30 p.m.

25 **Data transmission** by G. Humphreys. Society of Instrument Technology and I.E.E. At Spencer Works, Richard Thomas and Baldwins, Llanwern, Newport, 6 p.m.

Infra-red technology by Lt.-Col. G. D. Peyter. Society of Instrument Technology. At Berkeley Hotel, High Street, Cheltenham, 7.30 p.m.

27 **A practical character recognition machine** by H. A. Bell and R. H. Britt. British Computer Society. At the City University, London, E.C.1, 4 p.m.

30 **The impact of the C.C.I.T.T. No. 6 signalling system on telecommunications** by E. P. G. Wright and D. L. Thomas. I.E.E. At Savoy Place, London, W.C.2, 5.30 p.m.

Résumés des principaux articles

Élément à mémoire à 16 chiffres binaires constitué de corps solides par Anh Nguyen-huu et R. H. Murphy

Résumé de l'article aux pages 604 à 608

Cet article décrit un circuit intégrateur à grande échelle—l'élément à 16 chiffres binaires—et son fonctionnement, ainsi que certaines des applications-type pour lesquelles il a été conçu.

Source d'énergie de 3kV, 60mA par C. W. Bodenhausen et G. Klein

Résumé de l'article aux pages 609 à 611

Les auteurs décrivent un bloc d'alimentation parfaitement stabilisé comportant un élément série se composant d'une lampe de transmission et d'un transistor. Ce dispositif permet d'obtenir une excellente stabilisation et un réglage instantané sans grand gain de circuit.

L'analyse du bruit des amplificateurs à réaction par P. J. Finnegan

Résumé de l'article aux pages 612 à 616

Le bruit à l'intérieur de toute invariante de temps à deux ouvertures peut être exprimé sous forme de deux sources de bruit à l'extérieur d'une invariante insonore, bien qu'équivalente, à deux ouvertures. En vertu de ce concept on peut obtenir des expressions approximatives mais généralement précises des générateurs de bruit global, du facteur de bruit et de la résistance de source optima de certaines catégories d'amplificateurs à réaction. Une étude a été effectuée sur la manière dont l'introduction de la réaction dégrade le facteur de bruit et altère la résistance de source optima, ainsi que sur la mise au point d'amplificateurs à dégradation négligeable du facteur de bruit en raison de la réaction. Finalement, une méthode simple est proposée pour l'analyse approximative d'une gamme plus étendue d'amplicateurs à réaction.

Réseau d'antennes à double fente ommidirectionnelles de bande X par T. Takeshima

Résumé de l'article aux pages 617 à 621

Cet article décrit un réseau d'antennes à fente ommidirectionnelles formé d'un guide d'ondes rectangulaire de bande X relativement mince et de plusieurs paires de fentes shunt longitudinales placées les unes en face des autres sur les côtés larges du guide d'ondes (ce dispositif étant sommairement appelé antenne à double fente). Les mesures effectuées ont montré que pour un guide d'ondes pont les dimensions extérieures seraient de 25mm×3mm, la courbe de radiation en azimut est circulaire à 1 dB près (fréquence mesurée: 9375MHz). Les résultats ont donné lieu à des comparaisons avec des guides d'ondes circulaires ou avec des antennes à fente du type coaxial. L'article conclut par une étude des méthodes de réalisation pratique pour la conductance de fente et de la capacité de transmission de puissance de l'antenne à double fente.

Minuteries à transistors à une jonction par J. F. Young

Résumé de l'article aux pages 621 à 623

L'utilisation du transistor à une jonction présente des avantages certains dans les circuits de minutage. industriels bien qu'il subsiste encore quelques difficultés. Deux circuits possibles sont décrits dans cet article: le premier produit un train d'impulsions après un retard initial mais ne réussit pas à fournir une puissance réuissance de sortie suffisante pour l'emploi direct avec un relais électromécanique; le second comprend des diodes permettant d'isoler le dispositif de minutage du relais, tous deux se trouvant dans le circuit émetteur. Le temps de retard est presque indépendant des variations de tension d'alimentation et de température ambiante.

Considérations sur la réalisation d'échelles à diodes tunnel montées en série par Z. C. Tan et J. B. Earnshaw

Résumé de l'article aux pages 624 à 629

Cet article traite des résultats de calculs se rapportant aux caracteristiques transitoires d'une paire de diodes tunnel similaires montées en série, polarisées par une source de courant idéal et déclenchées par des impulsions d'une source de tension à courant alternatif. Le but de cas calculs est d'étudier quantitativement les conditions de réalisation d'échelles utilisant des diodes tunnel montées en série. Une explication qualitative du fonctionnement de ces échelles est également présentée et ses limites sont indiquées. La principale conclusion de cette investigation est que les échelles à diodes tunnel montées en série, bien que pouvant être amenées à fonctionner de façon satisfaisante avec des composants choisis avec grand soin, n'en constituent pas moins des appareils d'une réalisation assez peu sûre du point de vue technique.

Une modèle de démonstration de conception simple par P. C. van Soest

Résumé de l'artcle aux pages 629 à 631

Afin de montrer certaines des particularités d'une système d'étude basé sur le modèle linéaire de Bush et Mosteller, l'auteur décrit une réalisation technique sommaire de ce système. Dans cette réalisation le vecteur de probabilité assigné aux classes de réponse est modifié suivant le modèle linéaire. L'acte d'omission, qui n'est pas pris en considération dans le modèle linéaire, est introduit. Un diagramme de montage du dispositif final est fourni.

Analyse de systèmes répétés de lignes de transmission avec charges équilibrées par J. N. Saha

Résumé de l'article aux pages 632 à 636

Les lignes de transmission à hyperfréquences sont souvent soutenues par un grand nombre d'adaptateurs de shunt en court-circuit sur de longues distances de leur parcours entre le transmetteur et l'antenne. Il est des plus souhaitables que cette ligne puisse transmettre la bande de fréquence la plus étendue possible tout en maintenant la réflexion dans la passe-bande à un minimum. Cet article détermine l'effet d'un grand nombre d'adaptateurs sur l'equilibrage et la largeur de bande. Les méthodes dites à matrice de dispersion ont été adoptées pour obtenir la formule du coefficient de transmission avant des sections à adaptateurs symétriques constituant la ligne. Différentes combinaisons de longeurs d'adaptateurs et d'espacements ont été envisagées dans un programme de calculatrice numérique et la réponse de fréquence a été relevée afin de démontrer que bon nombre de *ces combinaisons donnent lieu à des variations aléatoires du coefficient de transmission en fonction de la fréquence. Afin de réaliser une largeur de bande maxima tout en maintenant le coefficient de transmission à une valeur élevée, il a été démontré que, pour une charge équilibrée, des adaptateurs de shunt λ/8 en court-circuit à espacement de λ/4 constituent le meilleur dessin. La validité du processus a été confirmée par des observations expérimentales.*

Instrument de mesure de puissance à thermistor par S. M. Bozic et J. R. Whitbread

Résumé de l'article aux pages 637 à 640

L'instrument de mesure de puissance dont il est question ici utilise, comme élément sensible, un thermistor dont la puissance de chauffe est maintenue à un niveau quasi constant au moyen d'un système à réaction. Le circuit est analysé et ses principales caractéristiques sont étudiées. Un circuit pratique entièrement transistorisé est également indiqué. Ce dernier possède une loi de puissance réelle jusqu'à 10mW dans la gamme de fréquence de 100Hz à 10MHz. Les effets des variations de température ambiante ont été étudiés et rendus négligeables dans la gamme de 0 à − 55°C. La constante de temps du circuit de 18s est définie par le thermistor.

Analyse de l'erreur de capacité d'un relais modulateur à transistor à effet de champ et à isolement métallique par J. Dostál

Résumé de l'article aux pages 640 à 641

Cet article examine en détail la capacité entre électrodes en tant que source d'erreur dans le transistor à effet de champ semiconducteur à isolement métallique lorsqu'il est utilisé comme relais modulateur.

Compteur binaire transistorisé de 100MHz par R. J. Hood

Résumé de l'article aux pages 642 à 643

Deux compteurs binaires transistorisés sont décrits: un circuit de 50MHz basé sur le commutateur modulaire de courant et un élément pouvant fonctionner à des fréquences supérieures à 100MHz. Un compteur de 100MHz à trois étages est montré.

Traceur de caractéristiques de tension/courant fournissant des axes étalonnés par Min Wei Li et G. Hoffmann de Visme

Résumé de l'article aux pages 644 à 646

L'instrument dont il est question dans cet article est basé sur des principes fort simples pour relever et tracer les caractéristiques de tension/courant de diodes normales et à résistance négative et fournir des axes étalonnés. Les mêmes principes peuvent être appliqués pour traver les caractéristiques de tension/courant de n'importe quel dispositif. Le circuit se distingue par un équivalent électronique du commutateur rotatif qui fonctionne à partir du courant et dont le potentiel de contact est presque nul. Cet article indique également les conditions précises régissant la stabilité des diodes tunnel, en particulier, et des réseaux à deux bornes à résistance négative et à réglage de tension, en général.

Zusammenfassung der wichtigsten Beiträge

Ein 16-bit-HLTTL-Festkörperspeicherelement von Anh Nguyen-huu und R. H. Murphy

Zusammenfassung des Beitrages auf Seite 604-608

Der Beitrag beschreibt eine Grossintegrationsschaltung (LSI)—das 16-bit-Speicherelement—und seine Arbeitsweise, zusammen mit typischen Anwendungen, für die sie entworfen wurde.

Konstantstromversorgung für 3 kV, 60 mA von C. W. Bodenhausen und G. Klein

Zusammenfassung des Beitrages auf Seite 609-611

In diesem Beitrag wird eine hochkonstante Hochspannungsversorgung beschrieben, in der ein Längsglied aus einer Senderöhre und einem Transistor besteht. Auf diese Weise lässt sich ausgezeichnete Konstanthaltung und momentane Regelung ohne hohe Schleifenverstärkung erreichen.

Rauschanalyse rückgekoppelter Verstärker von P. J. Finnegan

Zusammenfassung des Beitrages auf Seite 612-616

Das Rauschen innerhalb jedes linearen, zeitlich unveränderlichen Vierpols kann durch zwei Rauschgeneratoren ausserhalb eines rauschlosen, sonst aber äquivalenten Vierpols ausgedrückt werden. Anwendung dieses Konzepts gestattet Ableitung von näherungsweisen, im allgemeinen aber genauen Ausdrücken für die Summenrauschgeneratoren, den Rauschfaktor und den optimalen Quellenwiderstand für gewisse Klassen rückgekoppelter Verstärker. Die Art und Weise, in der Anwendung von Rückkopplung den Rauschfaktor degradiert und den optimalen Quellenwiderstand ändert, sowie der Entwurf von Verstärkern mit vernachlässigbarer Degradierung des Rauschfaktors durch Rückkopplung werden untersucht. Abschliessend wird ein einfaches Verfahren für die näherungsweise Analyse einer breiten Auswahl rückgekoppelter Verstärker vorgeschlagen.

Rundstrahlendes Doppelschlitzstrahler-Antennensystem für das X-Band von T. Takeshima

Zusammenfassung des Beitrages auf Seite 617-621

Der Beitrag beschreibt ein rundstrahlendes Schlitzstrahler-system, das aus einem verhältnismässig dünnen X-Band-Rechteckhohlleiter mit einander auf den weiten Seiten gegenüberliegenden, parallelen Längsschlitzpaaren besteht. Diese Anordnung wird als Doppelschlitzantenne bezeichnet. Durch Messungen bei 9375MHz wird nachgewiesen, dass das Azimuth-Strahlungsdiagramm für einen geschlitzten Wellenleiter mit Aussenabmessungen von 25,4mm × 3,2mm innerhalb 1dB kreisrund ist. Weiterhin werden Vergleiche mit Rundhohlleitern und geschlitzten Koaxialantennen sowie praktische

Entwurfsmethoden für den Schlitzleitwert und die Leistungsaufnahme der Doppelschlitzantenne besprochen.

Zeitgeber mit Doppelbasisdioden von J. F. Young

Zusammenfassung des Beitrages auf Seite 621-623

Die Doppelbasisdiode hat vorteilhafte Anwendungsmöglichkeiten in industriellen Zeitgeberschaltungen, bei denen jedoch verschiedene Schwierigkeiten auftreten. Zwei Schaltungen werden beschrieben: die erste gibt nach Anfangsverzögerung eine Impulsreihe ab, deren Leistung für direkte Betätigung eines elektromechanischen Relais zu niedrig ist; in der zweiten Schaltung trennen Dioden die CR-Zeitschaltung vom Relais. Die Verzögerungszeit ist von Schwankungen der Speisespannung und der Umgebungstemperatur fast unabhängig.

Entwurfsüberlegungen für Untersetzer mit seriengeschalteten Tunneldioden von Z. C. Tan und J. B. Earnshaw

Zusammenfassung des Beitrages auf Seite 624-629

Dieser Beitrag behandelt die Ergebnisse von Berechnungen bezüglich der Einschwingeigenschaften eines seriengeschalteten Paares gleicher Tunneldioden, das durch eine ideale Stromquelle vorgespannt und durch Impulse von einer wechselstromgekoppelten Spannungsquelle getriggert wird. Zweck dieser Berechnungen ist die quantitative Untersuchung der Entwurfsbedingungen für Untersetzer mit Ketten seriengeschalteter Tunneldioden. Ferner wird eine qualitative Erläuterung der Arbeitsweise dieser Untersetzer mit Andeutung ihrer Begrenzung gegeben. Die Hauptschlussfolgerung dieser Untersuchung ist, dass Untersetzer mit seriengeschalteten Tunneldioden zwar mit kritisch ausgesuchten Bauelementen zufriedenstellend arbeiten können, vom technologischen Gesichtspunkt aus jedoch kaum ausführbar erscheinen.

Ein Demonstrationsmodell für eine einfache Lernsituation von P. C. van Soest

Zusammenfassung des Beitrages auf Seite 629-631

Eine einfache technische Verwirklichung eines auf dem linearen Modell von Bush und Mosteller beruhenden Lernsystems wird beschrieben, so dass die Eigenschaften eines solchen Systems vorgeführt werden können. In dieser Verwirklichung wird der den Reaktionsklassen zugeordnete Wahrscheinlichkeitsvektor den Anforderungen des linearen Modells entsprechend modifiziert. Das im linearen Modell nicht berücksichtigte Vergessen wird eingeführt. Für die endgültige Anordnung wird ein Schaltbild gegeben.

Analyse sich wiederholender Antennenleitungssysteme mit angepassten Lasten von J. N. Saha

Zusammenfassung des Beitrages auf Seite 632-636

VHF-Antennenleitungen werden oft über grosse Entfernungen zwischen Sender und Antenne durch kurzgeschlossene Stichleitungen unterstützt. Es ist sehr wünschenswert, dasse eine solche Leitung den breitmöglichsten Frequenzbereich übertragen kann und dass die Reflexion im Durchlassband so niedrig wie möglich gehalten wird. Dieser Beitrag bestimmt den Einfluss einer grossen Anzahl von Stichleitungen auf Anpassung und Bandbreite. In der Ableitung der Formel für den Vowärtsübertragungsfaktor für Abschnitte mit symmetrischer Stichleitungsanordnung, aus denen die Leitung besteht, werden Streumatrixmethoden angewendet. In einem Digitalrechnerprogramm wurden verschiedene Kombinationen von Leitungstunnellänge und- abstand untersucht, der Frequenzgang aufgenommen und gezeigt, dass viele dieser Kombinationen zu regellosen Schwankungen des Übertragungsfaktors mit der Frequenz führen. Es wird gezeigt, dass zur Erzielung maximaler Bandbreite bei hohem Übertragungsfaktor $\lambda/8$ kurzgeschlossene Parallelstichleitungen in $\lambda/4$ Abstand den besten Entwurf darstellen. Die Gültigkeit dieses Verfahrens wurde durch versuchsweise Beobachtungen bestätigt.

Thermistor-Leistungsmesser von S. M. Bozic und J. R. Whitbread

Zusammenfassung des Beitrages auf Seite 637-640

Der Messkopf des hier beschriebenen Leistungsmessers ist ein Thermistor, dessen Beheizung durch ein Rückwirkungssystem fast konstant gehalten wird. Die Schaltung wird analysiert und die Haupteigenschaften besprochen. Ausserdem wird eine praktische volltransistorierte Schaltung gegeben, die im Frequenzbereich 100Hz . . . 10MHz bis zu 10mW eine Wirkleistungskennlinie hat. Der Einfluss der Umgebungstemperaturschwankungen wird in Betracht gezogen und im Bereich 0 . . . + 55°C vernachlässigbar klein gemacht. Die 18-s-Zeitkonstante der Schaltung wird durch den Thermistor bestimmt.

Analyse des Kapazitätsfehlers eines MIS-FET-Choppermodulators von. J. Dostál

Zusammenfassung des Beitrages auf Seite 640 641

In dem Beitrag wird die Elektrodenkapazität als Fehlerquelle des in einem Choppermodulator verwendeten Metall-Nichtleiter-Halbleiter-Feldeffekttransistors besprochen und analysiert.

Transistorierter 100-MHz-Binärzähler von R. J. Hood

Zusammenfassung des Beitrages auf Seite 642-643

Es werden zwei transistorierte Binärzähler beschrieben: eine auf einem strombetätigten Schalter beruhende 50-MHz-Schaltung und ein Gerät, das mit Frequenzen von über 100MHz arbeiten kann. Ein dreistufiger 100-MHz-Zähler wird beschrieben.

Spannung-Strom-Kennlinienschreiber mit geeichten Koordinaten von Min Wei Li und G. Hoffmann de Visme

Zusammenfassung des Beitrages auf Seite 644 646

Der Beitrag beschreibt ein auf sehr einfachen Prinzipien beruhendes Gerät für das Aufnehmen der Strom-Spannungs-Kennlinien von normalen Dioden sowie solchen mit negativem Widerstand und Erstellung geeichter Koordinaten. Dieselben Prinzipien können für die Aufnahme von Strom-Spannungskennlinien beliebiger Elemente Anwendung finden. Ein Kennzeichen der Schaltung ist das elektronische Äquivalent eines spannungsgesteuerten Drehschalters, dessen Kontaktpotential fast null ist. Der Beitrag enthält auch eine Darlegung der genauen Bedingungen, die die Stabilität von spannungsgesteuerten Zweipolen mit negativem Widerstand im allgemeinen sowie von Tunneldioden im besonderen bestimmen.